IDENTIFICATION OF PIPELINE CRACKING AREA IN UNDERWATER ENVIRONMENT

CHONG CHEAN YEE

UNIVERSITI TEKNIKAL MALAYSIA MELAKA
UTeM
اونيۏرسيتي تيکنيکل مليسيا ملاک

BACHELOR OF MECHATRONICS ENGINEERING WITH HONOURS
UNIVERSITI TEKNIKAL MALAYSIA MELAKA

2019

IDENTIFICATION OF PIPELINE CRACKING AREA IN UNDERWATER ENVIRONMENT

CHONG CHEAN YEE

A report submitted
in partial fulfillment of the requirements for the degree of
Bachelor of Mechatronics Engineering with Honours

Faculty of Electrical Engineering

اونيۏرسيتي تيکنيکل مليسيا ملاک
UNIVERSITI TEKNIKAL MALAYSIA MELAKA

UNIVERSITI TEKNIKAL MALAYSIA MELAKA

2019

DECLARATION

I declare that this thesis entitled “IDENTIFICATION OF PIPELINE CRACKING AREA IN UNDERWATER ENVIRONMENT” is the result of my own research except as cited in the references. The thesis has not been accepted for any degree and is not concurrently submitted in candidature of any other degree.

Signature : .....

Name : .....

Date : .....

UNIVERSITI TEKNIKAL MALAYSIA MELAKA

APPROVAL

I hereby declare that I have checked this report entitled “IDENTIFICATION OF PIPELINE CRACKING AREA IN UNDERWATER ENVIRONMENT” and in my opinion, this thesis it complies the partial fulfillment for awarding the award of the degree of Bachelor of Mechatronics Engineering with Honours

Signature : .....

Supervisor Name : .....

Date : .....

UNIVERSITI TEKNIKAL MALAYSIA MELAKA

DEDICATIONS

To my beloved mother and father

UNIVERSITI TEKNIKAL MALAYSIA MELAKA

ACKNOWLEDGEMENTS

Throughout the entire project, I was contact with various people, researchers and academicians, all of whom plays a vital role in completing this report. All above, I would like to express my sincere appreciation to Universiti Teknikal Malaysia Melaka (UTeM) for providing me all the necessary facilities for the research. I feel grateful for having the chance to meet various of people and professionals who provide me a good experience throughout this bachelor program.

Next, I would like to express my special thanks of gratitude to my final year project (FYP) supervisor, Professor Madya Dr. Ahmad Zaki Bin Hj. Shukor, for his encouragement, guidance and patience. He had helped me when I faced any problem on the project. He had also given his valuable support cooperation and suggestions from time to time. I am very thankful to him.

My sincere appreciation also extends to all my friends who have provided many useful views and tips on my project. Last but not least, I am grateful to all my family members for their moral support.

اونيۏرسيتي تيکنيکل مليسيا ملاک
UNIVERSITI TEKNIKAL MALAYSIA MELAKA

ABSTRACT

Underwater pipelines are usually used to transport oil and natural gas in huge quantities and over long distances. Cracking in underwater pipelines is hard to be detected and the cracking had caused a large number of past accidents throughout the world. The main problem for detecting the cracking area or location is the poor visibility in underwater environment. The objectives of this study are to develop image processing method in identifying the cracking area using real underwater pipeline's images and analyse the pipeline cracking area in different types of artificial underwater environment. In the proposed system, the images of cracking pipeline were collected and undergoes image processing algorithm, which include grayscale image, image filtering, image thresholding and edge detection. Then, contour method was used to find the coordinates of the cracking area from the processed images. Two experiments were designed to fulfil the objectives. The first experiment is to identify the pipeline's crack using the images from real underwater environment, while other experiments are to determine the pipeline cracking area using images from artificial underwater environment in different conditions. In the first experiment, suitable filter, threshold method and edge detector are chosen for the system. The percent error of the proposed system is determined in Experiment 2 for different conditions. For the result of Experiment 1, the proposed system is including Gaussian filter, simple thresholding and Canny edge detection. From Experiment 2, the performance of the proposed system is the best in the condition of low turbidity level with high lighting level. The condition of high turbidity level with low lighting level had the worst performance as the resulted percent error had reached more than 70% and half of the cracking parts cannot be found in this condition. Therefore, turbidity and lighting conditions is important for image processing.

UNIVERSITI TEKNIKAL MALAYSIA MELAKA

ABSTRAK

Saluran paip bawah air biasanya digunakan untuk mengangkut sejumlah besar minyak dan gas melalaui jarak yang panjang. Bagaimanapun, retakan yang ada pada saluran paip bawah air susah untuk dikesan dan retakan tersebut telah menyebabkan berlakunya kemalangan yang berjumlah besar dalam seluruh dunia. Masalah yang terbesar bagi mengesan retakan tersebut adalah disebabakan penglihatan yang buruk ketika berada di bawah air. Tujuan kajian ini adalah untuk mengkaji penggunanaan teknik pemprosesan gambar dalam mengesan kawasan retakan pada saluran paip bawah air yang sebenar dan menganalisis kawasan retakan pada saluran paip yang berada dalam pelbagai keadaan persekitaran bawah air buatan. Dalam sistem yang dicadangkan, gambar-gambar retakan paip telah dikumpul dan teknik pemprosesan gambar telah dijalankan di mana teknik tersebut merangkumi menukar gambar asal kepada gambar skala kelabu, menapiskan gambar, mengambangkan gambar and *edge detection*. Selepas teknik pemprosesan gambar, teknik *Contour* telah digunakan untuk mencari koordinat kawasan retakan daripada gambar yang telah diproseskan. Dua eksperimen telah dijalankan untuk memenuhi tujuan kajian ini. Eksperimen pertama adalah untuk mengenal pasti retak saluran paip dengan menggunakan gambar dari persekitaran bawah air sebenar, manakala eksperimen lain adalah untuk menentukan saluran paip kawasan retak menggunakan imej daripada persekitaran bawah air buatan dalam keadaan yang berbeza. Dalam eksperimen pertama, penapis, kaedah ambang dan *edge detector* yang sesuai dipilih untuk system tersebut. Peratus kesilapan sistem ditentukan dalam Eksperimen 2 untuk keadaan yang berbeza. Untuk hasil Eksperimen 1, sistem yang dicadangkan termasuk penapis *Gaussian*, penguncian mudah dan *Canny edge detection*. Dari Eksperimen 2, prestasi sistem yang dicadangkan adalah yang terbaik dalam keadaan tahap kekeruhan yang rendah dengan tahap pencahayaan yang tinggi. Keadaan paras kekeruhan yang tinggi dengan tahap pencahayaan rendah mempunyai prestasi terburuk kerana kesilapan peratus telah mencapai lebih daripada 70% dan separuh daripada bahagian retak tidak dapat ditemui dalam keadaan ini. Oleh itu, tahap kekeruhan dan pencahayaan adalah penting untuk pemprosesan imej.

UNIVERSITI TEKNIKAL MALAYSIA MELAKA

TABLE OF CONTENTS

PAGE

DECLARATION

APPROVAL

DEDICATIONS

ACKNOWLEDGEMENTS **2**

ABSTRACT **3**

ABSTRAK **4**

TABLE OF CONTENTS **5**

LIST OF TABLES **7**

LIST OF FIGURES **8**

LIST OF APPENDICES **12**

CHAPTER 1 INTRODUCTION **13**
1.1 Motivation 13
1.2 Problem Statement 14
1.3 Objectives 16
1.4 Scopes 16
1.5 Thesis Outline 17

CHAPTER 2 LITERATURE REVIEW **18**
2.1 Underwater Pipeline System 18
2.2 Types of Crack in Underwater Pipeline 19
2.2.1 Stress Corrosion Cracking (SCC) 19
2.2.2 Hydrogen Induced Cracking (HIC) 20
2.2.3 Stress Oriented Hydrogen Induced Cracking (SOHIC) 21
2.2.4 Hook Crack 21
2.3 Related Works On Cracking Pipeline Detection Methods 21
2.3.1 Image Processing 22
2.3.2 Acoustic/Ultrasonic Sensor 24
2.3.3 Criteria Comparison 26
2.4 Summary 29

CHAPTER 3 METHODOLOGY **30**
3.1 System Overview 30
3.2 Image Acquisition 30
3.3 Image Processing Algorithm 31
3.3.1 Image Grayscaling 32
3.3.2 Image Filtering 32
3.3.3 Image Thresholding 32

UNIVERSITI TEKNIKAL MALAYSIA MELAKA

3.3.4 Edge Detection 33
3.4 Crack Area Determination 33
3.5 Experiments 34
3.5.1 Hardware Components 35
3.5.2 Experiment 1: Identification of Pipeline Cracking Area for Real Underwater Environment 36
3.5.3 Experiment 2: Identification of Pipeline Cracking Area for Artificial Underwater Environment with Different Conditions 37
3.6 Summary 41

CHAPTER 4 RESULTS AND DISCUSSIONS 42
4.1 Results and Analysis 42
4.1.1 Experiment 1: Identification of Pipeline Cracking Area for Real Underwater Environment 42
4.1.2 Experiment 2: Identification of Pipeline Cracking Area for Artificial Underwater Environment with Different Conditions 53
4.1.2.1 Low Turbidity Level and High Lighting Level 53
4.1.2.2 Low Turbidity Level and Low Lighting Level 57
4.1.2.3 High Turbidity Level and High Lighting Level 63
4.1.2.4 High Turbidity Level and Low Lighting Level 68
4.1.3 Summary 73

CHAPTER 5 CONCLUSION AND FUTURE WORKS 74
5.1 Conclusion 74
5.2 Future Works 75

REFERENCES 76

APPENDICES 81

UNIVERSITI TEKNIKAL MALAYSIA MELAKA

LIST OF TABLES

Table 2.1 Criteria Comparison on Pipeline Detection Methods from Previous Related Works 26

Table 2.2 Advantages and Limitations of Image Processing Method and Method using Acoustic/Ultrasonic Sensor 28

Table 3.1 Fulfilment of The Objectives Based on The Experiments 34

Table 3.2 Specification of SJCAM SJ4000 Wi-Fi Action Camera 35

Table 4.1 Crack Area Determination Results for Experiment 1 52

Table 4.2 Crack Area Determination Results for Experiment 2 Condition 1 57

Table 4.3 Crack Area Determination Results for Experiment 2 Condition 2 62

Table 4.4 Percent Error Results for Experiment 2 Condition 2 62

Table 4.5 Crack Area Determination Results for Experiment 2 Condition 3 67

Table 4.6 Percent Error Results for Experiment 2 Condition 3 67

Table 4.7 Crack Area Determination Results for Experiment 2 Condition 4 72

Table 4.8 Percent Error Results for Experiment 2 Condition 4 72

UNIVERSITI TEKNIKAL MALAYSIA MELAKA

LIST OF FIGURES

Figure 2.1 A Seafloor Oil Production Facility with A Number Of Components [23] 19

Figure 2.2 Underwater Acoustic Sensor Networks (UASN) [38] 25

Figure 2.3 Integrated Underwater Acoustic Sensor Networks [38] 25

Figure 3.1 Overview of Underwater Pipeline Cracking Area Identification System 30

Figure 3.2 Example real underwater pipe with cracks 31

Figure 3.3 Flow of Image Processing Algorithm 31

Figure 3.4 OpenCV-Python 31

Figure 3.5 (a) Horizontal Sobel Mask; (b) Vertical Sobel Mask 33

Figure 3.6 Boundary Rectangle with Coordinates 34

Figure 3.7 SJCAM SJ4000 Wi-Fi Action Camera 35

Figure 3.8 Flowchart for Experiment 2 37

Figure 3.9 Equipment Required for Experiment 2 38

Figure 3.10 Fish Aquarium Setup 39

Figure 3.11 Four Conditions for Experiment 2 40

Figure 3.12 Cracked PVC Pipes for Experiment 2 40

Figure 4.1 Original Image [33] and Grayscale Image for Crack 1 42

Figure 4.2 Original Image [34] and Grayscale Image for Crack 7 43

Figure 4.3 Original Image [36] and Grayscale Image for Crack 9 43

Figure 4.4 Original Image [20] and Grayscale Image for Crack 20 43

Figure 4.5 Original Image [49] and Grayscale Image for Crack 37 44

Figure 4.6 Image filtered using median and Gaussian filter for Crack 1 44

UNIVERSITI TEKNIKAL MALAYSIA MELAKA

Figure 4.7 Image filtered using median and Gaussian filter for Crack 7 45

Figure 4.8 Image filtered using median and Gaussian filter for Crack 9 45

Figure 4.9 Image filtered using median and Gaussian filter for Crack 20 45

Figure 4.10 Image filtered using median and Gaussian filter for Crack 37 46

Figure 4.11 Image resulted using simple and Otsu thresholding for Crack 1 46

Figure 4.12 Image resulted using simple and Otsu thresholding for Crack 7 47

Figure 4.13 Image resulted using simple and Otsu thresholding for Crack 9 47

Figure 4.14 Image resulted using simple and Otsu thresholding for Crack 20 47

Figure 4.15 Image resulted using simple and Otsu thresholding for Crack 37 48

Figure 4.16 Image resulted using different edge detector for Crack 1 48

Figure 4.17 Image resulted using different edge detector for Crack 7 49

Figure 4.18 Image resulted using different edge detector for Crack 9 49

Figure 4.19 Image resulted using different edge detector for Crack 20 49

Figure 4.20 Image resulted using different edge detector for Crack 37 50

Figure 4.21 Area for Crack 1 detected with their coordinates 50

Figure 4.22 Area for Crack 7 detected with their coordinates 51

Figure 4.23 Area for Crack 9 detected with their coordinates 51

Figure 4.24 Area for Crack 20 detected with their coordinates 51

Figure 4.25 Area for Crack 37 detected with their coordinates 52

Figure 4.26 Result of Proposed Image Processing Algorithm for Crack A1 53

Figure 4.27 Area for Crack A1 detected with their coordinates 54

Figure 4.28 Result of Proposed Image Processing Algorithm for Crack B1 54

Figure 4.29 Area for Crack B1 detected with their coordinates 55

Figure 4.30 Result of Proposed Image Processing Algorithm for Crack C1 55

Figure 4.31 Area for Crack C1 detected with their coordinates 56

UNIVERSITI TEKNIKAL MALAYSIA MELAKA

Figure 4.32 Result of Proposed Image Processing Algorithm for Crack D1 56

Figure 4.33 Area for Crack D1 detected with their coordinates 56

Figure 4.34 Result of Proposed Image Processing Algorithm for Crack A2 58

Figure 4.35 Area for Crack A2 detected with their coordinates 58

Figure 4.36 Result of Proposed Image Processing Algorithm for Crack B2 59

Figure 4.37 Area for Crack B2 detected with their coordinates 59

Figure 4.38 Result of Proposed Image Processing Algorithm for Crack C2 60

Figure 4.39 Area for Crack C2 detected with their coordinates 60

Figure 4.40 Result of Proposed Image Processing Algorithm for Crack D2 61

Figure 4.41 Area for Crack D2 detected with their coordinates 61

Figure 4.42 Result of Proposed Image Processing Algorithm for Crack A3 63

Figure 4.43 Area for Crack A3 detected with their coordinates 64

Figure 4.44 Result of Proposed Image Processing Algorithm for Crack B3 64

Figure 4.45 Area for Crack B3 detected with their coordinates 65

Figure 4.46 Result of Proposed Image Processing Algorithm for Crack C3 65

Figure 4.47 Area for Crack C3 detected with their coordinates 65

Figure 4.48 Result of Proposed Image Processing Algorithm for Crack D3 66

Figure 4.49 Area for Crack D3 detected with their coordinates 66

Figure 4.50 Result of Proposed Image Processing Algorithm for Crack A4 68

Figure 4.51 Area for Crack A4 detected with their coordinates 68

Figure 4.52 Result of Proposed Image Processing Algorithm for Crack B4 69

Figure 4.53 Area for Crack B4 detected with their coordinates 69

Figure 4.54 Result of Proposed Image Processing Algorithm for Crack C4 70

Figure 4.55 Area for Crack C4 detected with their coordinates 70

Figure 4.56 Result of Proposed Image Processing Algorithm for Crack D4 71

UNIVERSITI TEKNIKAL MALAYSIA MELAKA

Figure 4.57 Area for Crack D4 detected with their coordinates 71

UTeM
اونيۏرسيتي تيکنيکل مليسيا ملاک
UNIVERSITI TEKNIKAL MALAYSIA MELAKA

LIST OF APPENDICES

APPENDIX A	TIME FRAME FOR FYP	81
APPENDIX B	GANTT CHART FOR FYP	82
APPENDIX C	IMAGE PROCESSING ALGORITHM CODING	83
APPENDIX D	CRACK AREA DETERMINATION CODING	85
APPENDIX E	RESULTS FOR EXPERIMENT 1	86

UNIVERSITI TEKNIKAL MALAYSIA MELAKA

CHAPTER 1

INTRODUCTION

This chapter describes the motivation and problem statement to give an idea of the contribution of the research study. The objectives and scope of the study are also described.

1.1 Motivation

Nowadays, fluids such as water, oil, natural gas and carbon dioxide have been moved in huge quantities and long distances using pipelines. Pipelines system are generally divided into two: onshore pipelines (land pipelines) and offshore pipelines (underwater pipelines) [1]. For the underwater pipeline, financial losses in term of fluid losses and environmental problems may be occurred due to poor maintenance of the pipeline and safety issues [2]. From 2003 to 2018, there is a large number of underwater pipeline accidents that occurred throughout the world.

The British Petroleum (BP) company owns the largest offshore deepwater oil field, Thunder Horse field in Gulf of Mexico, that processes 200 million cubic feet of natural gas and 250 thousand barrels of oil per day [3,4]. After the occurrence of Hurricane Dennis in July 2005, Thunder Horse platform was found leaning badly. When the platform was being repaired, it was discovered that the underwater pipelines of platform are brittle and full of cracks due to poor welding job [5].

PETRONAS gas pipeline explosion in Sarawak, Malaysia occurred early in the morning of 10 June 2014. The location of the incident was in the district of Lawas, Sarawak. The people in Lawas town were shocked seeing the fireball that burned for almost 2 hours. The RM4 billion project (Sabah-Sarawak interstate gas pipeline) owned by PETRONAS had been temporarily stopped after the explosion occurred. Fortunately, there were no lives lost in the incident [6]. This incident is caused by the cracking pipeline due to soil movement [7].

In 2015, an underwater pipeline under Moscow's Moskva River in Russia that used to transport oil, exploded due to cracks in the pipeline. The flames and smoke

UNIVERSITI TEKNIKAL MALAYSIA MELAKA

could be seen 16 km away from the explosion site. Three bystanders, including a child were being admitted to the hospital for respiratory problems caused by the plumes of black smoke and there was no occurrence of death in this accident [8,9].

An oil spill from the Poplar pipeline into the Yellowstone River just upstream of Glendive, Montana was discovered on Jan 2015. More than 30 thousand gallons of Bakken crude oil was spilled into the Yellowstone River due to the cracked pipeline. The incident had affected the quality of drinking water near Glendive and the surrounding towns. The oil cleanup on Yellowstone River took a few months to complete since the ice on the river prevented the cleanup [10,11].

Alaska's Cook Inlet is well known for its marvelous mountain view and the habitat of the endangered beluga whales. In Feb 2017, a Hilcorp helicopter noticed that bubbles of natural gas were floating at the surface of Cook Inlet. The natural gas was bubbling up from the cracked underwater pipeline which used to transport natural gas to the offshore oil drilling platforms. It was then found out that the leakage was started a few months earlier in Dec 2016. 210,000 to 310,000 cubic feet of the natural gas had been leaked into the watershed every day and posed a toxic threat to the people and marine life of Cook Inlet [12,13].

On July 24, 2018, an oil spill occurred in Cliff Head Alfa platform, Perth. Australia-based Triangle Energy confirmed the incident and reported that the main cause of the incident was the small crack in the pipeline. Fortunately, there were no people or wildlife harmed since the oil spill was in the range of 0 to 10,000 litres [14].

UNIVERSITI TEKNIKAL MALAYSIA MELAKA

In conclusion, the cracking of underwater pipeline is the main reason causing most of the incidents mentioned above. The incidents had caused financial losses and human life or marine life losses. This has motivated me to do the research on the identification of underwater pipeline cracking area.

1.2 Problem Statement

Currently, pipelines are an effective medium to transport oil and natural gas in the underwater environment. After the pipeline has been used for years, failures may occur. The failures are generally due to inherent defects, external damage or old-aged pipelines. Underwater pipeline accidents have been increased occasionally because of the cracking in the pipelines [1]. There are some problems being faced when the cracking detection is carried out in underwater environment.

The main problem is the poor visibility in underwater environment. Visibility is commonly defined as the distance at which an object can been seen. The degree of visibility in underwater environment mainly depends on the light penetration and turbidity level. Light penetration depends on light level, incidence angle of light rays and roughness of water surface. Light level is low in cloudy or rainy day causing poor visibility in underwater environment. Water can absorb wavelength of light rays to different degree making the colour shift in the water. The characteristic coloration of the water will also cause the light level in the water drops. For the incidence angle, the higher the distance from equator of earth, the lower the incidence angle, more light being reflected, making less light enter the water. As an example, the seawater near the coast of New Jersey is more cloudy that that of Bonaire ocean which located near the equator. In the case of water surface's roughness, ocean with choppy waves will have poor underwater visibility since it reflects more light rays compared to calm ocean. Turbidity means the cloudiness of a fluid caused by the large number of suspended particles that absorb and scatter the light, and hence reduce the fluid visibility. Turbidity may be affected by decomposed plant and animal matter, algae, silt or clay. Tides, heavy rain, storm, urban run-off, landslide and bank erosion can also increase the number of suspended particles and affect the turbidity level. Sea with choppy waves in stormy day stirs up the sediments from the sea bottom, causing high underwater turbidity level. Runoff has caused almost 240 million tons of topsoil washed from Mississippi River to the Gulf of Mexico every year. The high turbidity level in underwater environment makes poor visibility and increases the difficulty in detecting the cracks and repairing work [15,20,21,22].

UNIVERSITI TEKNIKAL MALAYSIA MELAKA

Secondly, the use of inspection tools may have some errors when remoting the pipelines' conditions. Crack detection and repair works are done by divers or inspection tools such as remotely operated vehicles (ROV) and pipeline inspection gauges (PIG). By comparing to divers, inspection tools can be operated in greater depth of water and longer time, however they may have some weakness such as expensive, vulnerable to failure, uncontrollable and hard to adapt to changes in pipeline direction and diameter [18,19]. Inspection tools also face problem when they lose connection from the server system. The result of underwater pipeline survey cannot be received if the connection between the inspection tools and server system. Furthermore, fatal accidents may occur in underwater environment. In oil and gas industry, saturation

diver is the one who go to the seabed to do maintenance and reparation on underwater pipelines. The most dangerous thing for the divers is the differential pressure. The pressure differences are due to different depth where water rushes to a body with great force. The force can be hundred pounds per square inch making divers in high risk of drowning. When diving to any depth, divers are breathing pressurized air. Those inert gases in the pressurized air are compressed and dissolve in the blood and body tissues. If the gases do not diffuse out after the diver come out from the water, the gases will form bubbles and become millions of tiny explosives in the body of the diver. Decompression sickness may occur and cause fatality. The longer the time taken for diving, the higher the risk for the divers [16,17].

Due to the problems stated, an underwater pipeline cracking area identification system will be developed.

1.3 Objectives

The objectives of the research study are as follows:

a) To develop image processing algorithm to identify the cracking area in underwater pipeline from actual images.
b) To analyse the pipeline cracking area in different types of artificial underwater environment.

UNIVERSITI TEKNIKAL MALAYSIA MELAKA

1.4 Scopes

The scopes of the research study are:

a) The image processing algorithm is used to identify the crack area, not to detect the crack.
b) The pipeline cracks are identified in four different types of water environment: which are
    - low turbidity level with high lighting level
    - low turbidity level with low lighting level
    - high turbidity level with high lighting level
    - high turbidity level with low lighting level
b) The technique used are image processing method including grayscale image, image filter, thresholding, edge detection

c) Area is determined using contour method.
d) The images from real underwater environment may not mention the light and turbidity level.
e) OpenCV-Python is used for the image processing algorithm.
f) SJCAM SJ4000 Wi-Fi Action Camera is the only used camera for Experiment 2.
g) For Experiment 2, the cracked PVC pipes' images are captured at the water height of 20 cm.
h) For Experiment 2, the distance between the lenses and cracked PVC pipes is about 8cm.

1.5 Thesis Outline

This report and project is about an underwater pipeline cracking area identification system. In this report, motivation for developing this system is covered in Chapter 1. Besides, the objectives and scope of the system are also stated in this chapter. In the following chapter, the review of previous related work of the environment mapping is discussed. In Chapter 2 also, some basic principles and theories are defined and stated. The experiment setup and type of the experiment is discussed in Chapter 3. In Chapter 4, the results are analysed and discussed, followed by a conclusion in Chapter 5.

UNIVERSITI TEKNIKAL MALAYSIA MELAKA

CHAPTER 2

LITERATURE REVIEW

This chapter describes the background of underwater pipeline system and different types of cracking pipeline. Next, related works on cracking pipeline detection methods are discussed. Lastly, the advantages and limitations of each method are discussed and summarized.

2.1 Underwater Pipeline System

Pipelines are the most suitable method to transport oil and natural gas in underwater environment as pipelines can be constructed at the water depths that more than 1000m. The installation of underwater pipeline system includes several components such as well heads, risers and subsea manifolds. Figure 2.1 has shown the installation of the underwater pipeline system for oil production purpose [23].

The oldest underwater pipeline in the world was the outfalls that was built in 19th century. For oil industry, the earliest underwater pipeline was short and long loading pipelines. The pipelines were built on shore and linking them into the water. The first underwater pipeline for petroleum industry was constructed in Gulf of Mexico (1947), which is located 17km from the land and 6m into the water. Underwater pipelines in earlier stage were constructed within the depth that reachable for the divers, almost 300m deep. Nowadays, the underwater pipelines are mostly placed in the depth more than 1000m. There are several projects that having the pipeline placed between 1500m and 2500m in the water. For example, pipelines in Black Sea was installed up to almost 2200m [1].

In [23], the lifespan of a pipeline is mentioned can be over 40 years. Failure incidents are counted as a part of life for the pipeline. Inherent effects mainly cause post-commissioning failure per unit time increased. The design of pipeline generally depends on the following criteria: stress-related principles, material selection and welding requirement and lastly internal and external pressures. These criteria may affect indirectly affect the lifespan of a pipeline. Besides, failure incidents may also

UNIVERSITI TEKNIKAL MALAYSIA MELAKA

cause by external damage like storms and anchors. Therefore, the pipeline design may also need to consider many other issues such as the age-related issues, seabed type and condition, temperature, tidal currents, waves and submarine landslide.

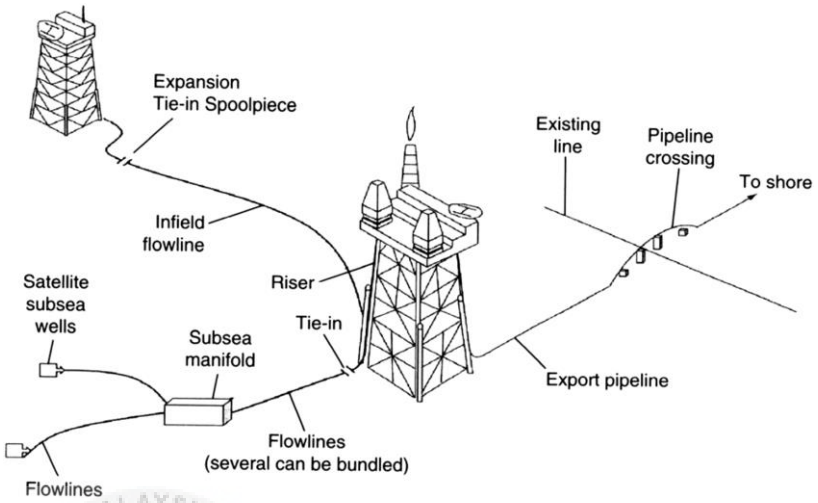

Figure 2.1 A Seafloor Oil Production Facility with A Number Of Components [23]

2.2 Types of Crack in Underwater Pipeline

Cracks weaken the structural integrity of pipeline. Cracking may happen due to the factors: base material of pipeline, welding work, heat affected zone (HAZ) and dents or defects. There are several types of cracking in underwater pipelines and four of them are discussed in this section.

UNIVERSITI TEKNIKAL MALAYSIA MELAKA

2.2.1 Stress Corrosion Cracking (SCC)

Stress corrosion cracking (SCC) is a crack formed from corrosive environment. It has a marked loss of mechanical stress with small amount of metal loss. It is a hazardous and fatal mechanism and may cause majority of subsea disaster. The vulnerability to SCC is affected by applied stress level, material of the pipeline and environmental conditions. Most of the underwater pipelines are made of steel. SSC happens due to the anodic reaction of the steel with the corrodents such as chloride ion (Cl-), oxidants, hydrogen sulphide (H2S) and oxidants like elemental sulphur present in the water. The synergistic action of H2S in acidic solution is known as sulphide

stress corrosion. Sulphide stress corrosion is resulted from localized alloy embrittlement by hydrogen atom [1,24,25,26].

There are three basic mechanisms of SCC which are active path dissolution, hydrogen embrittlement and film-induced cleavage. The most active path for the accelerated corrosion is the gain boundary where segregation of impurity element can trouble the passivation of a material. The gain boundary corrosion can occur without the presence of stress where the crack walls is still passivated. The presence of applied stress is to open up the cracks and faster the corrosion rate. The maximum crack growth rate for active path corrosion is 10-2 mm/s but the usual rate is 10-8 mm/s. In the case of hydrogen embrittlement, hydrogen is small enough to dissolve in all materials. Region of high triaxial tensile stress will attract hydrogen to it when the metal structure destroyed. The dissolved hydrogen will assist in the fracture of metal and then lead to metal embrittlement. The cracking of this mechanism may be intergranular or transgranular and the maximum crack growth rate is 1 mm/s. For film-induced cleavage, ductile material is generally passivated with brittle film. The crack that formed by corrosion in the brittle film can propagate the ductile material. De-alloyed layer is the brittle film that lead to film-induced cleavage. Transgranular cracking is expected from the film-induced cleavage process [26].

2.2.2 Hydrogen Induced Cracking (HIC)

UNIVERSITI TEKNIKAL MALAYSIA MELAKA

Hydrogen induced cracking (HIC) is one of the cracking that occurs in the steel underwater pipelines. The occurrence of HIC is due to metallurgical (strength, alloying element, microstructure, etc.) and environmental factors (pH, temperature, aggressive ions, etc.). Underwater pipeline is used to transport crude oil and natural gas. The formation of HIC is when the hydrogen sulphide (H2S) in the crude oil reacts with the water and hydrogen is formed. At the same time, hydrogen is also formed when H2S reacts with the iron in the steel pipeline. The hydrogen atom is small enough to diffuse through the wall of pipeline and cause embrittlement. The more the hydrogen being trapped in the space of pipe wall, the higher the hydrogen pressure. This causes the stress in the steel pipeline greater than its tensile strength. Steel is a ductile material and high stress may cause lamination. When the laminations are formed near to each other, stresses will force the lamination to join to form HIC. HIC's cracks are usually

positioned parallelly to the rolling plane. HIC may also occur during welding process [27,28,29].

2.2.3 Stress Oriented Hydrogen Induced Cracking (SOHIC)

Stress oriented hydrogen induced cracking (SOHIC) is like HIC but the lamination is formed on the top of each other. Formation of HIC is usually the initial step for the formation of SOHIC; however, SOHIC also can be formed in the HIC-resistant material. High pressure stresses of hydrogen will force the formation of crack instead of plastic deformation. Individual HIC cracks are formed as vertically stacked array and the array runs perpendicular to the applied stress. Significant through-thickness crack which is SOHIC is formed when the run through the thickness of the pipeline. For a non-ductile material, SOHIC usually formed adjacent to the heat affected zone (HAZ) of weld. SOHIC can be divided into two types: Type I and II. Type I is the traditional SOHIC with in-plane and linking cracks while Type II is SOHIC with no obvious in-plane cracks. For the formation of Type I SOHIC, in-plane cracks are initially formed and crack propagation rate of linking cracks is low, thus form the Type I SOHIC. Otherwise, it is the formation of Type II SOHIC [27,29,30].

2.2.4 Hook Crack

UNIVERSITI TEKNIKAL MALAYSIA MELAKA

Hook crack occurs during pipeline manufacturing or welding process. The occurrence of hook crack is due to non-metallic inclusions. Hook crack is formed when inclusion is turned out from the metal which gives the crack's appearance as "hook" or "J" shape. Hook cracks are small and always follow the weld flow lines. If there are too many hook cracks, it may open up the surface of the pipeline. Hook cracks will possibly pass the initial hydrotest; however, the cracks will later fail as fatigue-induced cracking [30,31].

2.3 Related Works On Cracking Pipeline Detection Methods

There are several methods that can be used to detect the cracks on the pipeline (either onshore or offshore pipeline) such as image processing, ultrasonic sensors,

negative pressure wave method, infrared thermography and others. Two out of these methods, which are usually used for detecting the defects, are discussed in this section.

2.3.1 Image Processing

Image processing method is mostly used to detect and identify the cracking pipeline. Visual inspection is carried out by trained divers or inspection tools to obtain the images of cracking pipelines [20]. Various researches on the image processing have been carried out.

The authors in [18] had developed an image processing protocol for the pipeline inspection. The protocol was claimed to be used for variety situations that can affect the imaging conditions and finally successfully to be demonstrated in Cork harbour, Ireland. The protocol is set up with two cameras to allow the photograph can be taken from different viewpoints simultaneously. The speciality of the protocol is the stereo imaging-based 3D shape recovery systems. The system is potentially to recover the full 3D information of the pipeline. The protocol tends to retain enough brightness and focus the enough of subject while minimizing the noise of the image.

[32] had introduced a vision-based quality inspection system to detect the defection for tube-sheet welding. The system contains welding robot, vision sensor and a control computer. Image processing, which is the most important part in this system, consists of two parts: image pre-processing and detection of the defect. In image pre-processing part, median filter is used to remove the noise of the image that captured by vision sensor. Otsu algorithm performs image segmentation automatically while morphological technology is used to make sure the continuity of edge. Region of interest (ROI) is then selected. Unlike the stereo imaging-based 3D shape recovery systems in [18], the system in [32] uses sum intensity for the defect detection. Accuracy of determining a defect and its location are determined using the sum intensity for the pipe tube. The results in [32] have shown the high accuracy of the vision-based quality inspection system.

UNIVERSITI TEKNIKAL MALAYSIA MELAKA

An image-based model for predicting pipeline's cracks had been proposed in [33]. Firstly, colour images are taken and converted into grayscale images (black and white) using MATLAB software. Next, image segmentation is carried out using threshold method while image enhancement is done using erosion and dilation operators. Then, the cracks are enhanced by applying Laplacian filter to the images.

The method used for detecting the edges is Canny edge detection. After edge detection, the crack width and length and the pixel resolution are calculated. Finally, the levels of cracks are classified by using fuzzy logic with crack width, crack length and number of pixels. The model proposed in [33] has the accuracy of 90% in detecting the cracks.

The procedure of the vision inspection system that introduced by [34] is similar to the one proposed in [33]. Both of system in [33] and [34] pre-process the pipeline images using image processing technique and then segment those images using thresholding. However, morphological method is also used in [34] for image segmentation. The additional thing of the system in [34] is the damage type of the pipeline can be identified using two recognitions: statistics recognition and back propagation neural network (BPNN) recognition. By using both recognitions, drainage pipelines can be detected and the damage situation of the inner wall of pipeline can also be identify.

Another image processing method mentioned in [35] is used to detect the cracks in the long-distance natural gas pipeline's inner wall. The algorithm is also divided into two parts which are image pre-processing and crack recognition. Image pre-processing part consists of converting images to grayscale images, median filtering, non-linear graying and binarization. Crack recognition algorithm involves the steps of partitioning the images, calculating the inflection point of images, analysing the centre point and radius minimum circle field where the image is and lastly judge the cracks using fuzzy judgement. By comparing to the accuracy in [33], the recognition rate of this algorithm has resulted more than 92% by testing on natural gas pipelines with different specifications [35].

Dou-edge evaluation (DEE) can be used as a computer vision algorithm for detecting the thin cracks on the pipeline automatically. DEE has advantages of extracting cracks from complicated and noisy environment when being compared to other edge filters such as Laplacian filter in [33]. The DEE algorithm is started by applying Sobel filter to the grayscale image to get a binary image. Morphological filter is then applied to the binary image to remove noise and fill objects; thus, a skeleton image will be obtained. The widths of the objects in the image is evaluated and then the objects other than the cracks will be filter out from the image. Lastly, random noise is removed by applying threshold filter to the image. The limitation of this DEE algorithm is cracks in different sizes' range cannot be detected at the same time [36].

UNIVERSITI TEKNIKAL MALAYSIA MELAKA

2.3.2 Acoustic/Ultrasonic Sensor

Acoustic sensors' nodes are generally installed on the outer pipeline surface. The pressure in a pipeline is always in a balance condition. When there is a leak, the pressure will be imbalance and the frequency of acoustic signal generated (noise) will exceed the audible range. Those acoustic sensors are used to collect the noise [2,15]. Ultrasonic sensors are used to emit and receive ultrasonic waves that travel through the pipeline's wall. A detailed mapping of the pipeline's wall will be obtained. There are two important information in the received waves, which are the time taken between emission and reception and the amplitude. The time taken can be used to determine the distance of the pipeline using Time-of-Flight (TOF). Then, by operating the ultrasonic sensor point-to-point through a region, the cracking area and location will be detected [24,36].

[37,38,39] have mentioned two types of networks using acoustic sensor for underwater pipelines: Underwater Acoustic Sensor Networks (UASN) and Integrated Underwater Acoustic Sensor Networks. UASN has a limitation where each node can only communicate with a few of neighbouring nodes, therefore there will be an error in information transmission to the control station. In Figure 2.2, only two out of all acoustic sensors is linked to a buoy which has the radio communication system that can communicate with the control station. This means that all the nodes have to transfer the signal to the neighbouring nodes until the signal reaches the node that connected to the buoy. Integrated UASN has overcome the problem of UASN by connecting each node to a wireless acoustic transceiver and a wired network interface. The status of each node can be checked periodically and maintenance can be carried out immediately. Faulty nodes may cause link breaks. With wider transmission range using wireless links with multiple nodes, the connectivity will remain even though there are several link breaks on several segments as shown in Figure 2.3.

UNIVERSITI TEKNIKAL MALAYSIA MELAKA

[40] proposed a system to monitor the pipeline wall for oil and gas station. The system is adopted by multi-crystal ultrasonic wave sensors. These sensors are used to monitor the thickness of the pipelines in circumferential direction. The sensors are used with 14 internal ultrasonic crystal in the system designed for the measurement of thickness. After the sensors have gathered the data, tendency analysis is operated to

give the tendency information. The different time periods analysed from the data tendency is then used for the prediction of pipeline crack area's location.

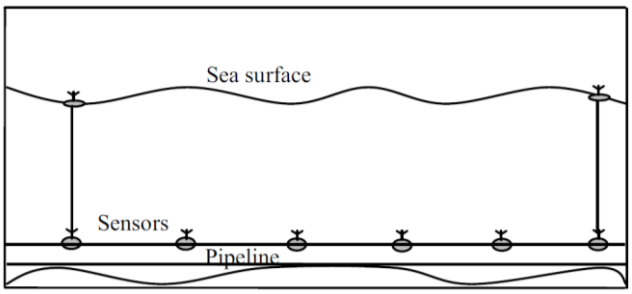

Figure 2.2 Underwater Acoustic Sensor Networks (UASN) [38]

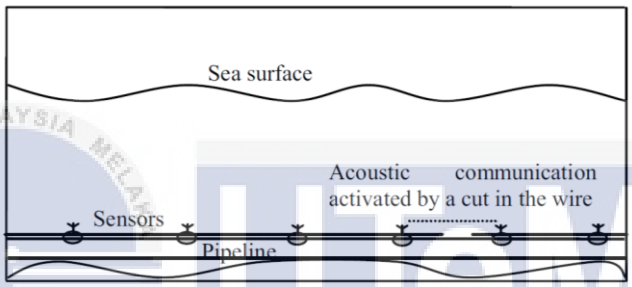

Figure 2.3 Integrated Underwater Acoustic Sensor Networks [38]

Similar to [40], [41] introduced a system for measuring the thickness of wall using ultrasonic multisensor. The proposed system has four main parts: tube transmission line for transporting pipes in constant speed, ultrasonic wave continuously detection equipment for acquire signals of the detection of steel pipe wall thickness, a data acquisition card (HY.6070C board) and computer inspecting software (Visual C++ 6.0 software) for calculation of pipe wall thickness. The detecting speed of this proposed system reaches approximately 0.417 m/s and its accuracy is ±1 mm.

Acoustic emission sensors are used for leak detection and the leak location for gas pipelines. The sensors, which are installed on the outer wall of the gas pipelines, collect the leak acoustic emission signals available for the leak detection. An adaptive time delay estimator is used to estimate the time delay between two leak acoustic emission signals. The time delay is then used to locate the leak location by combining with the sonic speed in gas pipeline and the distances between two acoustic emission sensors. The experimental result shows that there is only 1% error in locating the leakage when the system is tested over the 80m pipeline [42].

UNIVERSITI TEKNIKAL MALAYSIA MELAKA

The authors in [43] also developed a simulation system with the use of acoustic emission for locating the crack in stainless steel pipelines. The transducer used in the system is piezoelectric sensor. The acoustic emission signals are collected using the same way in [42]. The difference of the system in [43] when compared to the one in [42], is timing parameters such as peak definition time, hit definition time and hit lockout time are defined clearly. By using these timing parameters, the sound localization accuracy is achieved in the experimental part. From the experimental results, the locating error of the system is approximately to 1% when the distance between the two piezoelectric sensors is 1.8 m [43].

2.3.3 Criteria Comparison

Table 2.1 Criteria Comparison on Pipeline Detection Methods from Previous Related Works

Conference / Journal	**[18]**	**[32]**	**[33]**	**[34]**
Algorithm Method	Stereo Imaging Image Processing	Image Processing	Image Processing	CCD Vision System
Sensor Used	Two Cameras	Vision Sensor	SONY-DSC T5 Digital Camera	Vison Sensor
Environment	Underwater	Tube-sheet Welding	Onshore and Offshore Sewer Pipes	Drainage Pipelines
Image Filter		Median Filter	Laplacian Filter	Smooth Filter
Image Segmentation		Otsu Algorithm	Threshold	Threshold and Morphology
Edge Detection			Canny Edge Detector	
Area/Location Determination		Sum intensity	Fuzzy Logic	Statistics Recognition and BPNN Recognition
Accuracy		High accuracy	90% accuracy	Not Stated

Conference / Journal	**[35]**	**[36]**	**[40]**
Algorithm Method	Image Processing	Image Processing	Ultrasonic Monitoring System
Sensor Used	Camera	Camera	Multi-crystal Ultrasonic Wave Sensors
Environment	Natural Gas Pipelines' Inner Wall	Onshore and Offshore Sewer Pipelines	Oil and Gas Pipelines
Image Filter	Median Filter	Morphological filter	
Image Segmentation	Not Stated		
Edge Detection		Sobel edge detector	
Area/Location Determination	Crack recognition	With the aid of skeleton images	Using time periods from data tendency
Accuracy	92% recognition rate	Not stated	High accuracy

Conference / Journal	**[41]**	**[42]**	**[43]**
Algorithm Method	On-line High-speed Inspection	Acoustic Emission Technique	Acoustic Emission Technique
Sensor Used	Ultrasonic Multisensor	Acoustic Emission Sensors	Acoustic Emission Sensors
Environment	Underground Oil or Gas Pipeline	Gas Pipelines	Stainless Steel Pipelines
Area/Location Determination	Visual C++ 6.0 software	Time delay between two leak acoustic emission signals.	Timing parameters
Accuracy	Error of ±1 mm	1% error over 80m pipeline	1% error over 1.8m pipeline

UNIVERSITI TEKNIKAL MALAYSIA MELAKA

Table 2.2 Advantages and Limitations of Image Processing Method and Method using Acoustic/Ultrasonic Sensor

Methods	Advantages	Limitations
Image Processing [32,33,35,36]	• Low cost • High accuracy • Thin cracks can be identified • Location and area of the crack can be known • Easy usage	• Time to detect the leak may be slow. • Need the help of trained divers or inspection tools to obtain the images of pipeline.
Acoustic / Ultrasonic Sensor [2,38,40,41,42,43]	• Moderately high cost • Moderately high accuracy • Time to detect the leak is fast.	• Inefficient for detecting small cracks due to high background and noise conditions • Limited bandwidth among nodes due to distance in between and frequency of the acoustic sensors • High propagation delays of the acoustic signals in underwater environment • Nodes need battery power to operate. The power consumed is high and the lifespan of the battery will reduce. • Ultrasound may harm the marine wildlife

UNIVERSITI TEKNIKAL MALAYSIA MELAKA

2.4 Summary

The discussion of the underwater pipelines' background and different type of underwater pipeline's cracks has been done. The reviews on different methods for detecting and identifying the cracks of either onshore or offshore pipelines is also done. A table is constructed to compare the advantages and limitations of those methods.

From the literature review, vision sensor and acoustic sensor networks are the most popular method to detect the pipeline cracks. Although method using acoustic sensors can detect the crack in a faster rate, this method has a limitation in identifying the crack area. Image processing, the well-known method to identify the cracks using the images taken by the vision sensor, is the trend that is going strong in recent years. From the reviews, there is only a few researchers implement the cracking area identification method. Mostly of the researcher only use the method on detecting whether there is a crack in the pipelines. For this reason, this thesis would like to propose an image processing method including the algorithm of identifying the crack area in underwater pipelines.

UNIVERSITI TEKNIKAL MALAYSIA MELAKA

CHAPTER 3

METHODOLOGY

This chapter starts with the overview of the pipeline cracking area identification system. Next, the identification system is discussed briefly according to the flow chart of system. Finally, the experiments' setup and procedure are explained.

3.1 System Overview

An overview of the proposed underwater pipeline cracking area identification system is discussed in this subchapter. There will be three basic operations in the system, which are image acquisition, image processing and crack area determination. Images of underwater pipeline with cracks will be snapped or collected. Then, the images undergo image pre-processing step which includes image graying, image filtering, image thresholding and others. After being processed, the crack area of the pipelines will be determined. The flowchart for the overview of system is shown in Figure 3.1. Experiments are designed and carried out to implement the system.

The progress of the project is shown using flowchart in APPENDIX A. The detailed timeline is displayed using Gantt chart in APPENDIX B.

UNIVERSITI TEKNIKAL MALAYSIA MELAKA

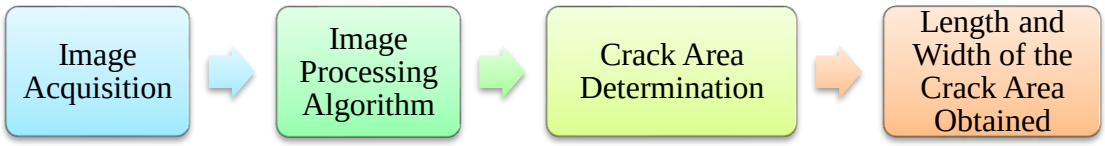

Figure 3.1 Overview of Underwater Pipeline Cracking Area Identification System

3.2 Image Acquisition

Images of underwater pipeline with cracks will be collected. Those images may be gathered from internet. The turbidity and lighting level of the images are not stated clearly.

Besides, by putting a cracked pipeline into water under certain depth, the images of the pipeline will be captured with known water environment.

Figure 3.2 Example real underwater pipe with cracks

3.3 Image Processing Algorithm

Image processing algorithm is the main role in the underwater pipeline cracking area identification system. The image processing algorithm of the system will be carried out using OpenCV-Python software. The flow of the image processing algorithm is shown in Figure 3.3. The first step is to read an image and convert it into a grayscale image. Next, the grayscale image will be filtered to remove noise. Thresholding will then be applied to the filtered image to create a binary image. Edge detection will be used to find the boundaries of the object in the image. Each stage of the image processing algorithm is discussed briefly in the following sections.

UNIVERSITI TEKNIKAL MALAYSIA MELAKA

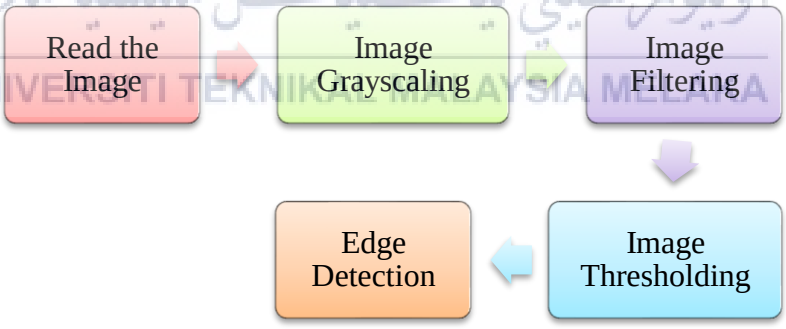

Figure 3.3 Flow of Image Processing Algorithm

Figure 3.4 OpenCV-Python

3.3.1 Image Grayscaling

Image grayscaling is the first step for any image processing algorithm. It is a process to convert a colour image into grayscale image. Grayscale image has 256 gray levels which are from 0 (black) to 255 (white). Grayscale image contains all the detailed information of the image and it is easier for understanding. Grayscale image can improve the process rate of the image processing algorithm compared to a colour image.

3.3.2 Image Filtering

Image filtering is aimed to remove the noise of an image. There are many filters that can be used, such as smoothing linear filters, weighted average filter, median filters and others. In this proposed identification system, median filter, Gaussian filter and unsharp masking will be used. The results of the filter used will be compared and discussed after the experiments are carried out.

Median filter is a non-linear filter which is simpler to be used for reducing noises in an image while keeping the edges. Gaussian filter is a linear filter that used to reduce noises, but it may also blur the edges and reduce contrast of the image.

اونيۏرسيتي تيکنيکل مليسيا ملاک
UNIVERSITI TEKNIKAL MALAYSIA MELAKA

3.3.3 Image Thresholding

Thresholding is one way for image segmentation. Image thresholding is used to convert a filtered image into binary (black and white) image and focus on the object or area of interest in an image. Two types of threshold, which are simple threshold and Otsu threshold will be used in this proposed identification system. Both types of the threshold will be analysed and discussed after the experiments are done.

Simple thresholding is an image thresholding using a set level. When the pixel value is larger than the threshold value being set, the pixel is assigned to a standard value 0 (black), else the pixel is assigned to 255 (white).

Otsu threshold is a multi-level thresholding. Otsu threshold value is selected by referring the minimum within-class variance of two groups of pixels separated by threshold operator. A threshold value is selected, the pixel value smaller than the threshold value is known as background pixels, else as foreground pixels.

3.3.4 Edge Detection

Edge detection is used to determine the boundaries of the object in the image by detecting the sharply changes of brightness. Common edge detection algorithms such as Sobel and Canny will be used and compared in the system.

Sobel edge detection is the use of a first order derivate mask that can detect the edges of objects in an image in vertical and horizontal direction. Figure 3.5 shows the mask of 3x3 Sobel operator.

Canny edge detection is a multistage edge detection with the steps of pre-processing, calculation of gradients, non-maximum suppression and thresholding with hysteresis. Firstly, an image is smoothed by applying Gaussian filter. Next, the gradient magnitude is determined using any gradient operator. Next, the edges of object in the image is thinned by suppressing non-maximum pixels to the gradient magnitude. Lastly, the edges of object in the image is detected by using Double Thresholding with two threshold value, τ_1 and τ_2.

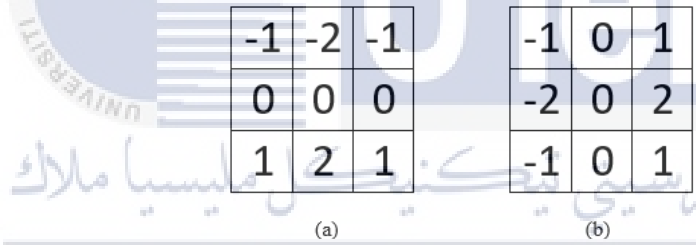

UNIVERSITI TEKNIKAL MALAYSIA MELAKA

Figure 3.5 (a) Horizontal Sobel Mask; (b) Vertical Sobel Mask

3.4 Crack Area Determination

Contour method is initially used to segment the interest region in the edge detected image. This method can use to find the pipeline crack area. When contour function is applied to the edge detected image, a boundary box is drawn around the interested region and the coordinates of the box are determined. By using the coordinates, the length and width of the crack area can be calculated using the Equation (3.1) and (3.2) respectively.

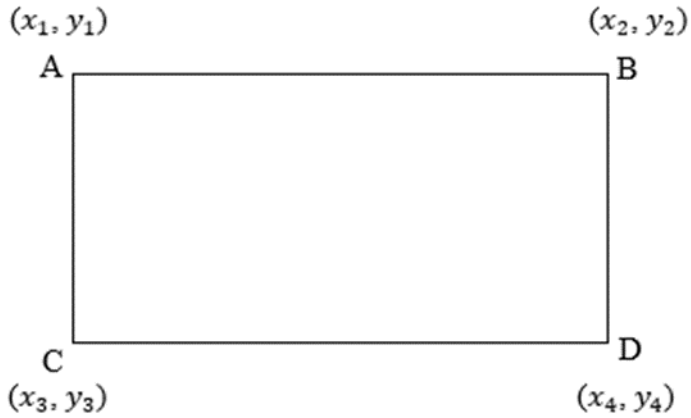

Figure 3.6 Boundary Rectangle with Coordinates

$$Length, l = x_2 - x_1 \quad (3.1)$$

$$Width, w = y_3 - y_1 \quad (3.2)$$

$$Area, A = l \times w \quad (3.3)$$

The percent error of the system can be calculated by the actual value and experimental value of crack area, as shown in Equation (3.4).

$$\%\ error = \frac{|experimental\ value - actual\ value|}{actual\ value} \times 100\% \quad (3.4)$$

UNIVERSITI TEKNIKAL MALAYSIA MELAKA

3.5 Experiments

In order to test the proposed underwater pipeline cracking area identification system, two experiments were conducted to validate the proposed method. Experiment 1 was carried out to identify the pipeline cracking area using the images from real underwater environment. For Experiment 2, pipeline cracking area was determined using images from artificial underwater environment in different conditions.

Table 3.1 Fulfilment of The Objectives Based on The Experiments

	Objective 1	**Objective 2**
Experiment 1	✓	
Experiment 2	✓	✓

3.5.1 Hardware Components

The selection of hardware part is important to ensure the proposed system work efficiently. For Experiment 2, the main hardware part in the proposed system was the underwater camera. SJCAM SJ4000 Wi-Fi Action Camera was chosen to capture the images of pipeline. The specification of this camera is shown in Table 3.2.

Figure 3.7 SJCAM SJ4000 Wi-Fi Action Camera

Table 3.2 Specification of SJCAM SJ4000 Wi-Fi Action Camera

Specifications	**Descriptions**
Lens	170° Ultra Wide Angle Lens
Image format	JPG
Resolution of Image	12MP / 10MP / 8MP / 5MP / 3MP
Storage	Slot for microSD card (maximum 32GB)
Battery Capacity	900 mAh
Operating Time	Approximate 70 minutes (for 1080p)
Connections	USB 2.0 / HDMI / Wi-Fi

Polyvinyl Chloride (PVC) pipe was used as the prototype for underwater cracking pipelines in Experiment 2. Soldering iron was used to make the cracks on the PVC pipe. Fish aquarium was used as the container filled with water for illustrating the artificial underwater environment.

UNIVERSITI TEKNIKAL MALAYSIA MELAKA

3.5.2 Experiment 1: Identification of Pipeline Cracking Area for Real Underwater Environment

For Experiment 1, the goal is to identify the pipeline cracking area for the real underwater environment. The aim of the experiment is to determine the suitable filter, threshold and edge detector to be used for the proposed image processing algorithm.

To carry out this experiment, the equipment required was only the laptop with OpenCV-Python software. Firstly, the cracked underwater pipeline images from internet or oil and gas company were collected. Total of 43 images were collected since Warner encouraged considering the minimum sample size is 20 [44]. Next, the images were inputted into the image processing algorithm. The original images were converted to grayscale images. For the image filtering process, the grayscale images were filtered using median filter and Gaussian filter respectively to remove the noise in the images. Then, the filtered images were undergone two types of thresholding process which are simple threshold and Otsu threshold respectively. The edge detection processes were carried out using Sobel, Laplacian and Canny edge detector respectively. The most suitable filter, threshold and edge detector were chosen for the Experiment 2. Lastly, the area of cracks was determined using contour method.

اونيۏرسيتي تيكنيكل مليسيا ملاك
UNIVERSITI TEKNIKAL MALAYSIA MELAKA

3.5.3 Experiment 2: Identification of Pipeline Cracking Area for Artificial Underwater Environment with Different Conditions

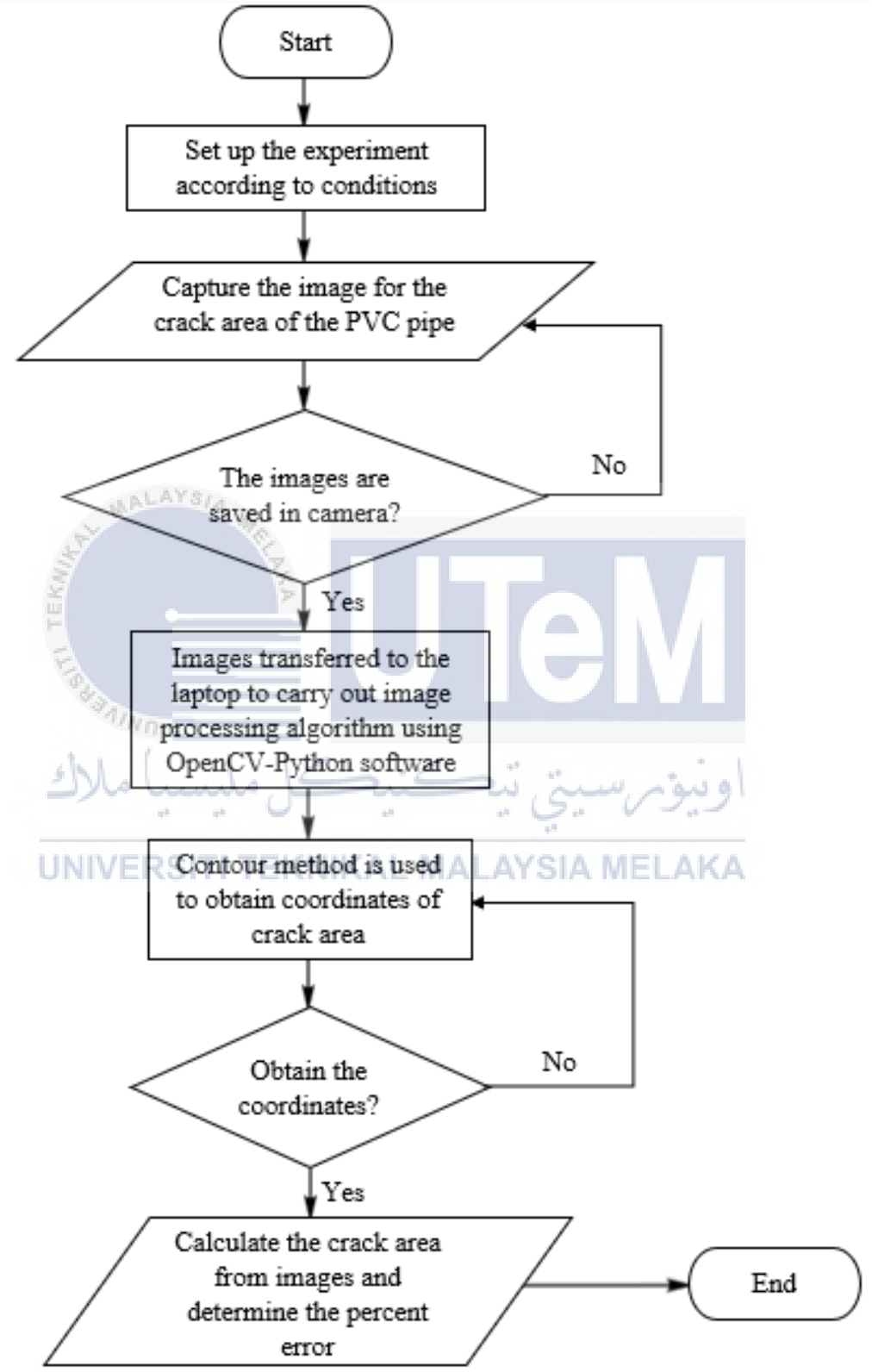

Figure 3.8 Flowchart for Experiment 2

For Experiment 2, the goal is to identify the pipeline cracking area for different conditions of artificial underwater environment. The aim of the experiments is to find the crack area of the pipeline using image processing algorithm and calculate the percent error. The flowchart of this experiments is shown in Figure 3.8

Equipment Required

- Laptop with OpenCV-Python software
- Fish Aquarium
- PVC Pipes
- SJCAM SJ4000 Wi-Fi Action Camera
- Selfie Stick
- Soldering Iron
- Smartphones with SJCAM App
- Ruler
- Sandpaper
- Marker
- Double-sided Tape
- Water (Clear and Murky)
- Scissors

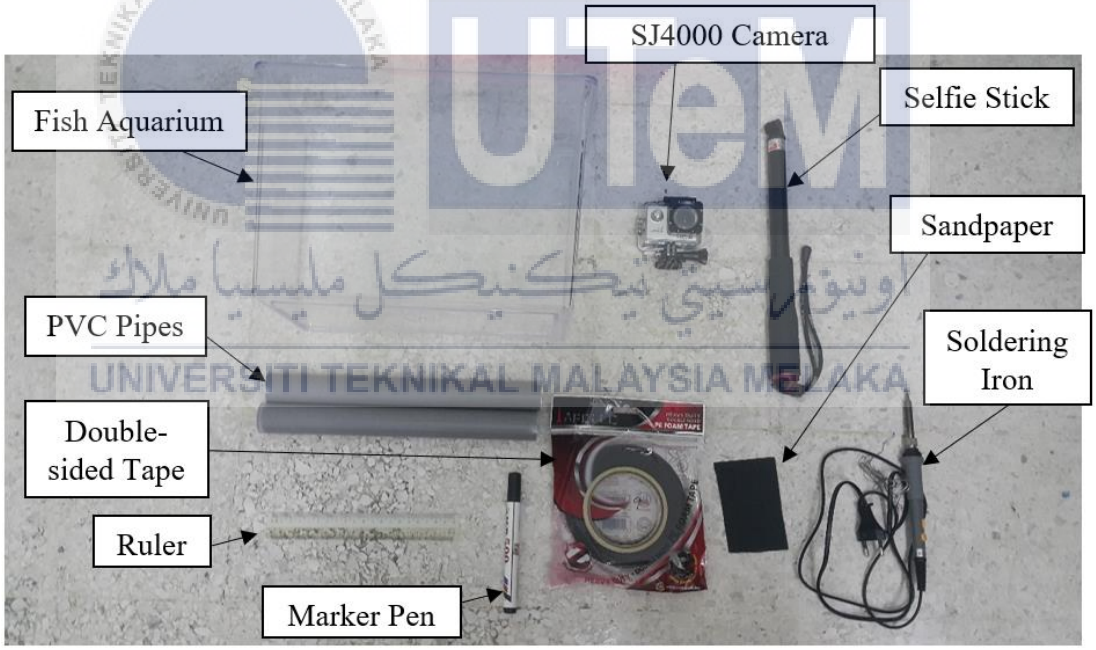

Figure 3.9 Equipment Required for Experiment 2

Procedure

Before starting this experiment, the cracks were made on the PVC pipes using soldering iron. SJCAM SJ4000 Wi-Fi Action Camera had to be connected with the SJCAM app in a smartphone via Wi-Fi. Experiment 2 was carried out by preparing a fish aquarium in a bright room. The cracked PVC pipe was set up in the aquarium using double-sided tape. SJCAM SJ4000 Wi-Fi Action Camera was inserted into the water and placed above the cracked pipe in the distance of 8cm. This is due to the camera was able to capture the cracking part perfectly in 8cm. Then, the images of the cracked PVC pipe were captured by operating the camera using the SJCAM app in the smartphone. The images were saved to the smartphone via SJCAM app and transferred to the laptop using Bluetooth. In the laptop, the image processing algorithm was carried out with the chosen filter, threshold and edge detector from Experiment 1. Later, the area of cracks was determined. The procedures were repeated with the following 4 conditions:

- low turbidity level and high lighting level - using the aquarium filled with clear water and setting the equipment in a bright room.
- low turbidity level and low lighting level - using the aquarium filled with clear water and setting the equipment in a dark room.
- high turbidity level and high lighting level - using the aquarium filled with murky water and setting the equipment in a bright room.
- high turbidity level and low lighting level - using the aquarium filled with murky water and setting the equipment in a dark room.

Finally, the percent error for each condition was calculated using Equation 3.4.

UNIVERSITI TEKNIKAL MALAYSIA MELAKA

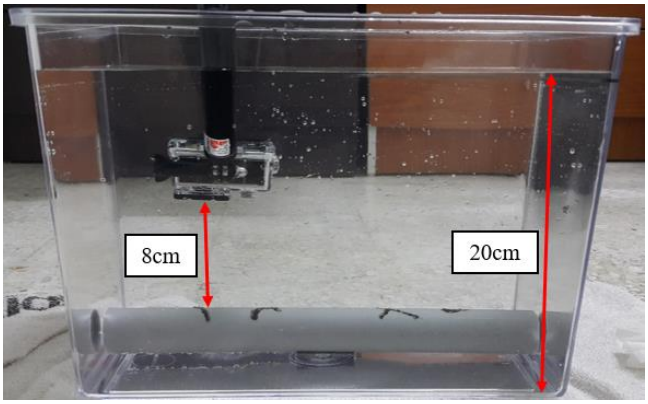

Figure 3.10 Fish Aquarium Setup

(a) Clear Water in Bright Room

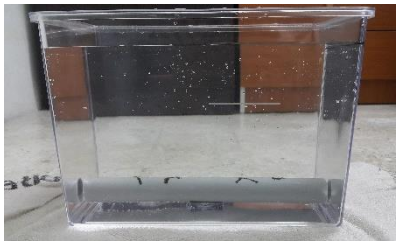

(b) Clear Water in Dark Room

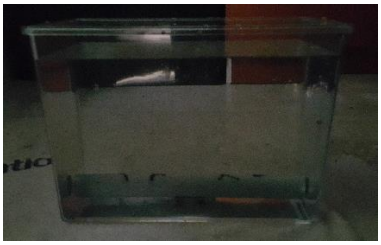

(c) Murky Water in Bright Room

(d) Murky Water in Dark Room

Figure 3.11 Four Conditions for Experiment 2

UNIVERSITI TEKNIKAL MALAYSIA MELAKA

Crack A

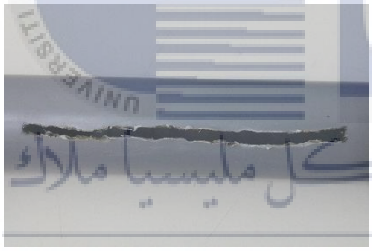

Crack B

Crack C

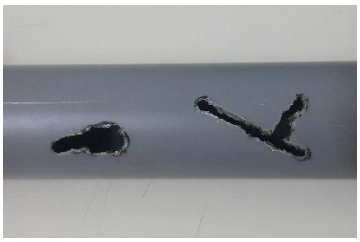

Crack D

Figure 3.12 Cracked PVC Pipes for Experiment 2

3.6 Summary

A proposed underwater pipeline cracking area identification system using image processing method was designed. Two experiments were carried out. Experiment 1 was conducted to identify the pipeline cracking area for the real underwater environment. The suitable filter, threshold and edge detector to be used for the proposed image processing algorithm is determined. Next, Experiment 2 was focused on the artificial underwater environment with different conditions. By using the chosen filter, threshold and edge detector from Experiment 1, the images of cracked PVC pipes were undergone the proposed image processing algorithm Lastly, the percent error of the proposed system in different conditions were compared and analysed in Experiment 2.

UNIVERSITI TEKNIKAL MALAYSIA MELAKA

CHAPTER 4

RESULTS AND DISCUSSIONS

This chapter illustrates the results and analysis for the proposed underwater pipeline cracking area identification system. The first part is to show the result of Experiment 1, which is to identification of pipeline cracking area for real underwater environment. The second part is to analysis and calculate the accuracy of the proposed underwater pipeline cracking area identification system from the results of Experiment 2.

4.1 Results and Analysis

4.1.1 Experiment 1: Identification of Pipeline Cracking Area for Real Underwater Environment

For Experiment 1, the simulation results for the image processing algorithm are shown. The simulation was performed using OpenCV-Python and the coding is shown in APPENDIX B. For obtaining the results, 43 real underwater pipeline images were used to undergo the image processing algorithm. 5 images from the 43 real underwater pipeline images were chosen as the samples for the comparison and analysis in this section. The analysis for the rest of the images are shown in APPENDIX C. Figure 4.1 to Figure 4.5 shows the original and grayscale images of the 5 sample real underwater pipeline images.

UNIVERSITI TEKNIKAL MALAYSIA MELAKA

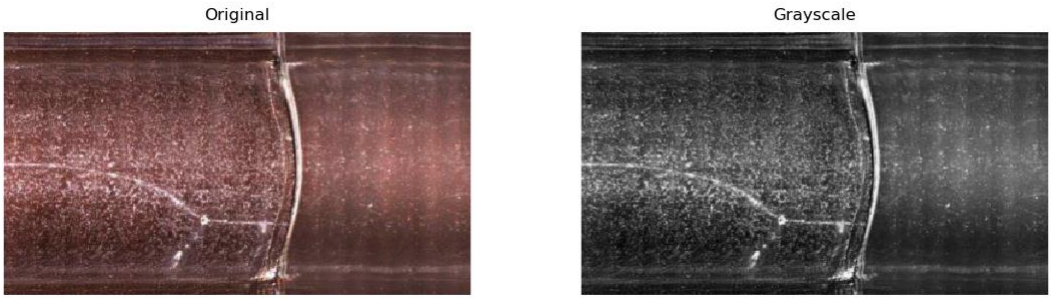

Figure 4.1 Original Image [33] and Grayscale Image for Crack 1

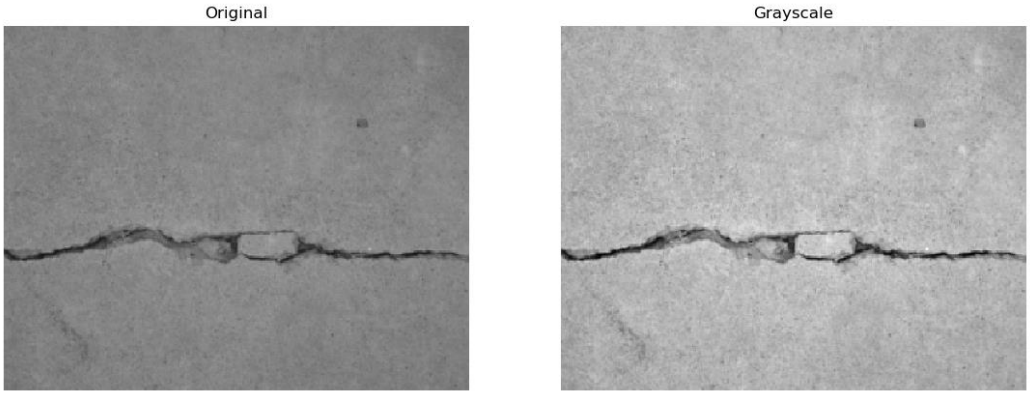

Figure 4.2 Original Image [34] and Grayscale Image for Crack 7

Figure 4.3 Original Image [36] and Grayscale Image for Crack 9

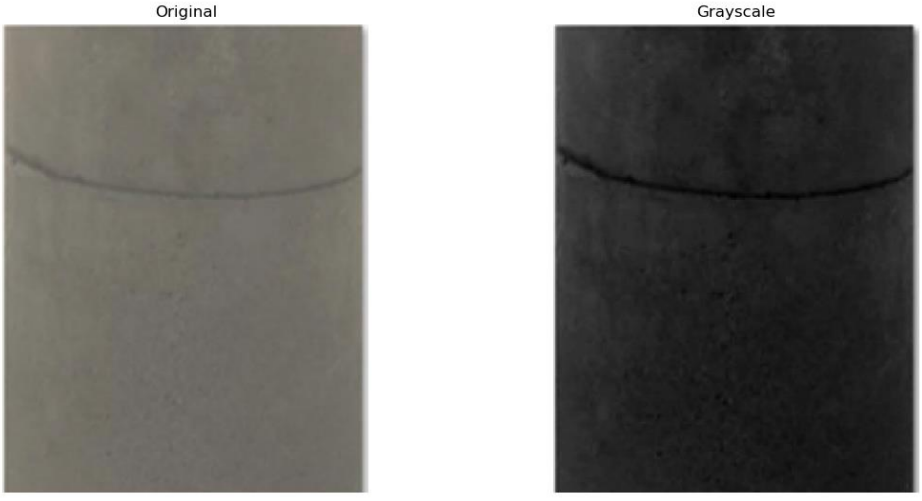

Figure 4.4 Original Image [20] and Grayscale Image for Crack 20

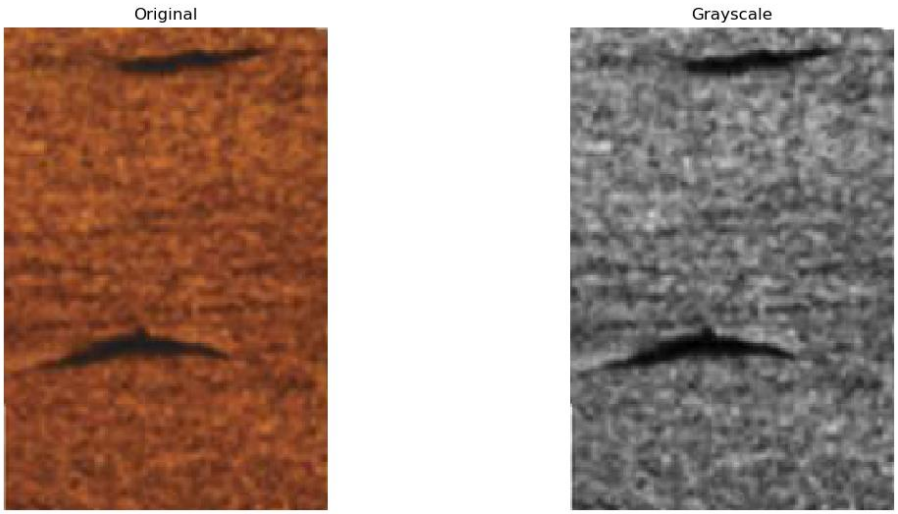

Figure 4.5 Original Image [49] and Grayscale Image for Crack 37

The grayscale images were filtered to remove the noises of the images. Two image filters, which are median filter and Gaussian filter, were used and compared. Results for image filtering process is shown in Figure 4.6 to Figure 4.10. From these figures, Gaussian filter is a better method for image filtering process. Median filter is efficient for removing salt and pepper noise. However, the noises for real underwater environment are mostly Gaussian noise. Gaussian filter is better for filtering the images to blur the edge of object in the images. Therefore, Gaussian filter was selected for the proposed image processing algorithm.

UNIVERSITI TEKNIKAL MALAYSIA MELAKA

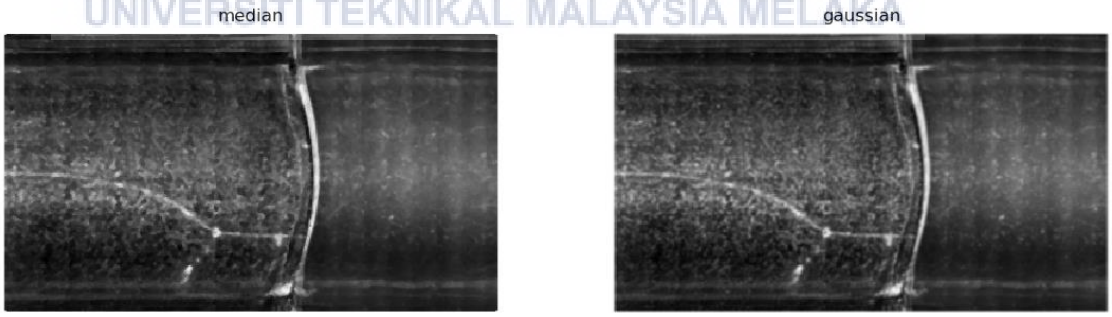

Figure 4.6 Image filtered using median and Gaussian filter for Crack 1

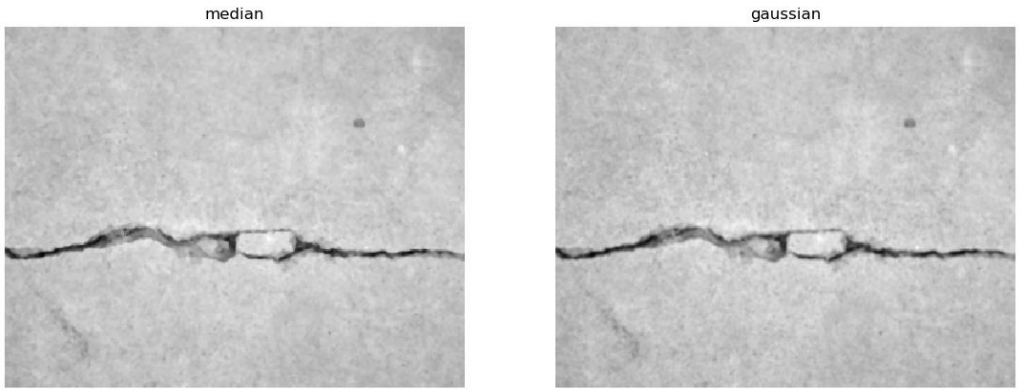

Figure 4.7 Image filtered using median and Gaussian filter for Crack 7

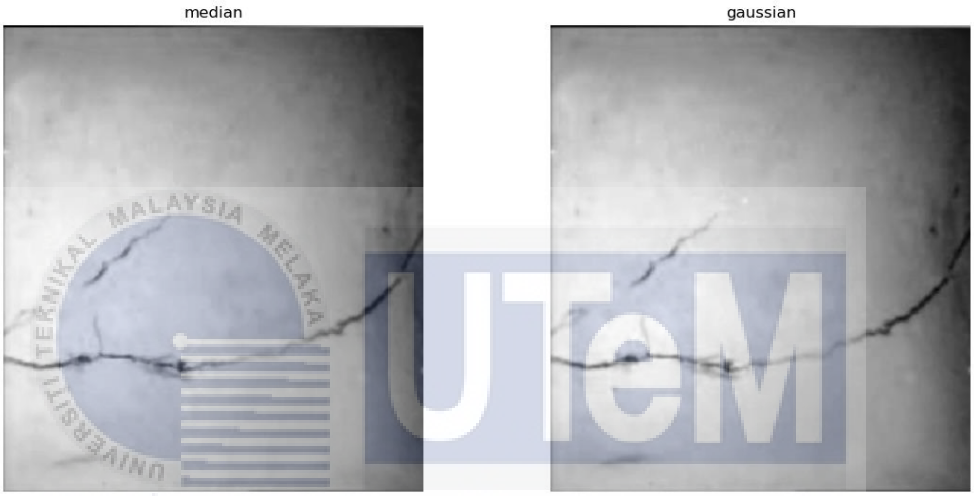

Figure 4.8 Image filtered using median and Gaussian filter for Crack 9

Figure 4.9 Image filtered using median and Gaussian filter for Crack 20

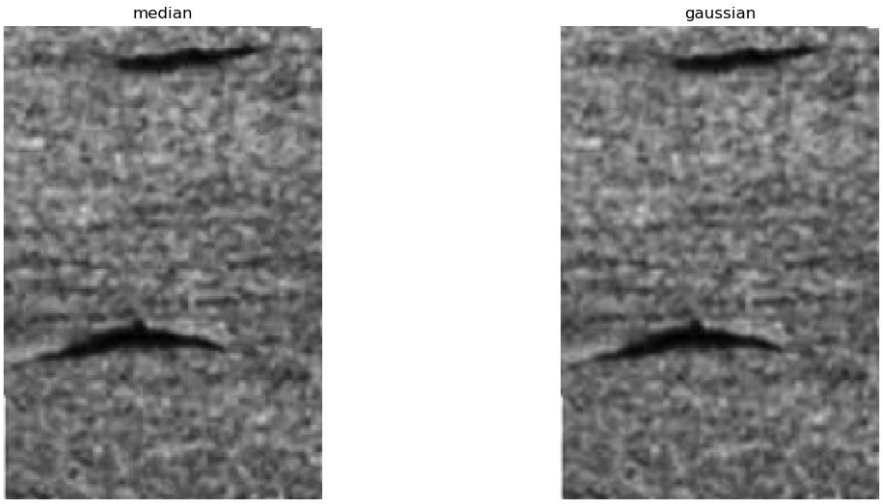

Figure 4.10 Image filtered using median and Gaussian filter for Crack 37

The Gaussian filtered images were then used to undergo image thresholding process. The results for the image thresholding are shown in Figure 4.10 to 4.15. For simple thresholding, the threshold value for simple thresholding was selected manually while for the Otsu thresholding, the threshold value was chosen arbitrary according to the images. From Figure 4.13, 4.14 and 4.15, the cracking part could be recognized for simple thresholding while the resulted image of Otsu thresholding does not show the perfect output since the cracking part could not be clearly shown. Therefore, simple threshold was used to apply for the image thresholding process.

UNIVERSITI TEKNIKAL MALAYSIA MELAKA

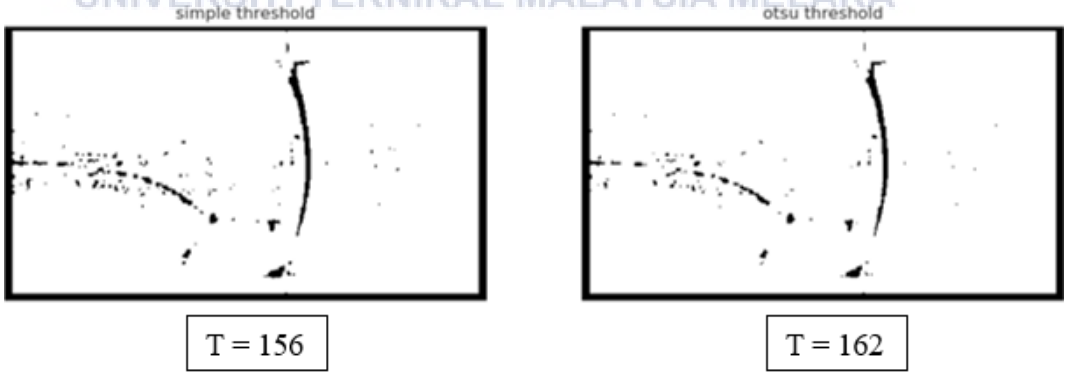

Figure 4.11 Image resulted using simple and Otsu thresholding for Crack 1

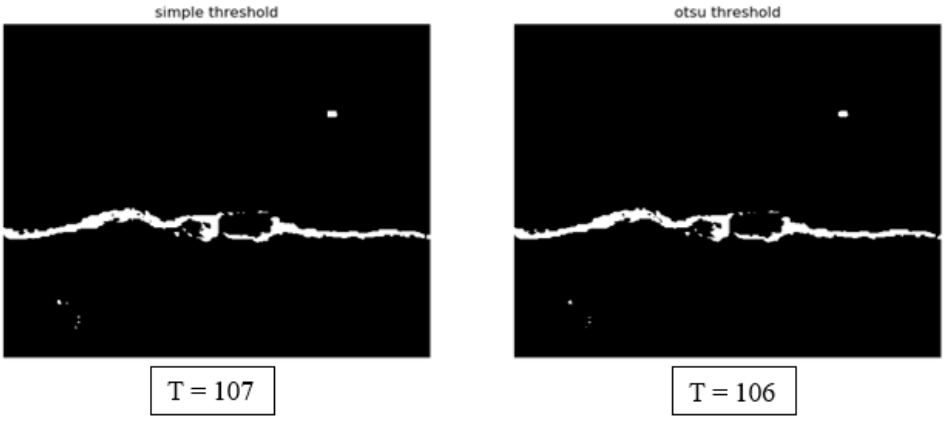

Figure 4.12 Image resulted using simple and Otsu thresholding for Crack 7

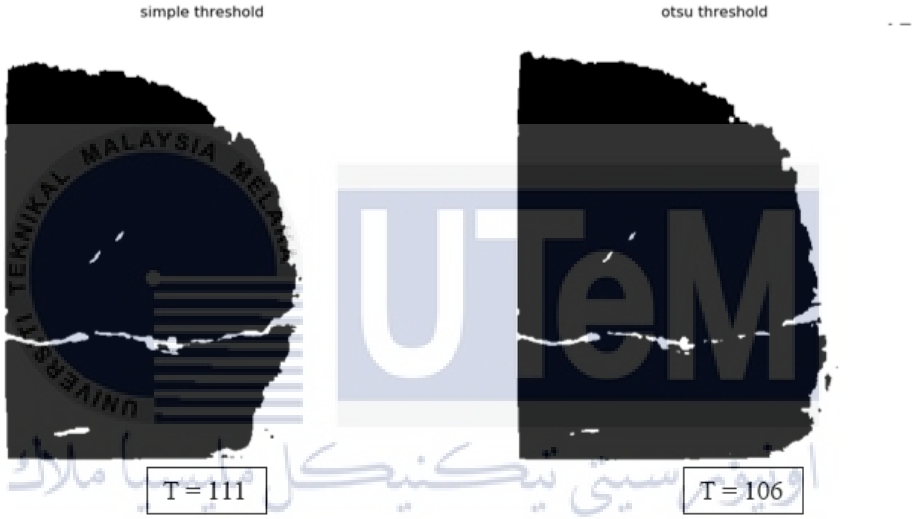

Figure 4.13 Image resulted using simple and Otsu thresholding for Crack 9

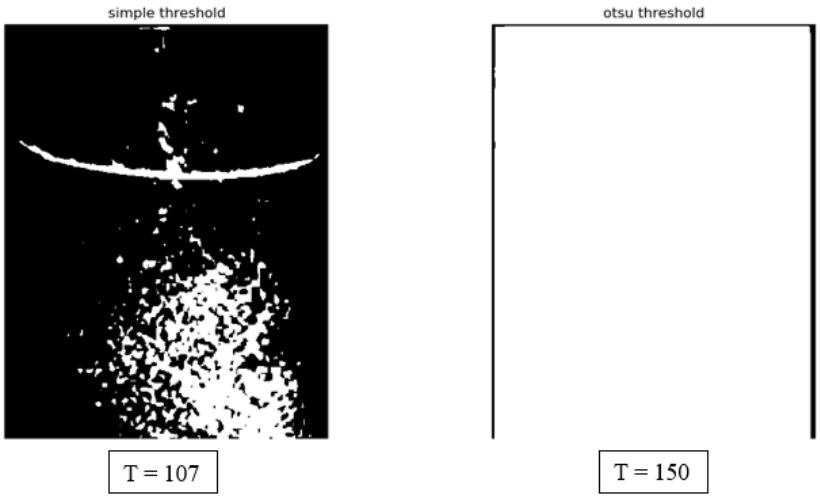

Figure 4.14 Image resulted using simple and Otsu thresholding for Crack 20

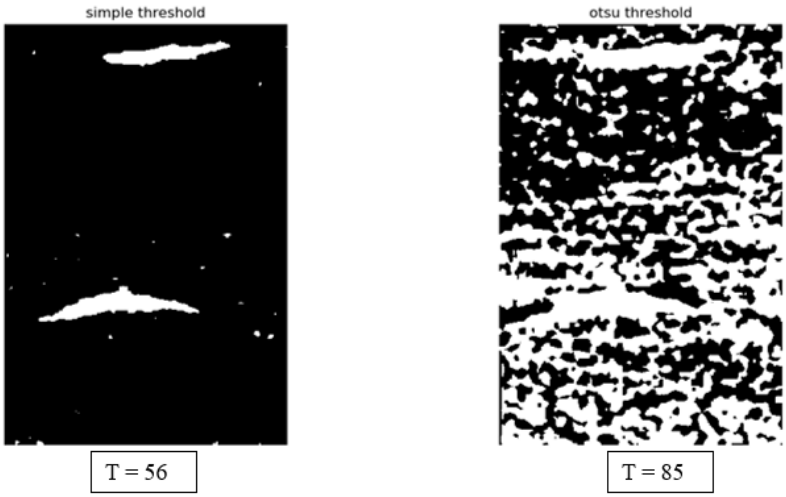

Figure 4.15 Image resulted using simple and Otsu thresholding for Crack 37

The resulted images from simple thresholding were undergone Sobel and Canny edge detection. The results of both edge detections were shown in Figure 4.16 to 4.20. Sobel x detects the edges of object in the image in vertical direction only while Sobel y detects the edges in horizontal direction only. Sobel x and y cannot detect the edges accurately. From the results obtained from Experiment 1, Canny edge detector had detected the edges more accurate compared to Sobel edge detector. Therefore, Canny edge detection is selected for the proposed underwater pipeline cracking area identification system.

UNIVERSITI TEKNIKAL MALAYSIA MELAKA

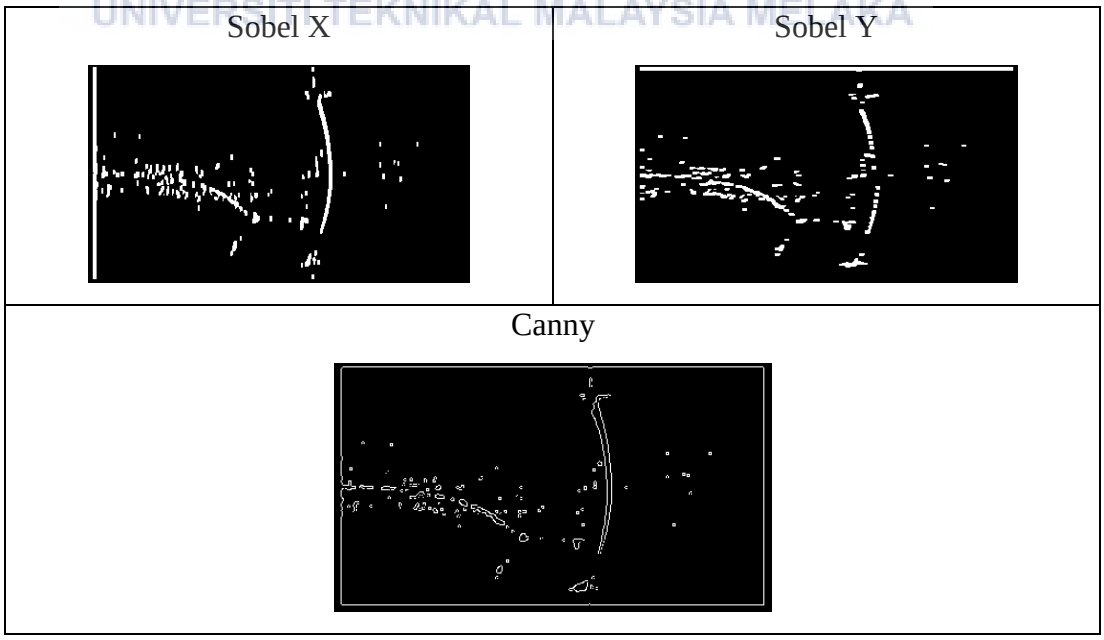

Figure 4.16 Image resulted using different edge detector for Crack 1

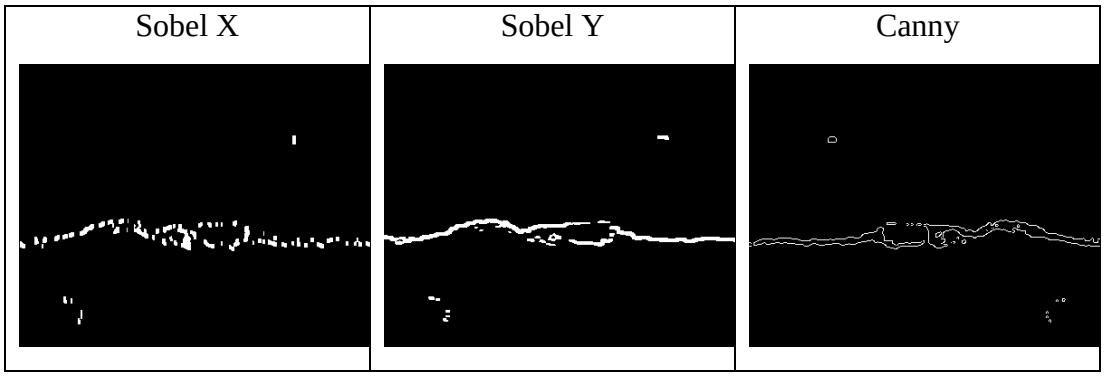

Figure 4.17 Image resulted using different edge detector for Crack 7

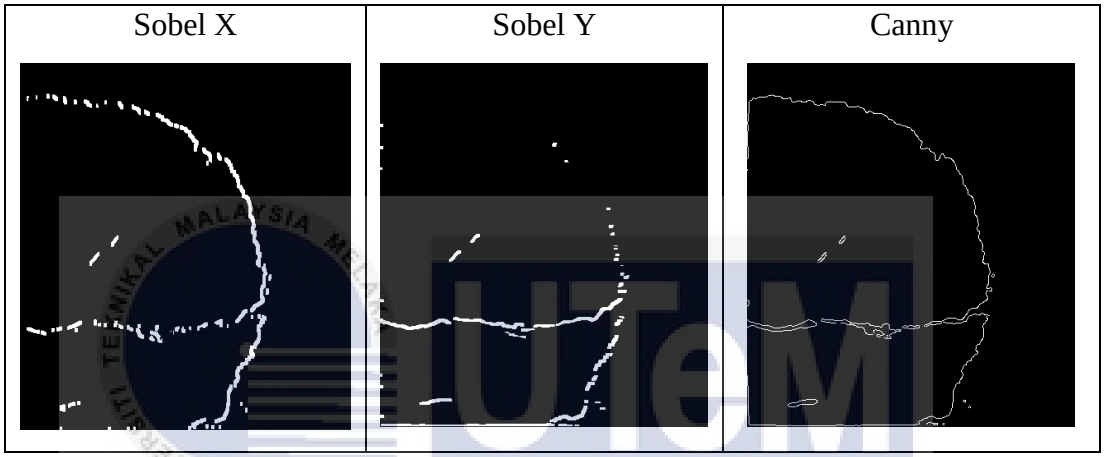

Figure 4.18 Image resulted using different edge detector for Crack 9

UNIVERSITI TEKNIKAL MALAYSIA MELAKA

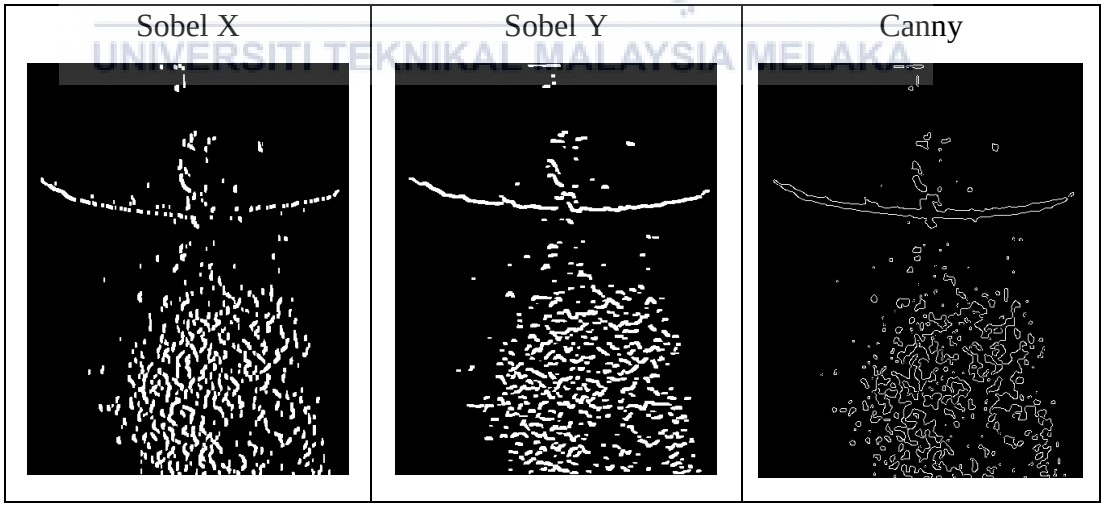

Figure 4.19 Image resulted using different edge detector for Crack 20

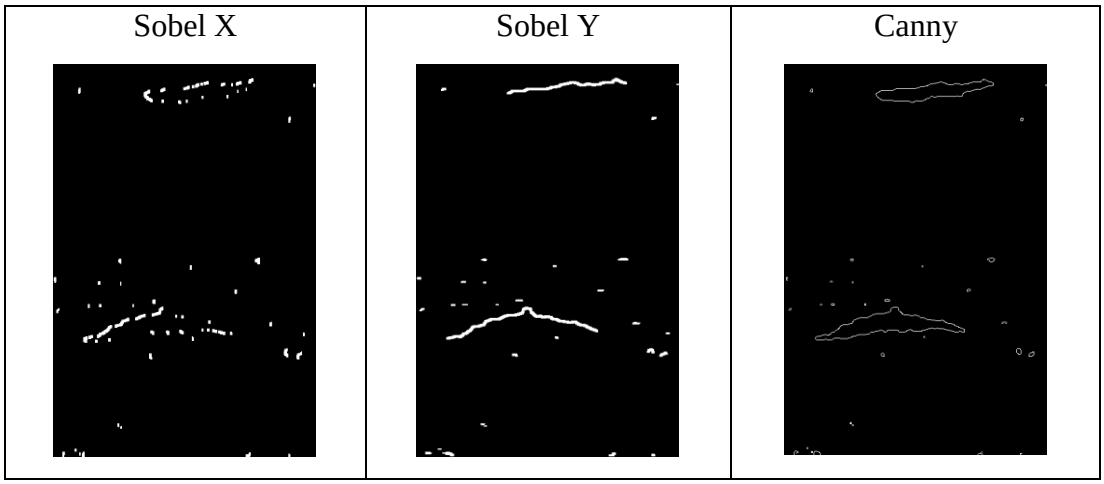

Figure 4.20 Image resulted using different edge detector for Crack 37

After image processing algorithm, contour method was used to find the pipeline's crack area. Figure 4.21 to 4.25 and Table 4.1 show the results for the crack area determination. The boundary rectangle (in green colour) was drawn on the crack part. However, the rectangle might not enclose the whole crack due to the simple threshold value set and the lighting condition when the images are captured. The starting point (red x mark) and ending point (blue x mark) were determined for the need of fixing the crack part in the future. The number of rectangle box formed for a crack pipeline image was displayed when running the Python coding. The crack part's rectangle box was selected manually.

UNIVERSITI TEKNIKAL MALAYSIA MELAKA

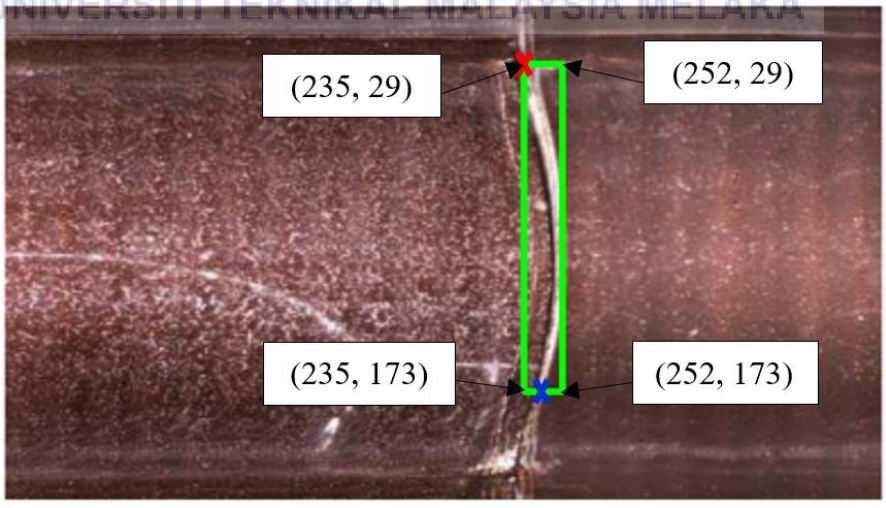

Figure 4.21 Area for Crack 1 detected with their coordinates

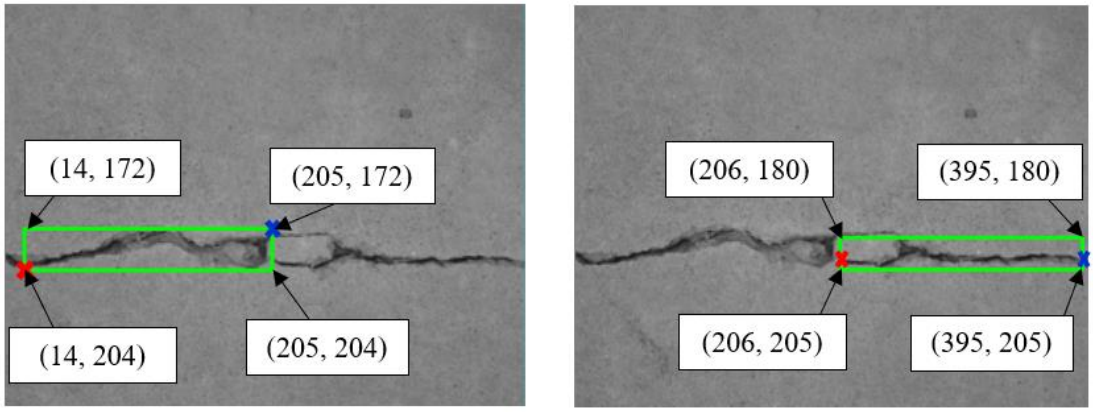

Figure 4.22 Area for Crack 7 detected with their coordinates

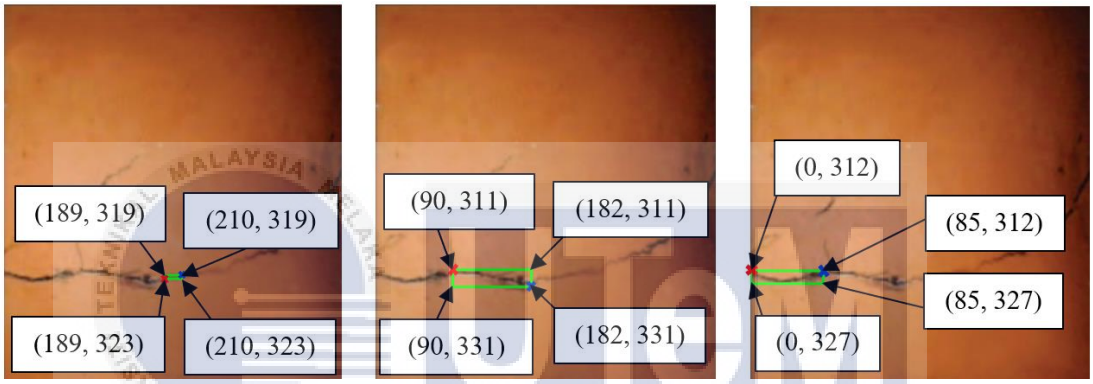

Figure 4.23 Area for Crack 9 detected with their coordinates

UNIVERSITI TEKNIKAL MALAYSIA MELAKA

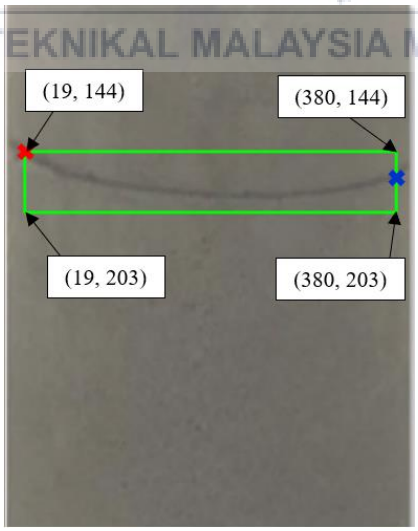

Figure 4.24 Area for Crack 20 detected with their coordinates

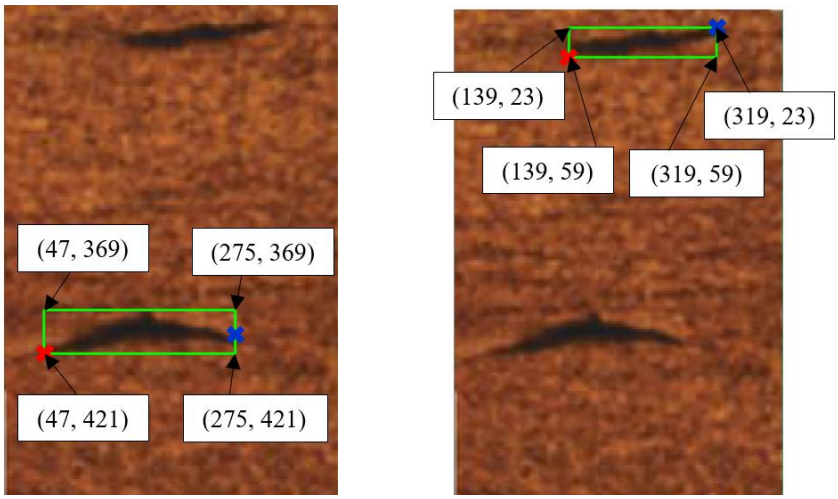

Figure 4.25 Area for Crack 37 detected with their coordinates

Table 4.1 Crack Area Determination Results for Experiment 1

Crack	Length, l (mm)	Width, w (mm)	Area, A (mm^2)	Starting Point	Ending Point
1	17	144	2448	(235, 29)	(260, 173)
7	191	32	6112	(14, 204)	(205, 172)
	189	25	4725	(206, 197)	(395, 197)
9	21	4	84	(189, 323)	(210, 319)
	92	20	1840	(90, 311)	(182, 331)
	85	15	1275	(0, 312)	(85, 312)
20	361	59	21299	(19, 144)	(380, 173)
37	228	52	11856	(47, 421)	(275, 395)
	180	36	6480	(139, 59)	(319, 23)

UNIVERSITI TEKNIKAL MALAYSIA MELAKA

4.1.2 Experiment 2: Identification of Pipeline Cracking Area for Artificial Underwater Environment with Different Conditions

4.1.2.1 Low Turbidity Level and High Lighting Level

Condition 1 for Experiment 2 is low turbidity level and low lighting level which means that this part of the experiment was carried out by using the aquarium filled with clear water and setting the equipment in a bright room. The original image captured by the camera was converted to grayscale image and the grayscale image was then filtered using Gaussian filter. Next, simple thresholding was applied to the filtered image with the threshold value that being selected manually. The edge of the crack for the threshold image was detected using Canny edge detector before determining the crack area. The results of proposed image processing system for Crack A, B, C and D in Condition 1 were shown in Figure 4.26, 4.28, 4.30 and 4.32 respectively. After completing the image processing algorithm, contour method was used to draw a rectangle box around the crack part and crack areas were calculated using Equation 3.1, 3.2 and 3.3. The crack area determination results for this condition were shown in Table 4.2. These results are used as reference to determine the percent error of the proposed system for the following conditions.

UNIVERSITI TEKNIKAL MALAYSIA MELAKA

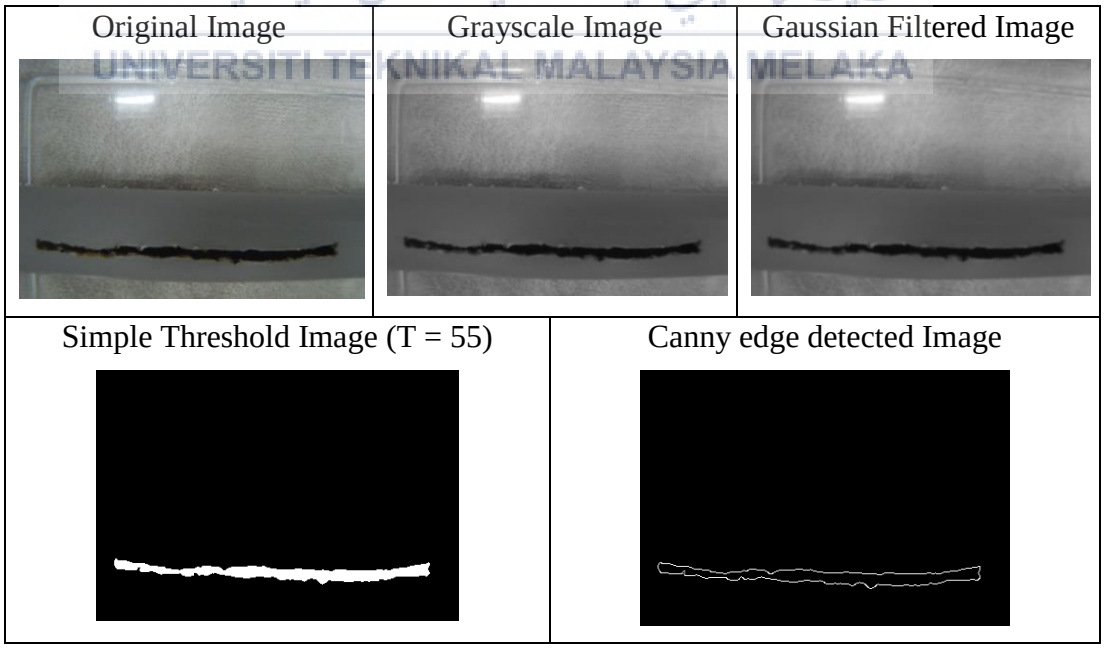

Figure 4.26 Result of Proposed Image Processing Algorithm for Crack A1

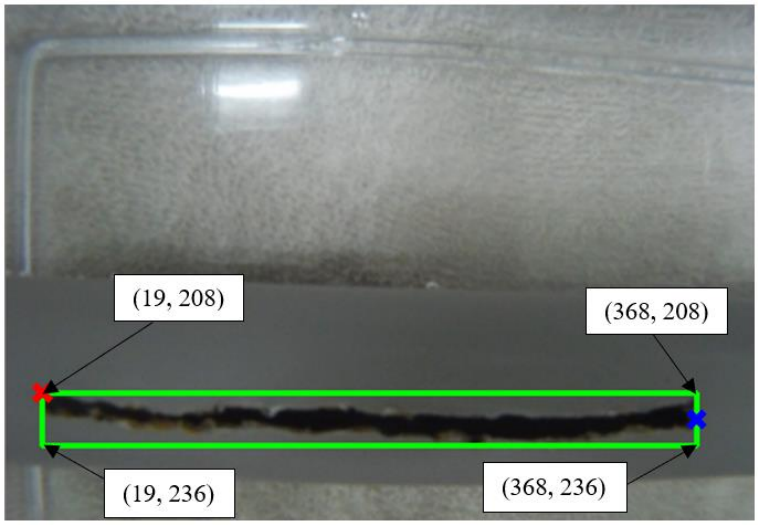

Figure 4.27 Area for Crack A1 detected with their coordinates

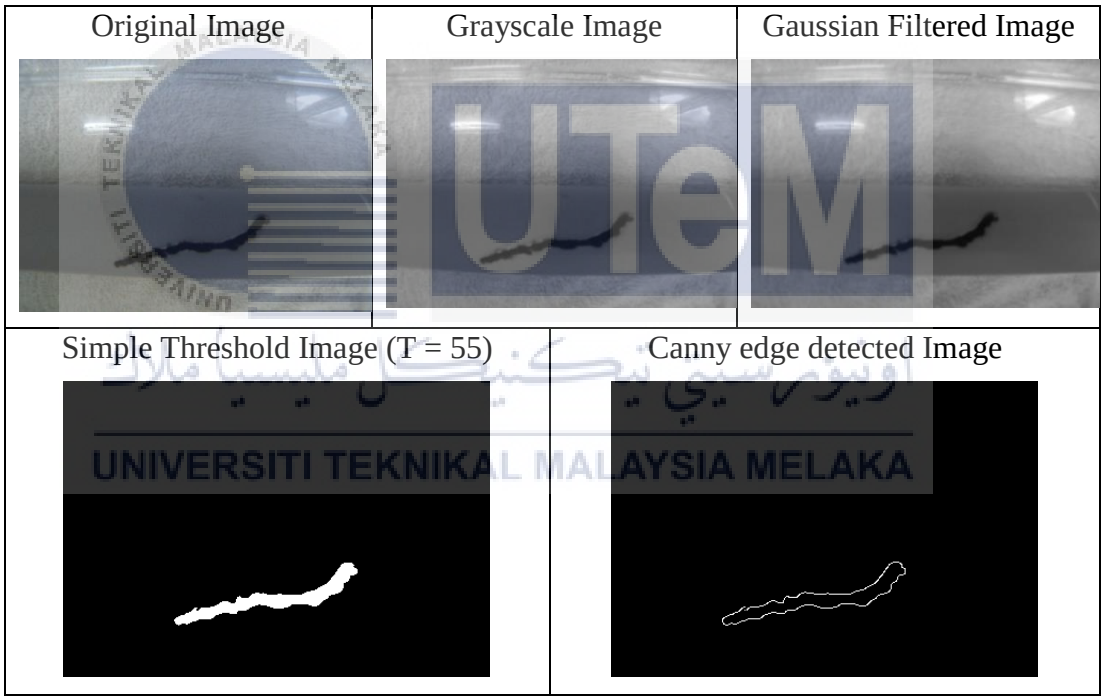

Figure 4.28 Result of Proposed Image Processing Algorithm for Crack B1

UNIVERSITI TEKNIKAL MALAYSIA MELAKA

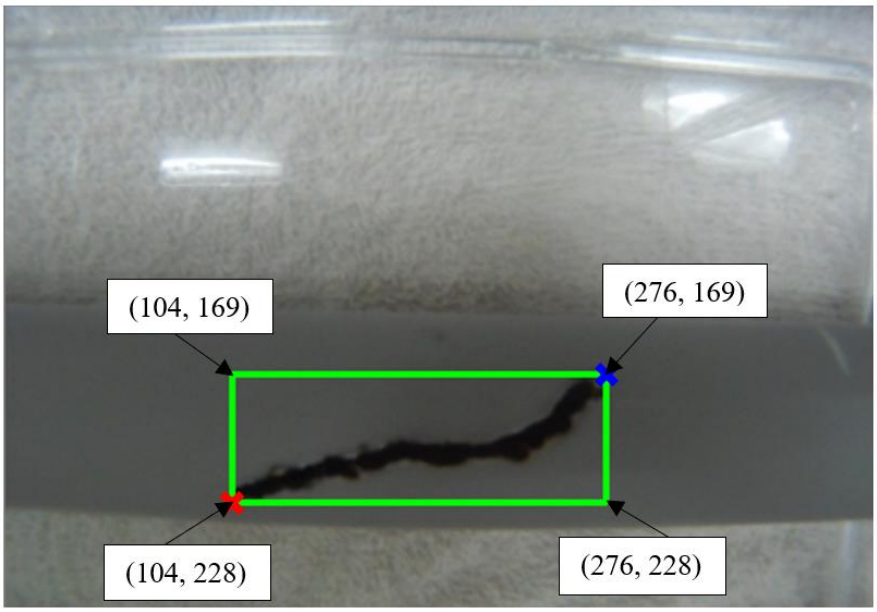

Figure 4.29 Area for Crack B1 detected with their coordinates

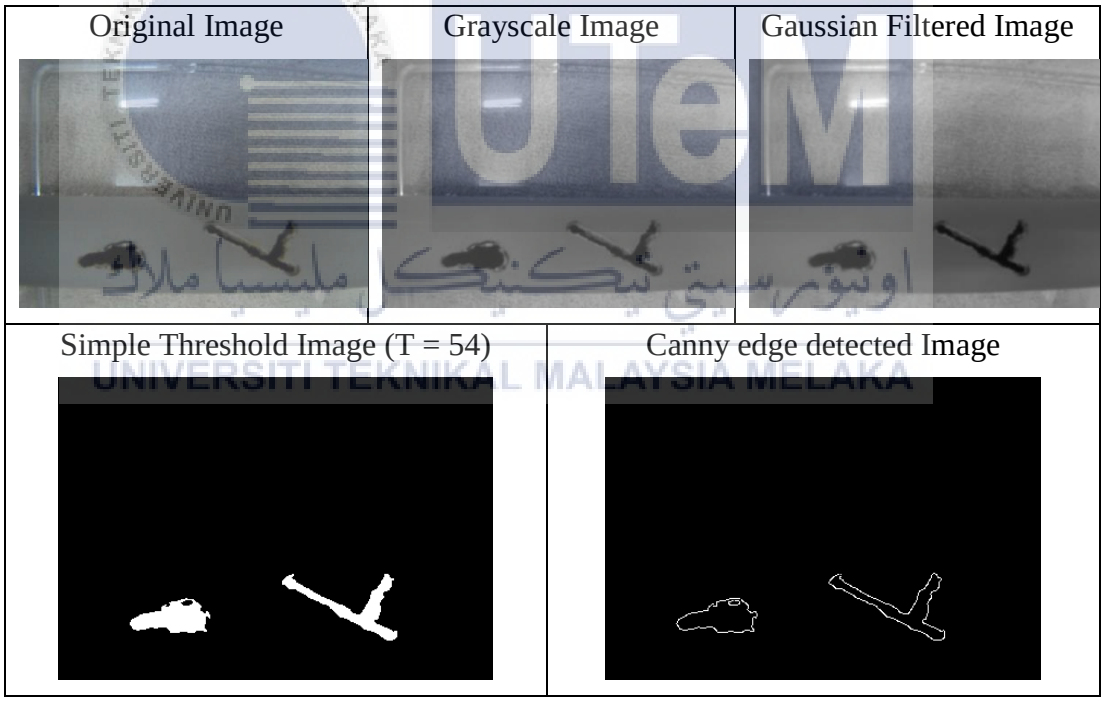

Figure 4.30 Result of Proposed Image Processing Algorithm for Crack C1

UNIVERSITI TEKNIKAL MALAYSIA MELAKA

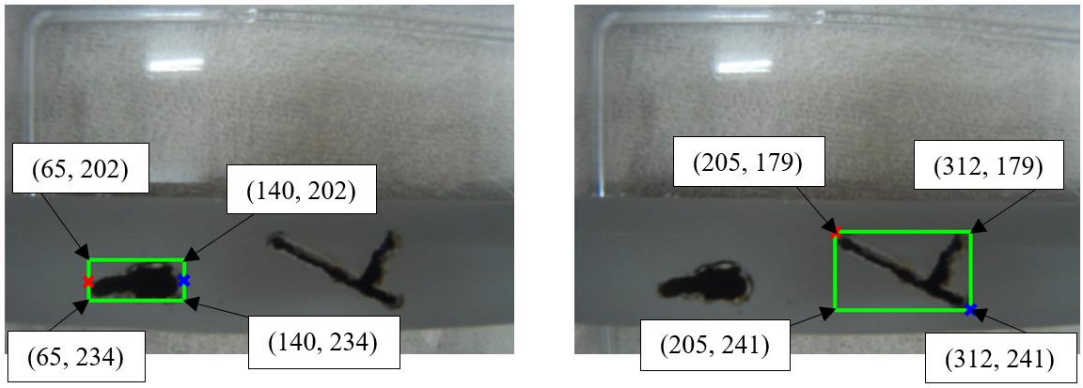

Figure 4.31 Area for Crack C1 detected with their coordinates

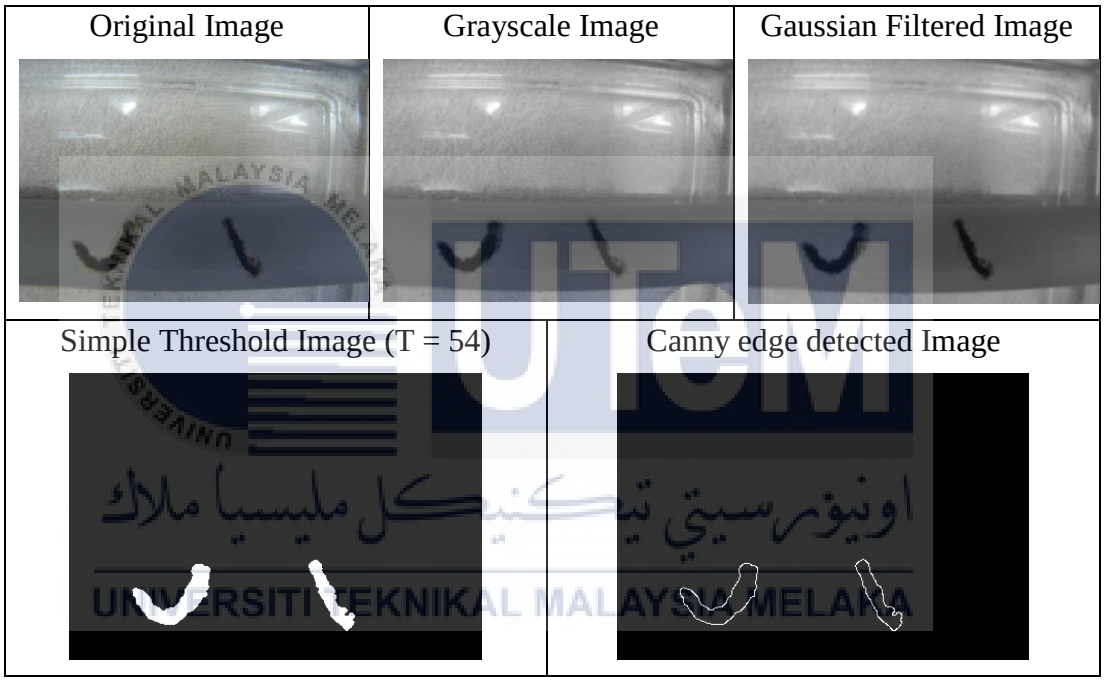

Figure 4.32 Result of Proposed Image Processing Algorithm for Crack D1

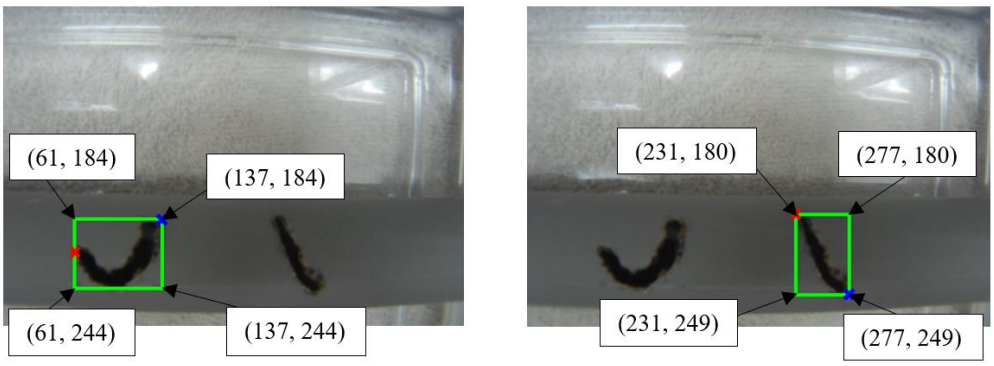

Figure 4.33 Area for Crack D1 detected with their coordinates

Table 4.2 Crack Area Determination Results for Experiment 2 Condition 1

Crack	**Length, l (mm)**	**Width, w (mm)**	**Area, A (mm^2)**	**Starting Point**	**Ending Point**
A1	349	31	10819	(19, 208)	(368, 208)
B1	172	59	10148	(104, 228)	(276, 169)
C1	75	32	2400	(65, 218)	(140, 218)
	107	62	6634	(205, 179)	(312, 241)
D1	76	60	4560	(61, 214)	(137, 184)
	46	69	3174	(231, 180)	(277, 249)

4.1.2.2 Low Turbidity Level and Low Lighting Level

This part of the experiment was carried out by using the aquarium filled with clear water and setting the equipment in a dark room (Condition 2). Similar to Condition 1, the images captured by SJCAM SJ4000 Wi-Fi Action Camera were undergone image processing algorithm. The results of proposed image processing system for Crack A, B, C and D in this condition were shown in Figure 4.34, 4.36, 4.38 and 4.40 respectively. Lastly, the contour method was used to determine the crack area. The contour method results for Crack A, B, C and D in this condition were manifested in Figure 4.35, 4.37, 4.39 and 4.41 respectively. The crack area determination results for Condition 2 were shown in Table 4.3. The results of the percent error of the proposed system for this condition area shown in Table 4.4.

UNIVERSITI TEKNIKAL MALAYSIA MELAKA

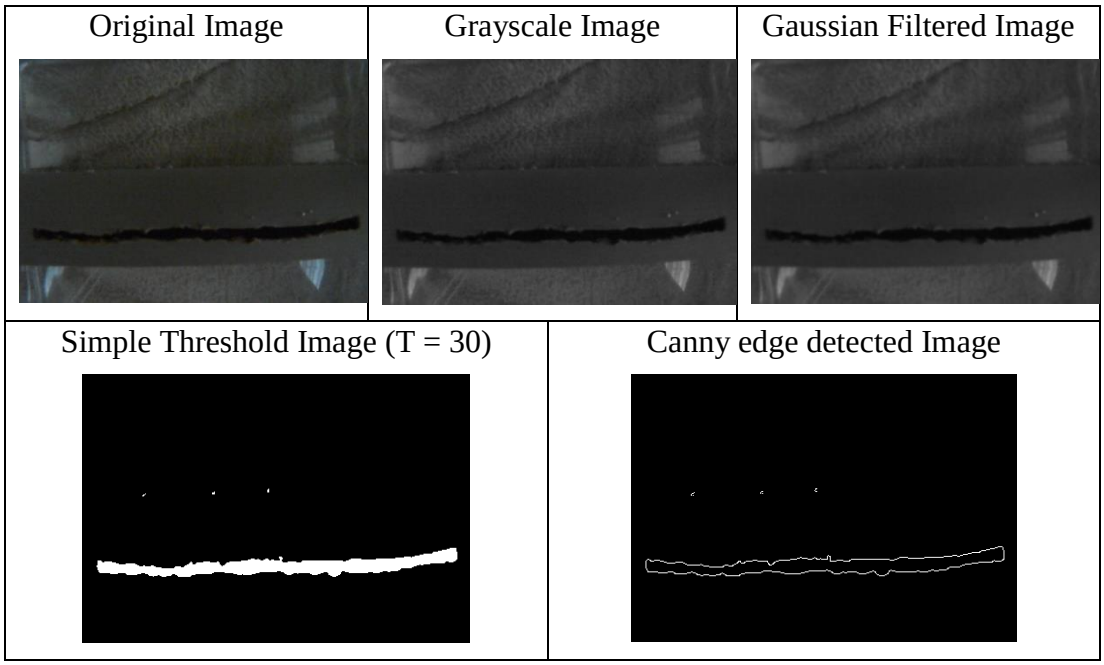

Figure 4.34 Result of Proposed Image Processing Algorithm for Crack A2

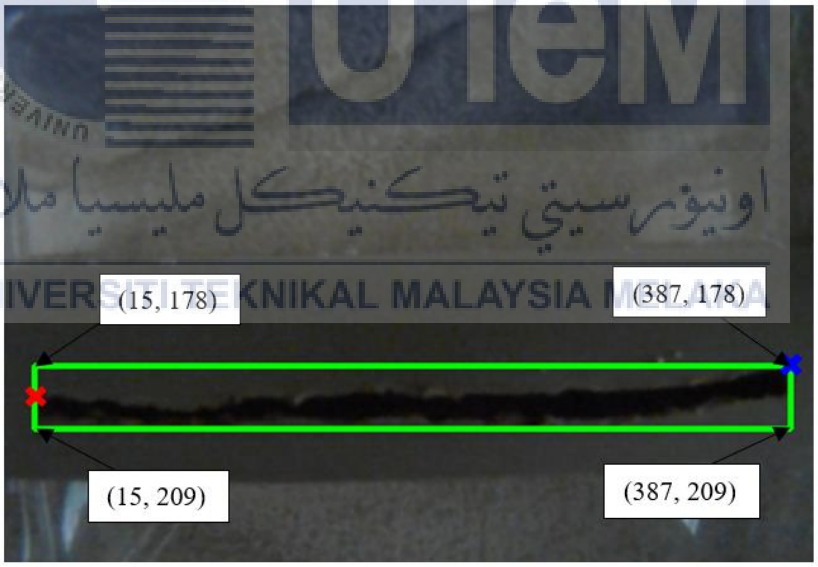

Figure 4.35 Area for Crack A2 detected with their coordinates

UNIVERSITI TEKNIKAL MALAYSIA MELAKA

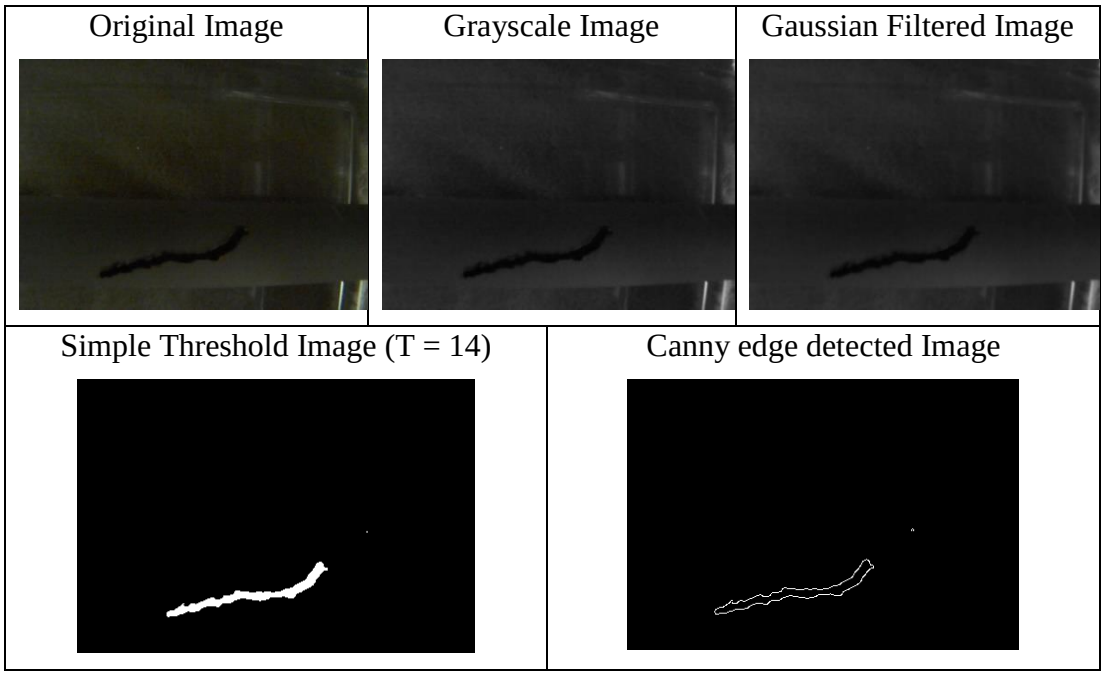

Figure 4.36 Result of Proposed Image Processing Algorithm for Crack B2

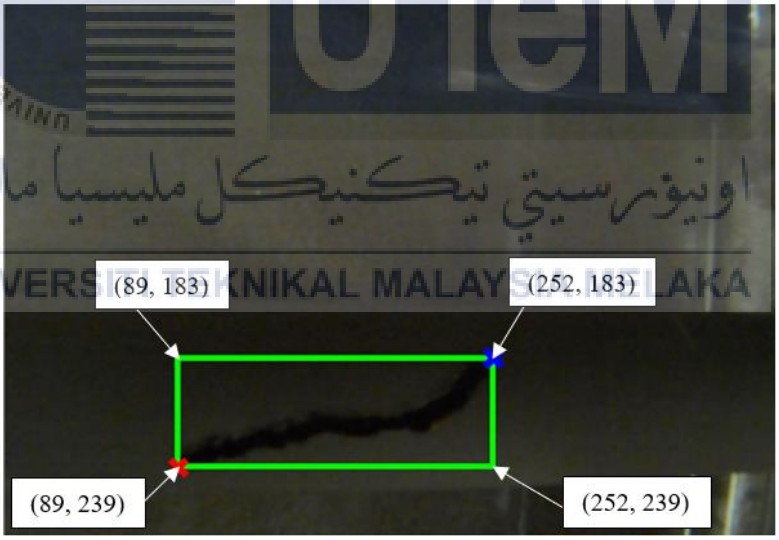

Figure 4.37 Area for Crack B2 detected with their coordinates

UNIVERSITI TEKNIKAL MALAYSIA MELAKA

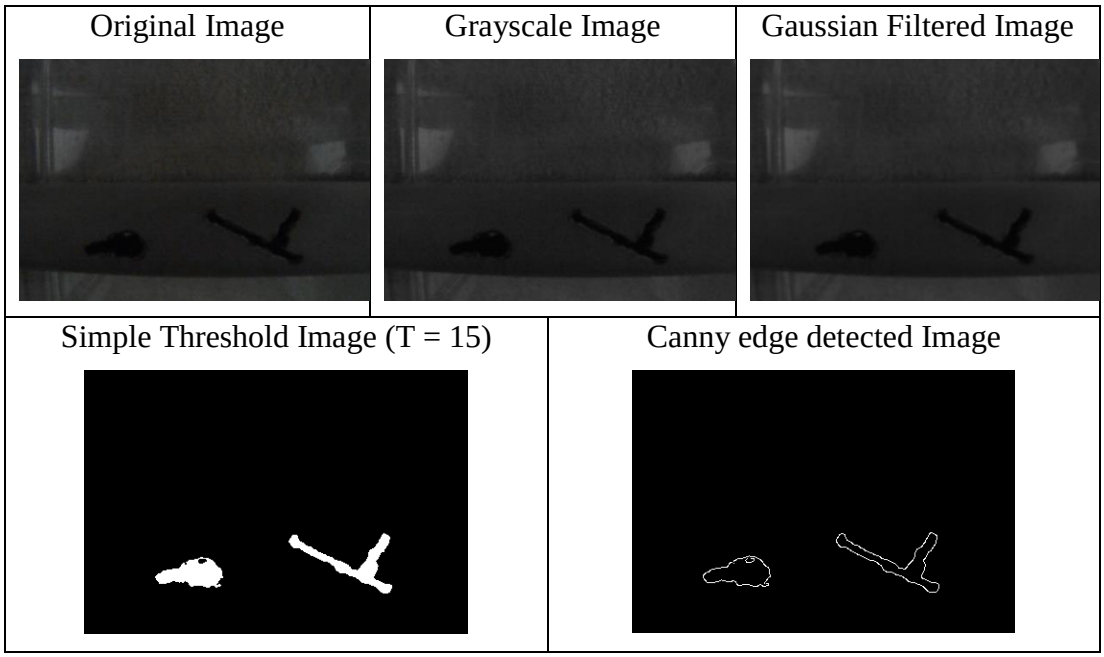

Figure 4.38 Result of Proposed Image Processing Algorithm for Crack C2

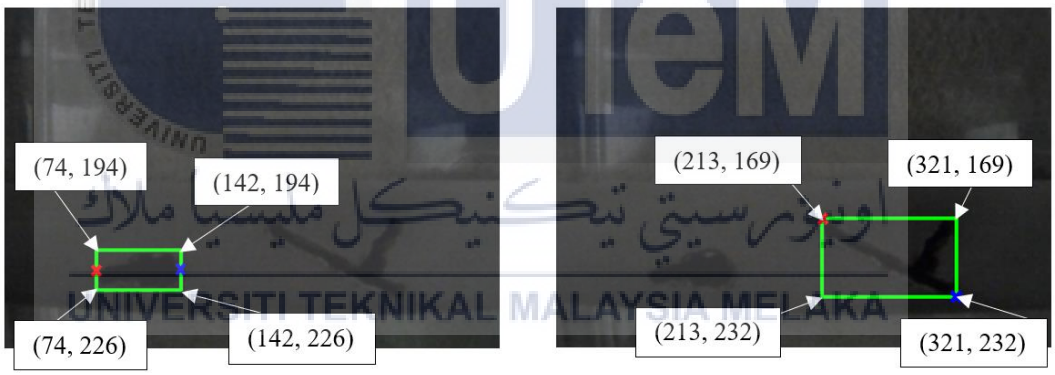

Figure 4.39 Area for Crack C2 detected with their coordinates

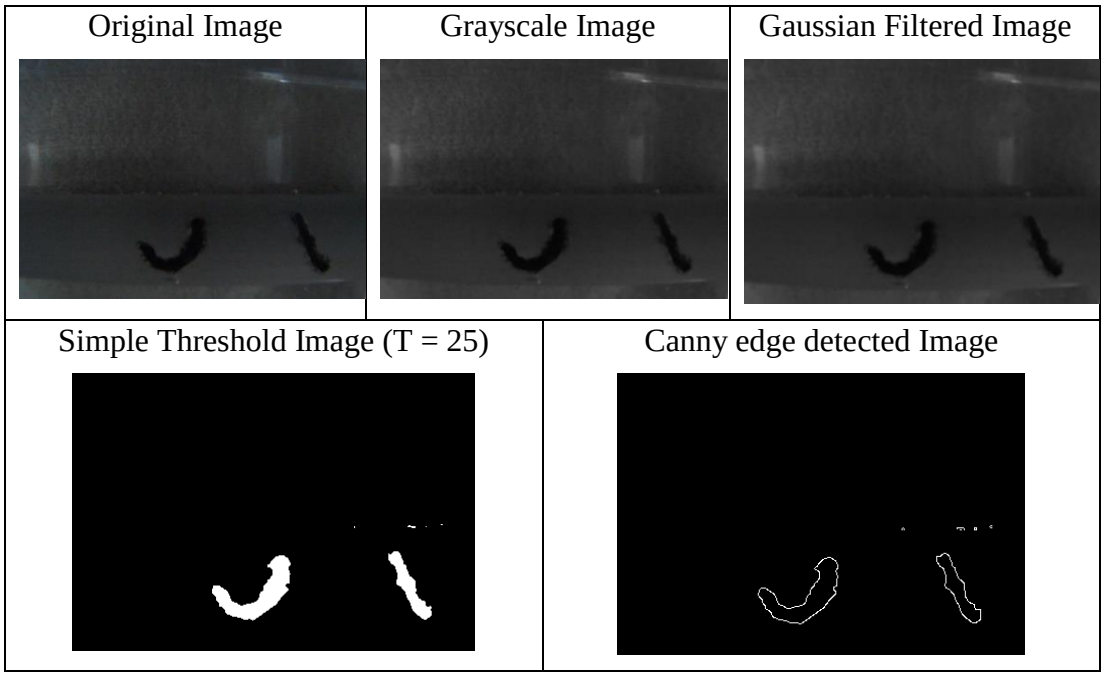

Figure 4.40 Result of Proposed Image Processing Algorithm for Crack D2

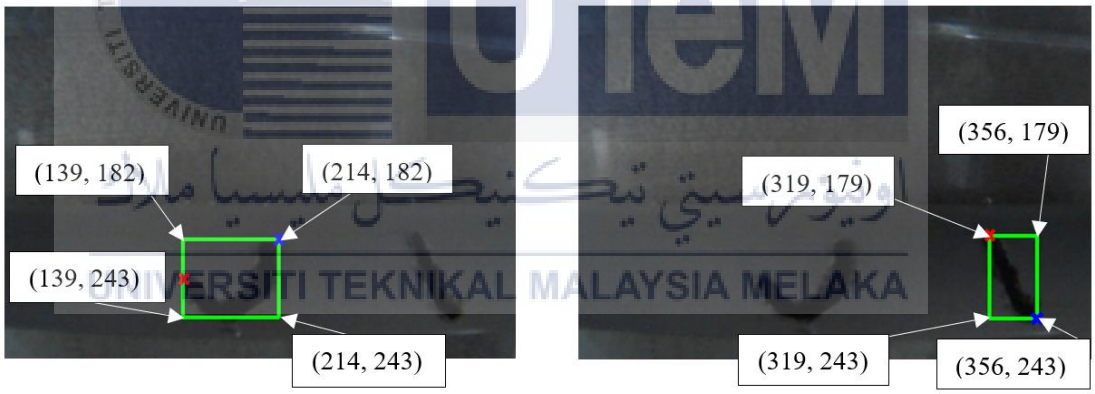

Figure 4.41 Area for Crack D2 detected with their coordinates

UNIVERSITI TEKNIKAL MALAYSIA MELAKA

Table 4.3 Crack Area Determination Results for Experiment 2 Condition 2

Crack	Length, l (mm)	Width, w (mm)	Area, A (mm^2)	Starting Point	Ending Point
A2	372	31	11532	(15, 193)	(387, 178)
B2	163	56	9128	(89, 239)	(252, 183)
C2	68	32	2176	(74, 210)	(142, 210)
	108	63	6804	(213, 169)	(321, 232)
D2	75	61	4575	(139, 212)	(214, 182)
	37	64	2368	(319, 179)	(356, 243)

Table 4.4 Percent Error Results for Experiment 2 Condition 2

Crack	Reference Area (mm^2)	Experimental Area (mm^2)	Percent Error (%)
A	10819	11532	6.59
B	10148	9128	10.05
C	2400	2176	9.33
	6634	6804	2.56
D	4560	4575	0.33
	3174	2368	25.39

From Table 4.4, the percent error of Condition 2 for all crack images are mostly less than 11%, except for the second crack in Crack D.

UNIVERSITI TEKNIKAL MALAYSIA MELAKA

4.1.2.3 High Turbidity Level and High Lighting Level

Condition 3 for Experiment 2 is carried out by using the aquarium filled with murky water and setting the equipment in a bright room. Similar to the previous conditions, the image processing algorithm was applied to the images captured by the camera in this condition and followed by crack area determination. The image processing results for Crack A, B, C and D in this condition were shown in Figure 4.42, 4.44, 4.46 and 4.48 respectively. The results of contour method for Crack A, B, C and D in this condition were displayed in Figure 4.43, 4.45, 4.47 and 4.49 respectively. The crack area determination results for this condition were shown in Table 4.5. The percent error results of each crack for the proposed system in Condition 3 are manifested in Table 4.6.

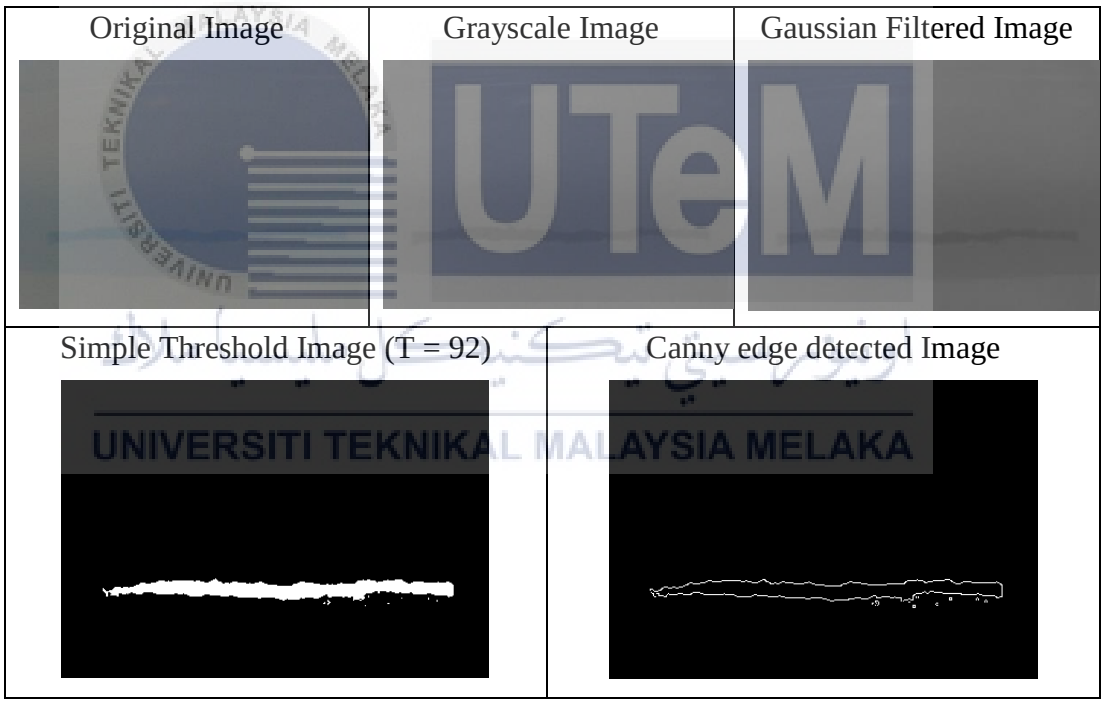

Figure 4.42 Result of Proposed Image Processing Algorithm for Crack A3

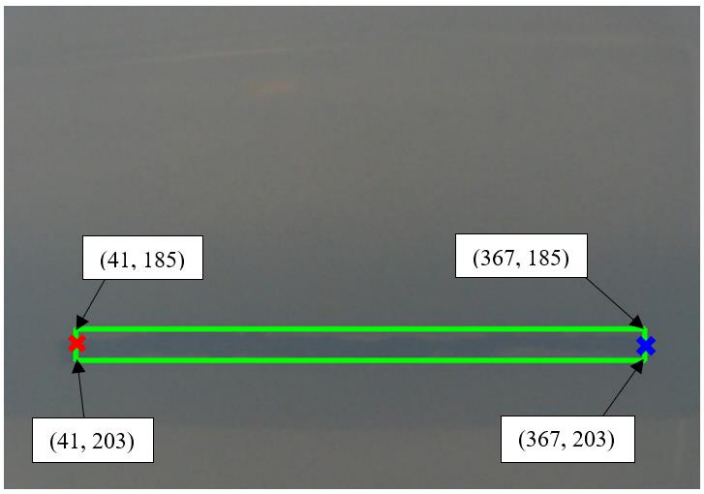

Figure 4.43 Area for Crack A3 detected with their coordinates

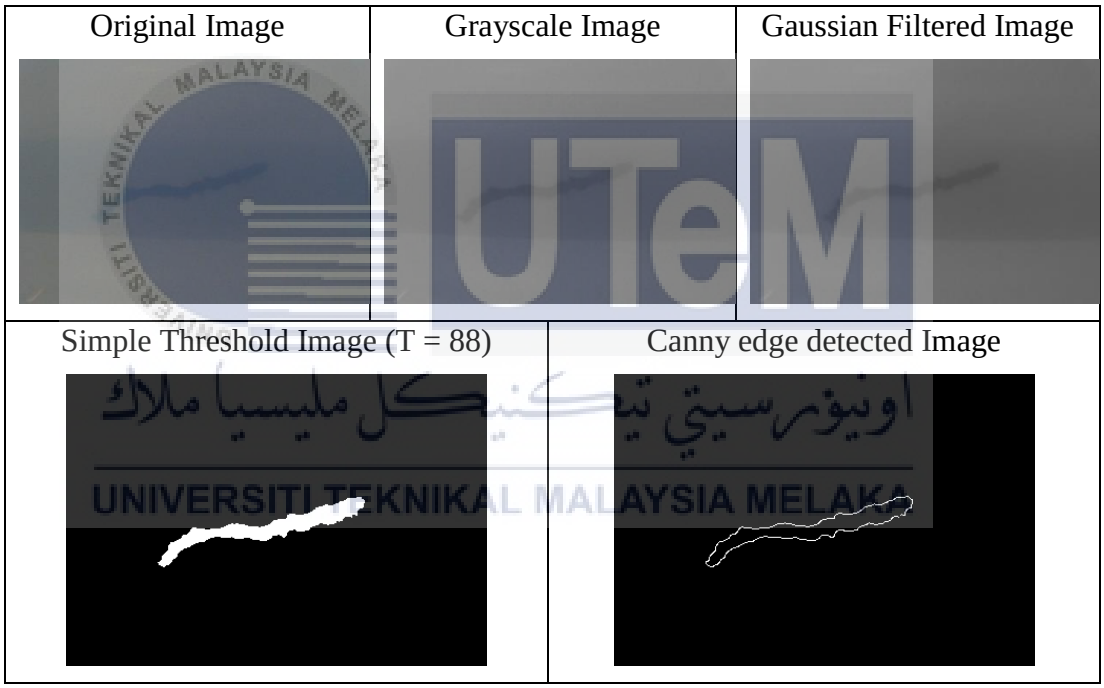

Figure 4.44 Result of Proposed Image Processing Algorithm for Crack B3

UNIVERSITI TEKNIKAL MALAYSIA MELAKA

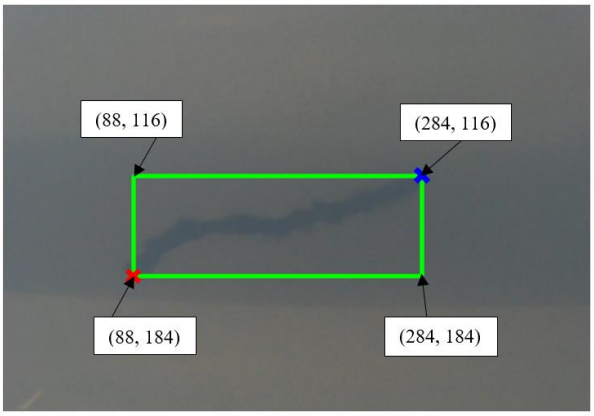

Figure 4.45 Area for Crack B3 detected with their coordinates

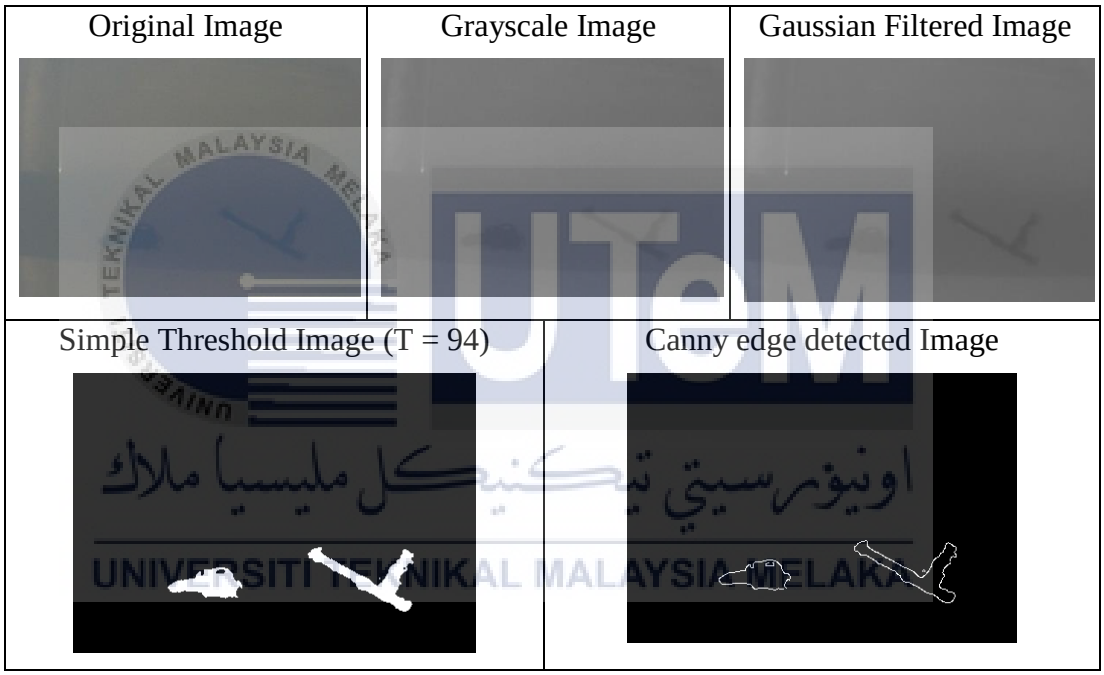

Figure 4.46 Result of Proposed Image Processing Algorithm for Crack C3

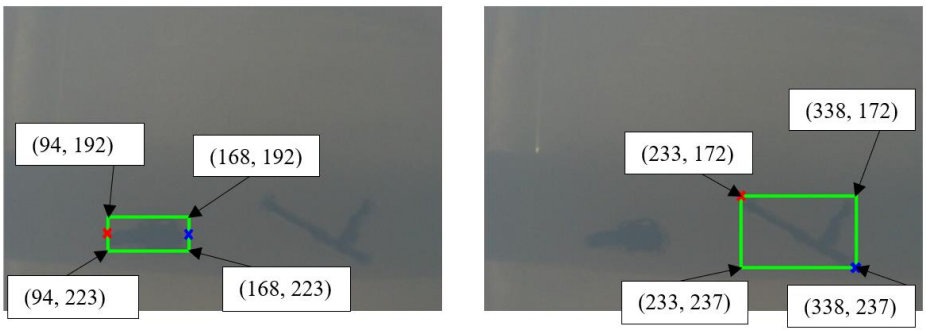

Figure 4.47 Area for Crack C3 detected with their coordinates

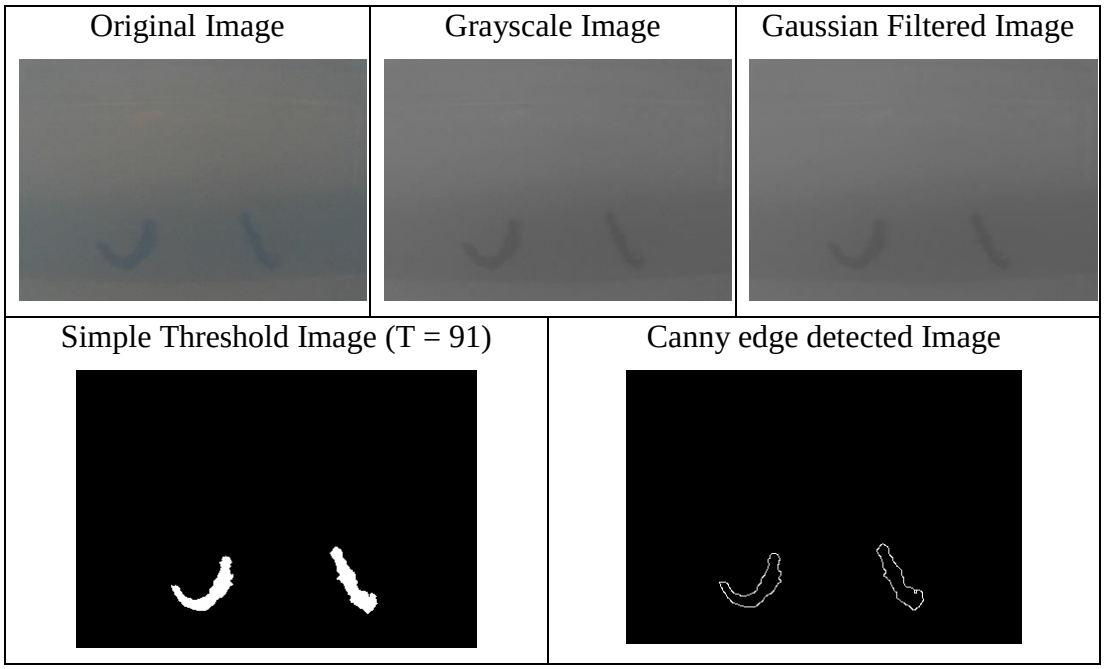

Figure 4.48 Result of Proposed Image Processing Algorithm for Crack D3

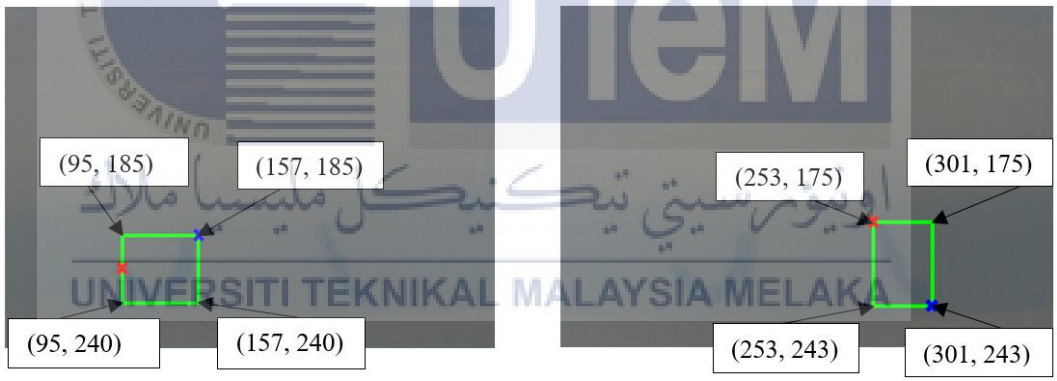

Figure 4.49 Area for Crack D3 detected with their coordinates

UNIVERSITI TEKNIKAL MALAYSIA MELAKA

Table 4.5 Crack Area Determination Results for Experiment 2 Condition 3

Crack	Length, l (mm)	Width, w (mm)	Area, A (mm^2)	Starting Point	Ending Point
A2	326	18	5868	(41, 194)	(367, 194)
B2	196	68	13328	(88, 184)	(284, 116)
C2	74	31	2294	(94, 207)	(168, 207)
	105	65	6825	(233, 172)	(338, 237)
D2	62	55	3410	(95, 212)	(157, 185)
	48	68	3264	(253, 175)	(301, 243)

Table 4.6 Percent Error Results for Experiment 2 Condition 3

Crack	Reference Area (mm^2)	Experimental Area (mm^2)	Percent Error (%)
A	10819	5868	45.76
B	10148	13328	31.34
C	2400	2294	4.42
	6634	6825	2.88
D	4560	3410	25.22
	3174	3264	2.84

The highest percent error in Condition 3 is happened in Crack A, which had reached more than 45%, followed by Crack B (31.34%). The percent error for the first crack part of Crack D was 25.22%. The percent errors for other crack parts were less than 5%.

UNIVERSITI TEKNIKAL MALAYSIA MELAKA

4.1.2.4 High Turbidity Level and Low Lighting Level

The last condition for Experiment 2 is carried out by using the aquarium filled with murky water and setting the equipment in a dark room. As mentioned in previous conditions, the images captured by the camera was undergone image processing and followed by crack area determination. The image processing and contour method results for Crack A, B, C and D in Condition 4 were shown in Figure 4.50 to 4.57. The crack area determination and percent error results of each crack for the proposed system in Condition 4 were shown in Table 4.7 and Table 4.8 respectively.

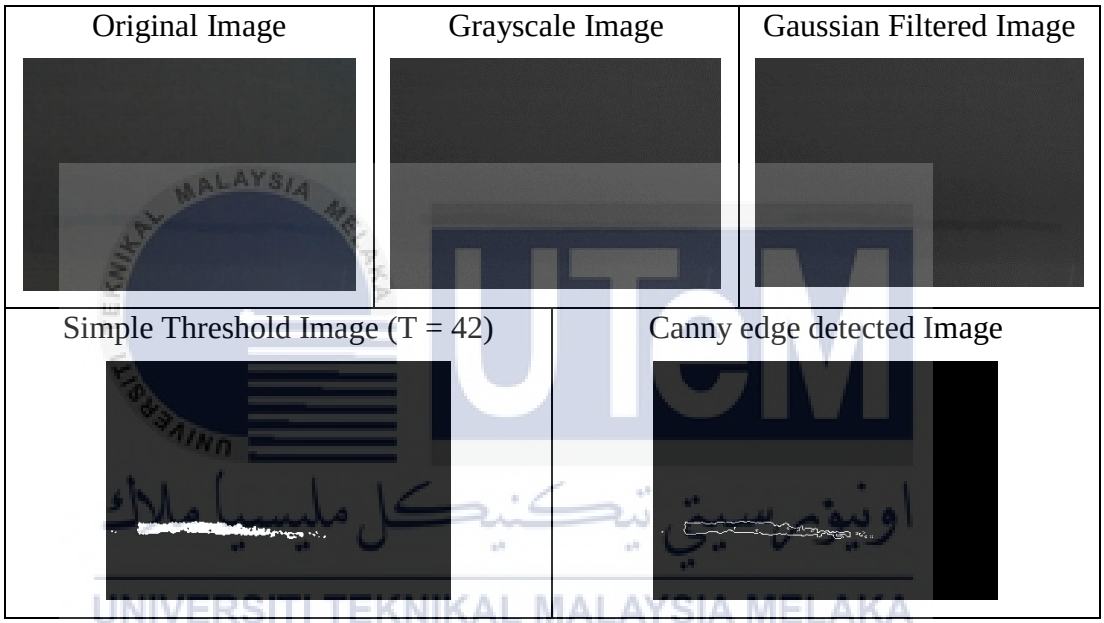

Figure 4.50 Result of Proposed Image Processing Algorithm for Crack A4

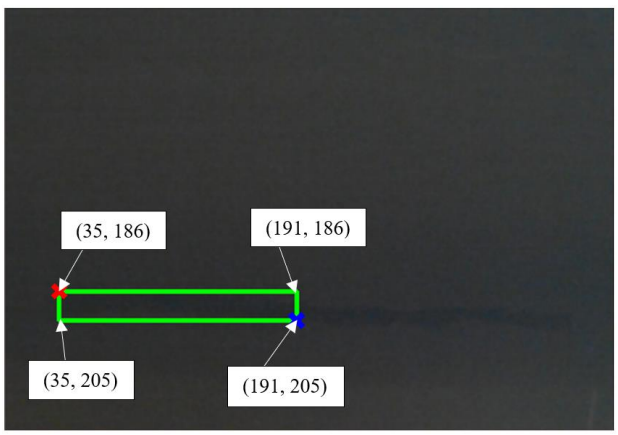

Figure 4.51 Area for Crack A4 detected with their coordinates

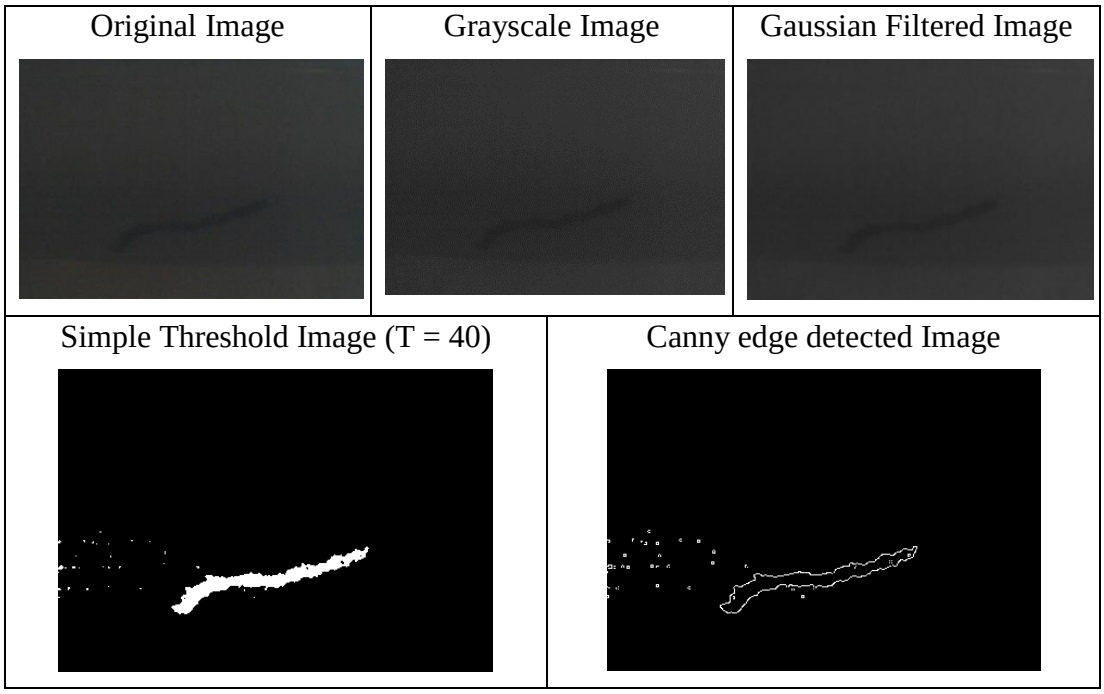

Figure 4.52 Result of Proposed Image Processing Algorithm for Crack B4

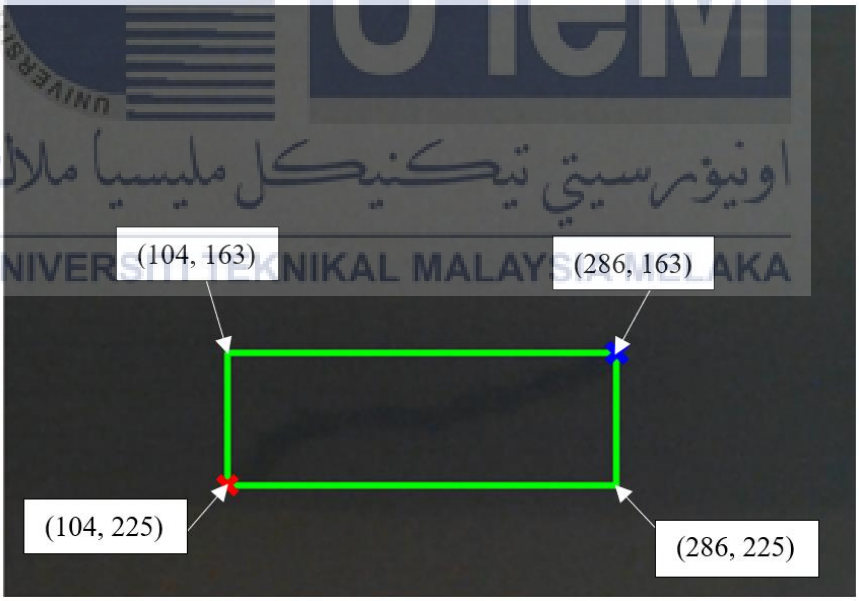

Figure 4.53 Area for Crack B4 detected with their coordinates

UNIVERSITI TEKNIKAL MALAYSIA MELAKA

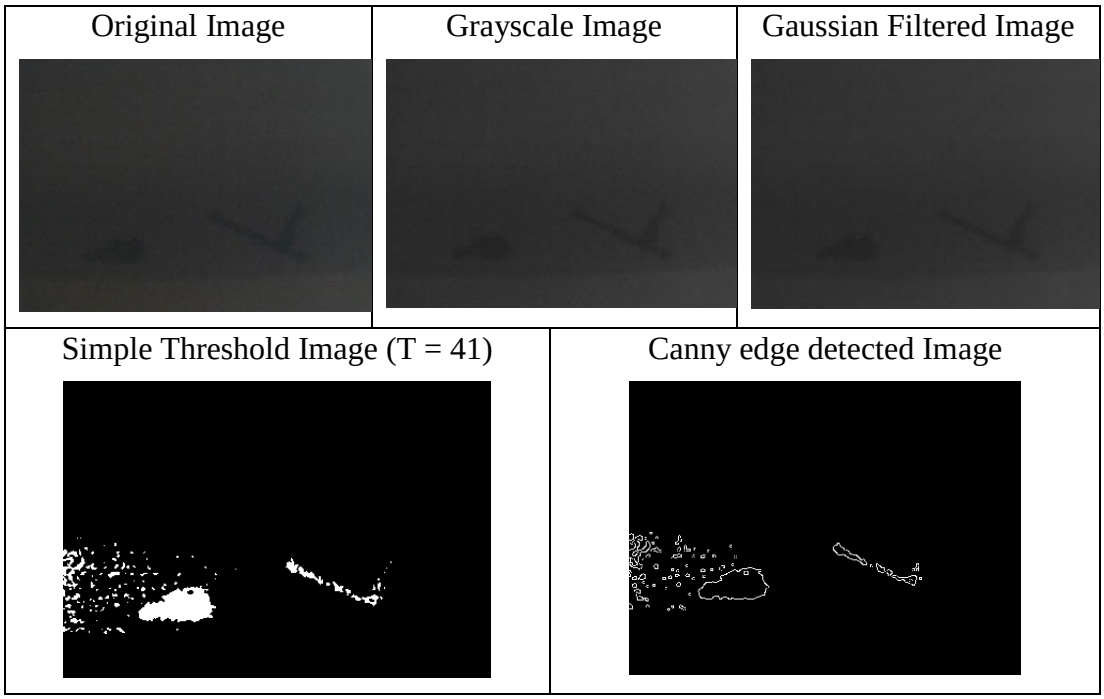

Figure 4.54 Result of Proposed Image Processing Algorithm for Crack C4

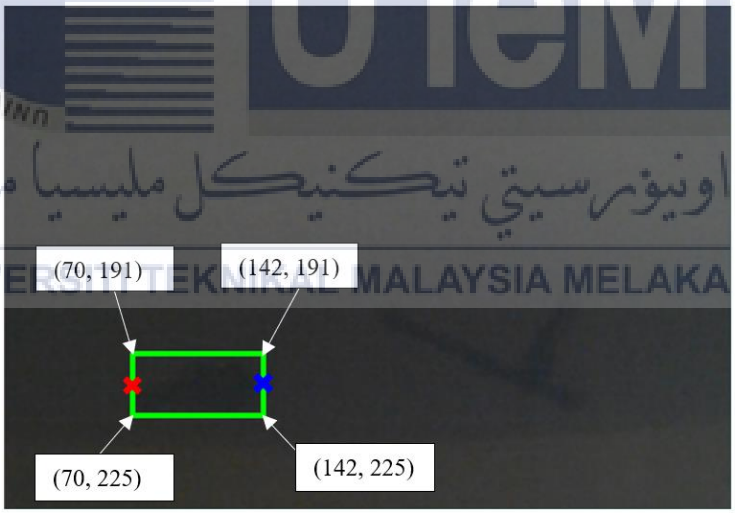

Figure 4.55 Area for Crack C4 detected with their coordinates

UNIVERSITI TEKNIKAL MALAYSIA MELAKA

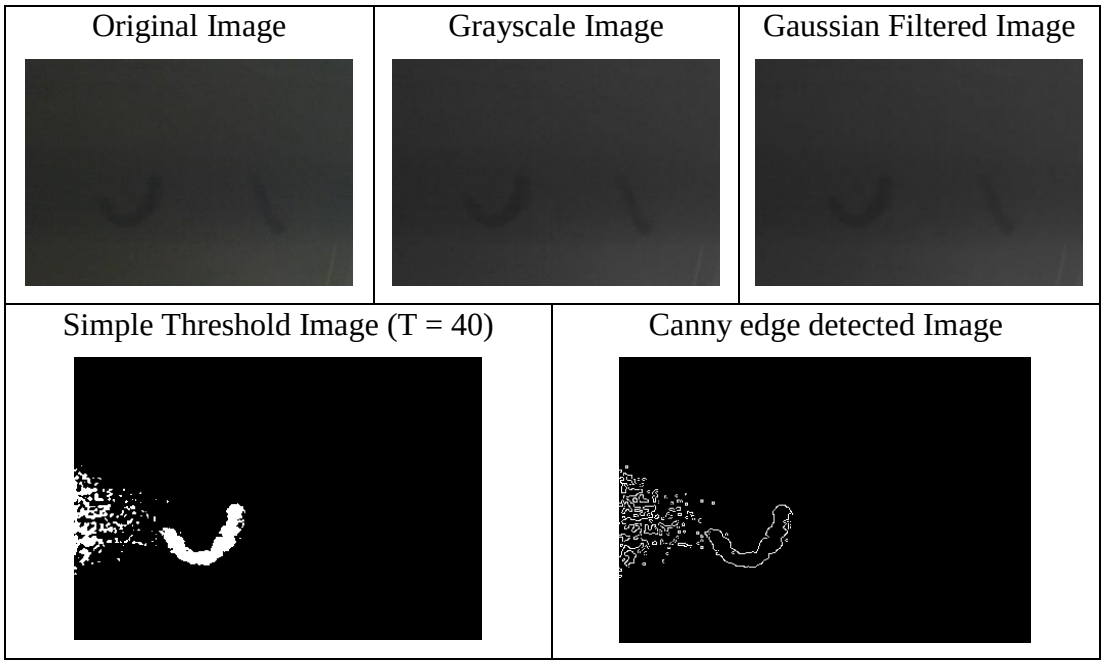

Figure 4.56 Result of Proposed Image Processing Algorithm for Crack D4

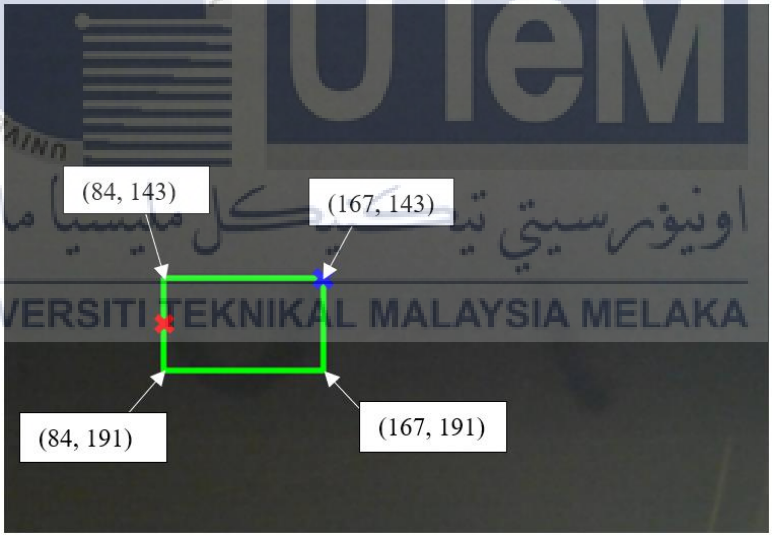

Figure 4.57 Area for Crack D4 detected with their coordinates

UNIVERSITI TEKNIKAL MALAYSIA MELAKA

Table 4.7 Crack Area Determination Results for Experiment 2 Condition 4

Crack	Length, l (mm)	Width, w (mm)	Area, A (mm^2)	Starting Point	Ending Point
A2	156	19	2964	(35, 186)	(191, 205)
B2	182	62	11284	(104, 225)	(286, 225)
C2	72	34	2448	(70, 208)	(142, 208)
	None	None	None	None	None
D2	83	48	3984	(84, 167)	(167, 143)
	None	None	None	None	None

Table 4.8 Percent Error Results for Experiment 2 Condition 4

Crack	Reference Area (mm^2)	Experimental Area (mm^2)	Percent Error (%)
A	10819	2964	72.60
B	10148	11284	11.19
C	2400	2448	2.00
	6634	None	None
D	4560	3984	12.63
	3174	None	None

UNIVERSITI TEKNIKAL MALAYSIA MELAKA

In Condition 4, some of the crack part in the images cannot be detected due to the problem of turbidity and lighting. For those crack parts that being detected, the percent error had reached more than 70%.

4.1.3 Summary

For Experiment 1, the proposed image processing algorithm was design. After converting the original image to grayscale image, Gaussian filter was chosen for filtering the noise from the image instead of median filter as the noise in the real underwater images were mostly Gaussian noises. Next, the Gaussian filtered image was converted to binary image using simple thresholding since the threshold value for simple thresholding can be chosen manually to produce a better binary image that can be more focus on the crack part when compared to that of Otsu thresholding. Then, the simple threshold image was undergone edge detection. Instead of Sobel edge detector, Canny edge detector was selected since it can be more accurate in detecting the edges of crack part. Lastly, the Canny edge detected image was used for determining the crack area using Contour method. The crack area was successfully be determined using the proposed image processing algorithm.

By using the proposed image processing algorithm from Experiment 1, the performance of the algorithm was compared under 4 conditions. The conclusion obtained for Experiment 2 is the proposed image processing method has the best performance in the condition of low turbidity level with high lighting level, followed by the condition of low turbidity level with low lighting level and high turbidity level with high lighting level the condition of The worst performance is when the images are captured in the condition of high turbidity level but low lighting level, as the system even cannot detect all the crack parts of the images in this condition.

UNIVERSITI TEKNIKAL MALAYSIA MELAKA

CHAPTER 5

CONCLUSION AND FUTURE WORKS

5.1 Conclusion

To be concluded, all the objectives were achieved successfully. First objective was achieved successfully by carrying out Experiment 1. An image processing algorithm was developed successfully to identify the cracking area. First of all, the real world image of cracking pipeline were collected from internet. The images were processed using OpenCV-Python software. The images were converted to grayscale images and filtered. Two filters, which were median and Gaussian filter, were used to remove the noise of image respectively and Gaussian filter was selected as the noise for the image were mainly Gaussian noises. Next, the Gaussian filtered images were undergone thresholding process using simple and Otsu threshold respectively. Simple threshold was chosen for the system since simple threshold had performed better than Otsu threshold. Simple threshold can select threshold value manually to get a better threshold image while Otsu threshold chooses the threshold value arbitrary according to the images. So, some of the cracking part cannot be clearly shown. Then, the simple threshold images were undergone edge detection using Sobel and Canny edge detector respectively. Canny edge detection was selected for the system as the Canny edge detector can detect the edges more accurately. Lastly, contour method was applied on the Canny edge detected images to draw a rectangle box for bounding the crack part. The coordinates of the rectangle box were determined and area of the crack part was obtained.

Second objective was also achieved in Experiment 2. An artificial underwater environment was prepared – a fish aquarium with clear or murky water and the crack PVC pipe. There were four conditions set for Experiment 2, which were low turbidity level with high lighting level (Condition 1), low turbidity level with low lighting level (Condition 2), high turbidity level with high lighting level (Condition 3) and high turbidity level with low lighting level (Condition 4). Firstly, the images of cracking PVC pipeline were captured by using SJCAM SJ4000 Wi-Fi Action Camera via the

UNIVERSITI TEKNIKAL MALAYSIA MELAKA

SJCAM app in smartphone for the first condition. Next, the image of cracking pipelines was transfer to laptop via Bluetooth. The cracking PVC pipelines images were processed through the image processing algorithm mentioned in previous paragraph and the area of crack part was determined. The areas obtained for Experiment Condition 1 were used as the reference value for calculating the percent error of the system in other 3 conditions. After finishing experiment in Condition 1, the procedures were repeated for other conditions. Then, the percent error for each condition were calculated. Condition 1 had performed the best among those 4 conditions. Percent error in Condition 2 was mostly less than 11% while the percent error in Condition 3 had reached more than 45%. Condition 4 had the worst performance as it reached the highest percent error which is more than 70%. Half of the cracking part even cannot be detected in Condition 4. This can be concluded that turbidity level and lighting level is important for the image processing.

5.2 Future Works

In order to improve the proposed underwater pipeline cracking area identification system, there are many suggestions that can be concluded. Instead of SJCAM SJ4000 Wi-Fi Action Camera, a more suitable camera, such as GoPro and Nikon brand, can be used for obtaining the image of cracking pipelines with better quality. Secondly, the contour method that used in this project needs to select the rectangle box manually for the cracking part. In order to get the area of cracking part faster for future, an automatic selection method is suggested the crack area determination process. Next, lighting and turbidity level are the factors that affect the performance of image processing for the underwater images. To improve the performance of image processing, the lighting and turbidity level must be considered when capturing the real world underwater images.

UNIVERSITI TEKNIKAL MALAYSIA MELAKA

REFERENCES

[1] A.C. Palmer and R.A. King, *Subsea Pipeline Engineering*, 2nd ed. Tulsa, USA: Pennwell, 2008, pp. 1-524.

[2] N.F. Adnan *et al.*, "Leak detection in gas pipeline by acoustic and signal processing," IOP Conf. Ser.: Mater. Sci. Eng., 2015.

[3] *Thunder Horse* [Online]. Available: https://web.archive.org/web/20120226230020/http://www.gvac.se/thunder-horse/

[4] Ray Tyson. (2005, Mar 06). *Still a mystery* [Online]. Available: http://www.petroleumnews.com/pntruncate/882142741.shtml

[5] Sarah Lyall. (2010, Jul 12). *In BP's Record, a History of Boldness and Costly Blunders* [Online]. Available: https://www.nytimes.com/2010/07/13/business/energy-environment/13bprisk.html

[6] Stephen Then. (2014, Jun 11). *Blast rips Sabah-Sarawak gas pipeline* [Online]. Available: https://www.thestar.com.my/news/nation/2014/06/11/blast-rips-sabahsarawak-gas-pipeline-no-one-hurt-in-2am-explosion-fire-is-out/

[7] Borneo Post Online, the largest English News site in Borneo. (2015, April 29). *Petronas consolidating final report on pipeline explosion in Lawas* [Online]. Available: http://www.theborneopost.com/2015/04/29/petronas-consolidating-final-report-on-pipeline-explosion-in-lawas/

[8] Mendeleyeev. (2015, Aug 16). *Pipeline Explodes Under Moscow River* [Online]. Available: https://russianreport.wordpress.com/2015/08/16/pipeline-explodes-under-moscow-river/

[9] Helen Whitehouse. (2015, Aug 13). *Oil pipeline leaks and dramatically bursts into flames in the middle of the Moscow River* [Online]. Available: https://www.mirror.co.uk/news/world-news/oil-pipeline-leaks-dramatically-bursts-6245523

[10] Montana Department of Justice. *Yellowstone River Oil Spill (January 15)* [Online]. Available: https://dojmt.gov/lands/yellowstone-river-oil-spill-january-2015/

UNIVERSITI TEKNIKAL MALAYSIA MELAKA

[11] Wendy Koch. (2015, Jan 20). *Oil Spills Into Yellowstone River, Possibly Polluting Drinking Water* [Online]. Available: https://news.nationalgeographic.com/news/energy/2015/01/150120-oil-spills-into-yellowstone-river/

[12] Voice of America (VOA) News, the largest U.S. international broadcaster. (2017. Apr 03). *Oil Leak Discovered by Workers in Alaska's Cook Inlet* [Online]. Available: https://www.voanews.com/a/oil-leak-discovered-by-workers-in-alaska-cook-inlet/3793738.html

[13] Katie Valentine. (2017, Apr 13). *Underwater pipeline has been leaking gas into a beluga whale habitat for 3 months* [Online]. Available: https://thinkprogress.org/underwater-pipeline-leaking-for-three-months-425a108b06c0/

[14] SAFETY4SEA, Maritime Portal. (2018, Jul 27). *Oil spill reported from Cliff Head Alfa platform off Perth* [Online]. Available: https://safety4sea.com/oil-spill-reported-from-cliff-head-alfa-platform-off-perth/

[15] A. Jasper, "Oil/Gas Pipeline Leak Inspection and Repair in Underwater Poor Visibility Conditions: Challenges and Perspectives," *Journal of Environmental Protection*, vol. 3, no.5, pp. 394-399, May. 2012.

[16] Interesting Engineering, a leading Science, Technology, Engineering and Mathematics (STEM) communicator. (2017, Jan 23). *Underwater Welding: One of the Most Dangerous Occupations in the World* [Online]. Available: https://interestingengineering.com/underwater-welding-one-of-the-most-dangerous-occupations-in-the-world

[17] Jen Banbury. (2018, May 09). *The Weird, Dangerous, Isolated Life of the Saturation Diver* [Online]. Available: https://www.atlasobscura.com/articles/what-is-a-saturation-diver

[18] M. O'Byrne *et al.*, "Protocols for Image Processing based Underwater Inspection of Infrastructure Elements," *Journal of Physics: Conference Series*, vol. 628, issue 1, Jul. 2015.

[19] G. H. Mills *et al.*, "Advances in the Inspection of Unpiggable Pipelines," *Robotics*, vol. 6, issue 4, 2017.

UNIVERSITI TEKNIKAL MALAYSIA MELAKA

[20] M. O'Byrne *et al.*, "An underwater lighting and turbidity image repository for analysing the performance of image-based non-destructive techniques," *Structure and Infrastructure Engineering*, vol. 14, issue 1, pp. 104-123, 2018.

[21] Robert N. Rossier. (2012). *What is visibility? Illuminating facts about an unclear situation* [Online]. Available: https://dtmag.com/thelibrary/visibility-illuminating-facts-unclear-situation/

[22] Scott Gietler. (2016, Mar 3). *Lighting your Subject Underwater* [Online]. Available: http://www.uwphotographyguide.com/underwater-photography-lighting

[23] P. Barrette, "Offshore pipeline protection against seabed gouging by ice: An overview," *Cold Regions Science and Technology*, vol. 69, issue 1, pp. 3-20, 2011.

[24] C. T. Mgonja, "The Consequences of cracks formed on the Oil and Gas Pipelines Weld Joints," *International Journal of Engineering Trends and Technology (IJETT)*, vol. 54, no. 4, pp. 223-232, Dec. 2017.

[25] T. L. Prakash *et al.*, "Studies on The Stress Corrosion Cracking (SCC) Behavior Of Various Metals and Alloys Used In The Desalination And Power Plants," unpublished.

[26] *Stress Corrosion Cracking*, National Physical Laboratory, Teddington, England, 2000.

[27] Ronald Frend. (2016, Aug 26). *HIC, SOHIC, SSC & Hydrogen Blisters - Why?* [Online]. Available: https://www.linkedin.com/pulse/hic-sohic-ssc-hydrogen-blisters-why-ronald-frend

[28] M. Elboujdaîni *et al.*, "Studies on Inhibition of Hydrogen-Induced Cracking of Linepipe Steels," *Corrosion*, vol. 62, issue 1, pp. 29-34, Jan. 2006.

[29] G. N. Haidemenopoulos *et al.*, "Investigation of Stress-Oriented Hydrogen-Induced Cracking (SOHIC) in an Amine Absorber Column of an Oil Refinery," *Metals*, vol. 8, issue 9, pp. 1-17, Sept. 2018.

[30] Offshore, magazine relative to offshore technology, oil and gas E&P operations. (2016, Aug 26). *PIPELINE MAINTENANCE: Magnetic leakage detection used to spot, measure pipeline cracks* [Online]. Available:

UNIVERSITI TEKNIKAL MALAYSIA MELAKA

https://www.offshore-mag.com/articles/print/volume-60/issue-11/news/pipeline-maintenance-magnetic-leakage-detection-used-to-spot-measure-pipeline-cracks.html

[31] S. Aminorroaya *et al.*, "Hook crack in electric resistance welding line pipe steel," *South East Asia Iron & Steel Institute Conference and Exhibition*, pp. 1-9, 2003.

[32] Hui-hui Chu *et al.*, "Quality Inspection Algorithm based on Machine Vision for Tube-Sheet Welding," in 2016 IEEE Workshop on Advanced Robotics and its Social Impacts (ARSO), Jul 2016, pp. 279-283.

[33] I. Khalifa *et al.*, "A New Image-Based Model For Predicting Cracks In Sewer Pipes," *International Journal of Advanced Computer Science and Applications (IJACSA)*, vol. 4, no. 12, pp. 65-71, 2013.

[34] XueLan Zhang *et al.*, "Research on Vision Inspection System for Drainage Pipeline's Damage based on Pattern Recognition," in 2007 IEEE International Conference on Robotics and Biomimetics (ROBIO), Dec 2007, pp. 697-701.

[35] Ding Qingxin *et al.*, "A Crack Recognition Way thru Images for Natural Gas Pipelines," in The 2nd International Conference on Information Science and Engineering, Dec 2010, pp. 859-862.

[36] P. Huynh *et al.*, "Dou-edge Evaluation Algorithm for Automatic Thin Crack Detection in Pipelines," in 2015 IEEE International Conference on Signal and Image Processing Applications (ICSIPA), Oct 2015, pp. 191-196.

[37] N. Mohamed *et al.*, "A Fault-Tolerant Acoustic Sensor Network for Monitoring Underwater Pipelines," in 2014 International Conference on High Performance Computing & Simulation, Bologna, Italy, July 2014, pp. 877-884.

[38] N. Mohamed *et al.*, "Monitoring Underwater Pipelines Using Sensor Networks," in 12th IEEE International Conference on High Performance Computing and Communications, Sept 2010, pp. 346-353.

[39] R. Ben-Mansour *et al.*, "Computational fluid dynamic simulation of small leaks in water pipelines for direct leak pressure transduction," *Computers & Fluids*, vol. 57, pp. 110-123, Mar. 2012.

[40] Bin Yang *et al.*, "Ultrasonic monitoring system for oil and gas pipeline corrosion," in 2012 Fourth International Conference on Multimedia Information Networking and Security, Nov 2012, pp. 381-383.

UNIVERSITI TEKNIKAL MALAYSIA MELAKA

[41] Wu Ang *et al*., "Measuring System for the Wall Thickness of Pipe Based on Ultrasonic Multisensor," in The Ninth International Conference on Electronic Measurement & Instruments (ICEMI), Aug 2009, pp. 1-641 - 1-644.

[42] Shuaiyong Li *et al*., "Leak Detection and Location for Gas Pipelines Using Acoustic Emission Sensors," in 2012 IEEE International Ultrasonics Symposium Proceedings, Oct 2012, pp. 957-960.

[43] Liying Sun and Yibo Li, "Acoustic Emission Sound Source Localization for crack in the pipeline," in 2010 Chinese Control and Decision Conference, May 2010, pp. 4298-4301.

[44] Warner, R. M. (2008). Applied statistics: From bivariate through multivariate techniques. Thousand Oaks, CA: Sage Publications.

[45] Nur Fatmala. (2016, Feb 17). *Crack on Offshore Pipeline* [Online]. Available: http://nfatmala.blogspot.com/2016/02/crack-on-offshore-pipeline.html

[46] Rizky Pitajeng. (2016, Feb 15). *Crack on Offshore Pipeline* [Online]. Available: http://rizkypitajeng.blogspot.com/2016/02/crack-on-offshore-pipeline.html

[47] C. Nageswaran *et al*. (2013, Sept). *Monitoring fatigue crack growth in subsea threaded components using ultrasonic phased array techniques* [Online]. Available: https://www.twi-global.com/technical-knowledge/published-papers/fatigue-crack-growth-ultrasonic-phased-array-techniques

[48] C. A. Stridsklev, "Sulfide Stress Corrosion Cracking Resistance of Modified ASTM A694 F60 Low Alloy Steel for Subsea Applications," Department of Materials Science and Engineering, Norwegian University of Science and Technology, Norway, June 2013.

[49] Shuqi Zheng *et al*., "Stress-Oriented Hydrogen-Induced Cracking ofL360QS Steel," in NACE International, Nov 2012, pp. 71-75.

[50] Hongxia Wan *et al.*, "Stress Corrosion Behavior of X65 Steel Welded Joint in Marine Environment," *International Journal of Electrochemical Science (IJACSA)*, vol. 4, no. 10, pp. 8437-8446, 2015.

UNIVERSITI TEKNIKAL MALAYSIA MELAKA

APPENDICES

APPENDIX A TIME FRAME FOR FYP

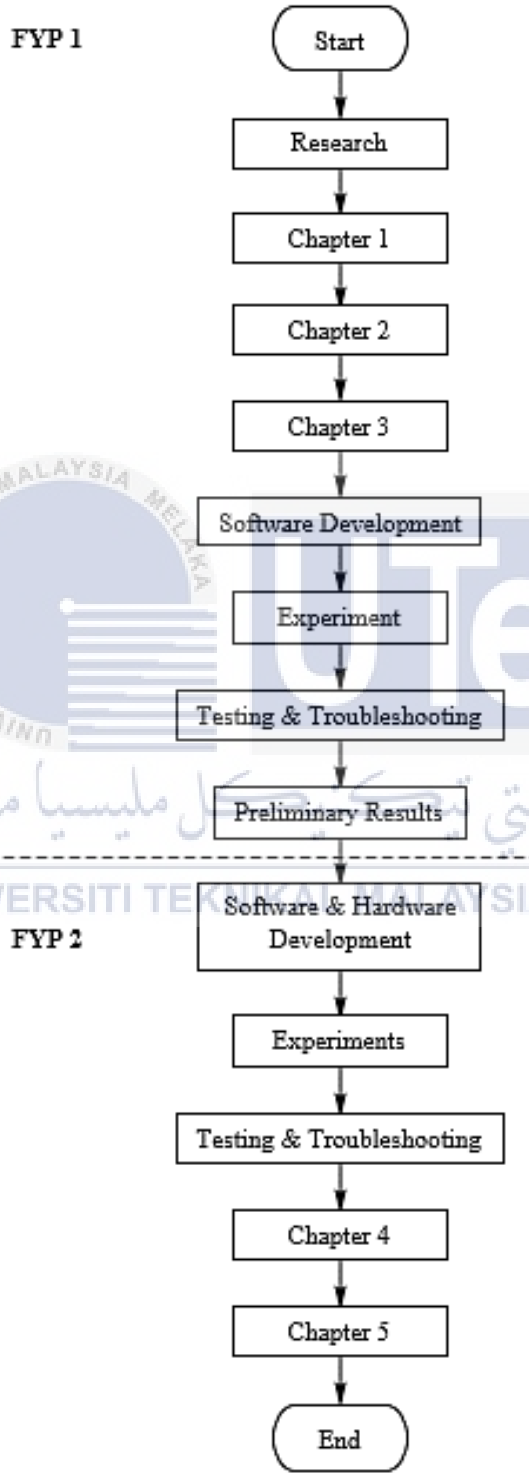

UNIVERSITI TEKNIKAL MALAYSIA MELAKA

APPENDIX B GANTT CHART FOR FYP

Project Activity	Sept 18				Oct 18				Nov 18				Dec 18	
FYP 1	**Week**													
	1	2	3	4	5	6	7	8	9	10	11	12	13	14
Title Discussion and Selection														
Research and Journal Findings														
Motivation & Problem Statement														
Objectives & Scope														
Literature Review														
Methodology -Experiment Designed														
Expected Results														
Submission for Draft of Progress Report														
FYP 1 Seminar														
Finalizing the Progress Report														
Submission for Final Report														

Project Activity	Feb 19	Mar 19					Apr 19				May 19				June 19		
FYP 2	**Week**																
	1	2	3	4	5	6	7	8	9	10	11	12	13	14	15	16	17
Software Development																	
Experiment 1																	
Experiment 2																	
Result & Discussions																	
Complete Draft of FYP 2 Report																	
Submission for Draft of FYP 2 Report																	
FYP 2 Seminar																	
Finalizing the FYP 2 Report																	
Submission for Final FYP 2 Report																	

UNIVERSITI TEKNIKAL MALAYSIA MELAKA

APPENDIX C IMAGE PROCESSING ALGORITHM CODING

```
import cv2
import numpy as np
import matplotlib.pylab as plt

#loading Image
img = cv2.imread('Crack B2.jpg')
r=400.0/img.shape[1]
dim=(400,int(img.shape[0]*r))
resized=cv2.resize(img,dim,interpolation=cv2.INTER_AREA)

#convert to grayscale image
gray = cv2.cvtColor(resized, cv2.COLOR_BGR2GRAY)
cv2.imwrite('gray.png',gray)
plt.subplot(121), plt.imshow(cv2.cvtColor(resized,
cv2.COLOR_BGR2RGB)), plt.axis('off'), plt.title('Original')
plt.subplot(122), plt.imshow(gray,cmap = 'gray'),
plt.axis('off'), plt.title('Grayscale')
plt.show()

#filtering to remove noise
median = cv2.medianBlur(gray,3)
cv2.imwrite('median.png', median)
gaussian= cv2.GaussianBlur(gray, (3,3), 0)
cv2.imwrite('gaussian.png', gaussian)
plt.subplot(121), plt.imshow(median,cmap = 'gray'),
plt.axis('off'), plt.title('median')
plt.subplot(122), plt.imshow(gaussian,cmap = 'gray'),
plt.axis('off'), plt.title('gaussian')
plt.show()

#simple thresholding
_, sthres = cv2.threshold(gaussian, 14, 255,
cv2.THRESH_BINARY_INV)
cv2.imwrite("simple threshold.png", sthres)

#otsu thresholding
ret,othres =
cv2.threshold(gaussian,0,255,cv2.THRESH_BINARY_INV+cv2.THRESH_O
TSU)
cv2.imwrite("otsu threshold.png", othres)
```

UNIVERSITI TEKNIKAL MALAYSIA MELAKA

```
print (ret)
plt.subplot(121), plt.imshow(sthres,cmap = 'gray'),
plt.axis('off'), plt.title('simple threshold')
plt.subplot(122), plt.imshow(othres,cmap = 'gray'),
plt.axis('off'), plt.title('otsu threshold')
plt.show()

#edge detection
sobelx = cv2.Sobel(sthres, cv2.CV_64F, 1, 0, ksize=5)
cv2.imwrite("sobelx.png", sobelx)
sobely = cv2.Sobel(sthres, cv2.CV_64F, 0, 1, ksize=5)
cv2.imwrite("sobely.png", sobely)
canny = cv2.Canny(sthres, 30, 190)
cv2.imwrite("canny.png", canny)
plt.subplot(131), plt.imshow(sobelx), plt.axis('off'),
plt.title('Sobel x edge')
plt.subplot(132), plt.imshow(sobely), plt.axis('off'),
plt.title('Sobel y edge')
plt.subplot(133), plt.imshow(canny), plt.axis('off'),
plt.title('Canny edge')
plt.show()

cv2.waitKey(0)
cv2.destroyAllWindows()
```

UNIVERSITI TEKNIKAL MALAYSIA MELAKA

APPENDIX D CRACK AREA DETERMINATION CODING

```
import cv2
import numpy as np
import matplotlib.pylab as plt

#Convert to grayscale image
img = cv2.imread('Crack 1.png')
r=400.0/img.shape[1]
dim=(400,int(img.shape[0]*r))
resized=cv2.resize(img,dim,interpolation=cv2.INTER_AREA)
gray = cv2.cvtColor(resized, cv2.COLOR_BGR2GRAY)

#Gaussian filter
gaussian= cv2.GaussianBlur(gray, (5,5), 0)

#Simple threshold & Canny edge detection
_, thres = cv2.threshold(gaussian, 41, 255, cv2.THRESH_BINARY)
canny = cv2.Canny(thres, 25, 190)
cv2.imshow("canny", canny)
cv2.imwrite("canny_edge.png", canny)

#Contour method
_, cnts, _ = cv2.findContours(canny, cv2.RETR_EXTERNAL,
cv2.CHAIN_APPROX_SIMPLE)
print("{} rectangle box are found\n".format(len(cnts)))

#select the rectanggle box by changing the number
cnts=cnts[0]

x,y,w,h = cv2.boundingRect(cnts)
cv2.rectangle(resized,(x,y),(x+w,y+h),(0,255,0),2)

cv2.imshow("contour", resized)
print("A : ",(x,y))
print("B : ",(x+w,y))
print("C : ",(x,y+h))
print("D : ",(x+w,y+h))

cv2.waitKey(0)
```

UNIVERSITI TEKNIKAL MALAYSIA MELAKA

APPENDIX E RESULTS FOR EXPERIMENT 1

Crack 2 [20]

Original Image	Grayscale Image	Median Filter	Gaussian Filter

Simple threshold (T = 106)	Otsu Threshold (T = 174)	Edge Detection		
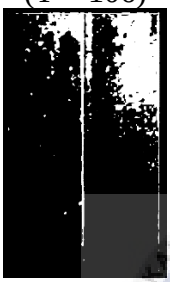		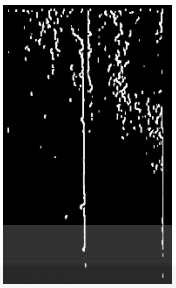	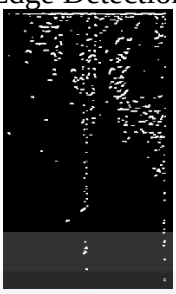	
		Sobel X	Sobel Y	Canny

Area Determination

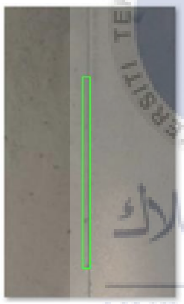

Coordinates = (181, 162) (197, 162) (181, 581) (197, 581)
Length, l = 16 mm
Width, w = 419 mm
Area, A = 6704 mm^2

UTeM
اونيۏرسيتي تيکنيکل مليسيا ملاک
UNIVERSITI TEKNIKAL MALAYSIA MELAKA

Crack 3 [20]

Original Image	Grayscale Image	Median Filter	Gaussian Filter
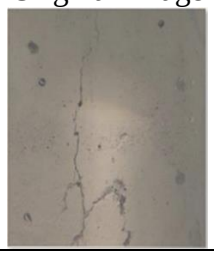	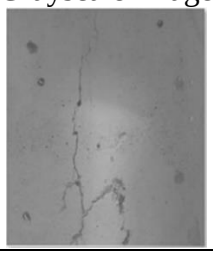	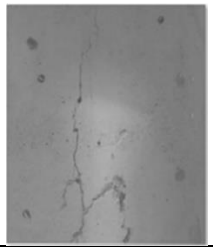	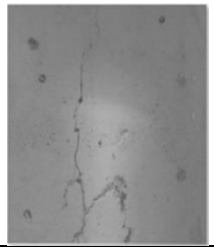

Simple threshold (T = 106)	Otsu Threshold (T = 174)	Edge Detection		
		Sobel X	Sobel Y	Canny

Area Determination

Coordinates = (118, 234) (171, 234) (118, 475) (171, 475)
Length, l = 53 mm
Width, w = 241 mm
Area, A = 12773 mm^2

Crack 4 [34]

Original Image

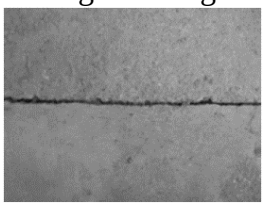

Grayscale Image

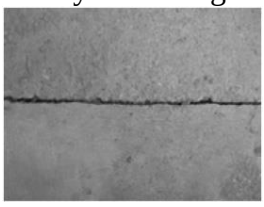

Median Filter

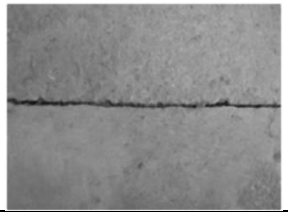

Gaussian Filter

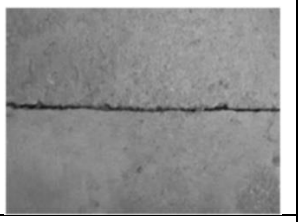

Simple threshold (T = 139)

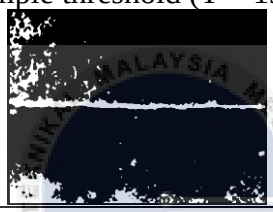

Otsu Threshold (T = 149)

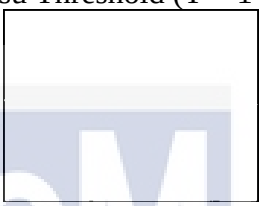

Edge Detection

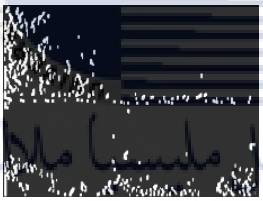

Sobel X

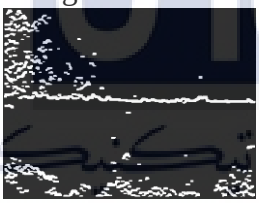

Sobel Y

Canny

Area Determination

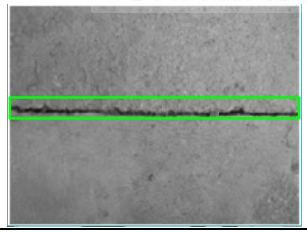

Coordinates = (2, 111) (347, 111) (2, 136) (347, 136)
Length, l = 345 mm
Width, w = 25 mm
Area, A = 8625 mm^2

Crack 5 [34]

Original Image

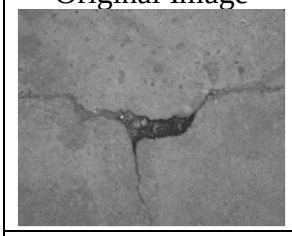

Grayscale Image

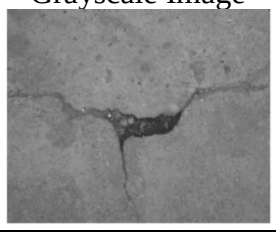

Median Filter

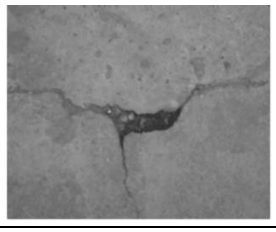

Gaussian Filter

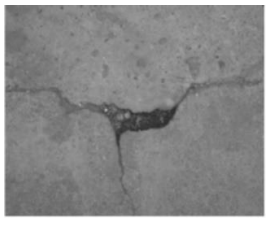

UNIVERSITI TEKNIKAL MALAYSIA MELAKA

Simple threshold (T = 114)	Otsu Threshold (T = 179)
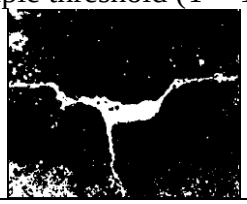	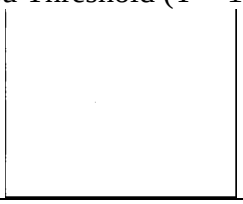

Edge Detection

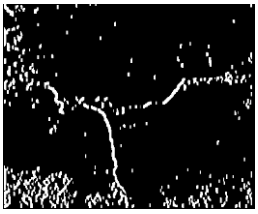
Sobel X

Sobel Y

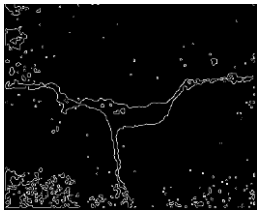
Canny

Area Determination

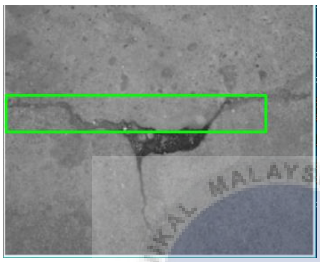

Coordinates = (2, 102) (294, 102) (2, 143) (294, 143)
Length, l = 292 mm
Width, w = 41 mm
Area, A = 11972 mm^2

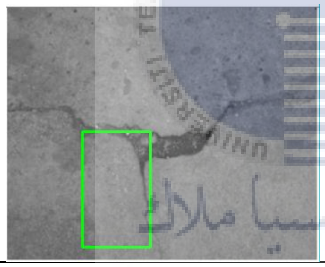

Coordinates = (85, 138) (161, 138) (85, 267) (161, 267)
Length, l = 76 mm
Width, w = 129 mm
Area, A = 9804 mm^2

UNIVERSITI TEKNIKAL MALAYSIA MELAKA

Crack 6 [34]

Original Image	Grayscale Image	Median Filter	Gaussian Filter
	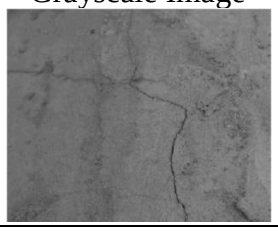	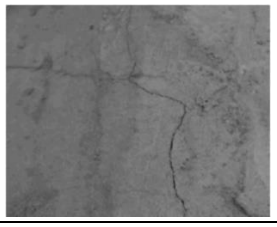	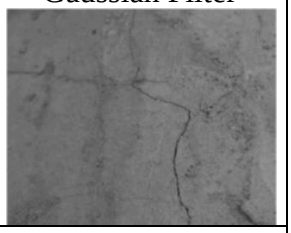

Simple threshold (T = 105)	Otsu Threshold (T = 155)
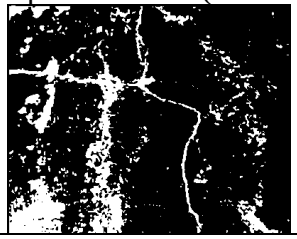	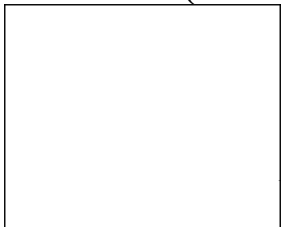

Edge Detection

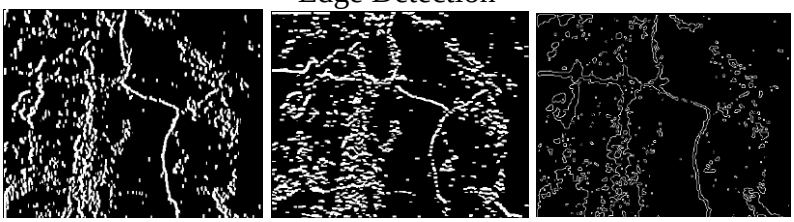

Sobel X | Sobel Y | Canny

Area Determination

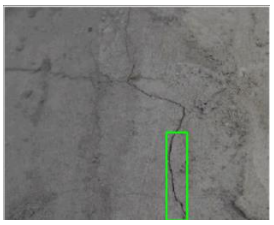

Coordinates = (244, 189) (275, 189) (244, 321) (275, 321)
Length, l = 31 mm
Width, w = 132 mm
Area, A = 4092 mm^2

Coordinates = (247, 140) (273, 140) (247, 192) (273, 192)
Length, l = 26 mm
Width, w = 52 mm
Area, A = 1352 mm^2

Crack 8 [36]

Original Image

Grayscale Image

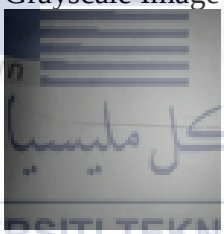

Median Filter

Gaussian Filter

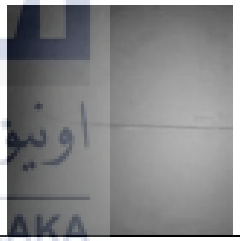

Simple threshold
(T = 165)

Otsu Threshold
(T = 99)

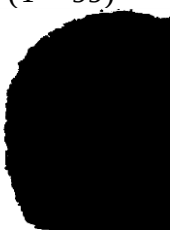

Edge Detection

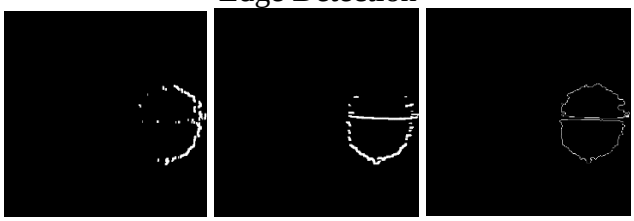

Sobel X | Sobel Y | Canny

Area Determination

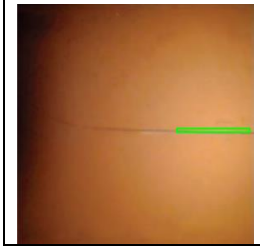

Coordinates = (267, 210) (389, 210) (267, 216) (389, 216)
Length, l = 122 mm
Width, w = 6 mm
Area, A = 732 mm^2

UNIVERSITI TEKNIKAL MALAYSIA MELAKA

Crack 10 [36]

Original Image	Grayscale Image	Median Filter	Gaussian Filter
	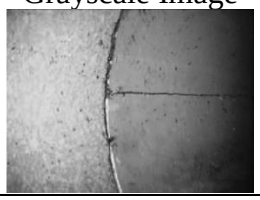		

Simple threshold (T = 100)	Otsu Threshold (T = 119)

Edge Detection

Sobel X | Sobel Y | Canny

Area Determination

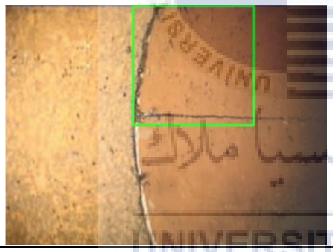

Coordinates = (158, 0) (307, 0) (158, 147) (307, 147)
Length, l = 149 mm
Width, w = 147 mm
Area, A = 21903 mm^2

Crack 11 [36]

Original Image	Grayscale Image	Median Filter	Gaussian Filter
	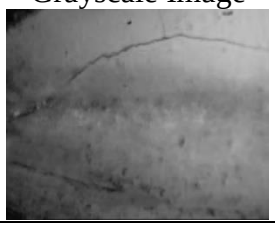	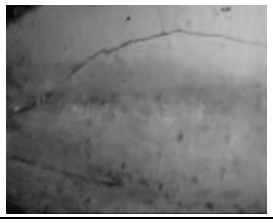	

Simple threshold (T = 125)	Otsu Threshold (T = 114)

UNIVERSITI TEKNIKAL MALAYSIA MELAKA

Edge Detection

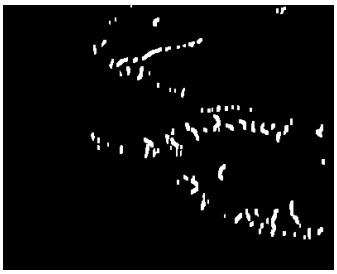

Sobel X

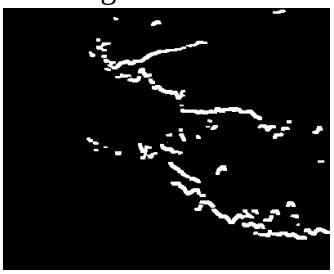

Sobel Y

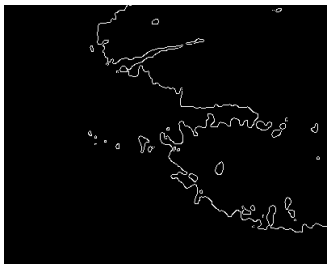

Canny

Area Determination

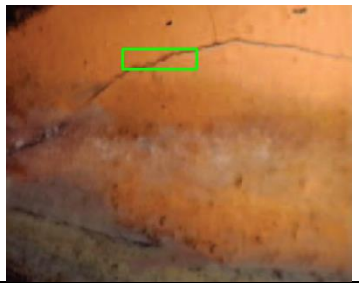

Coordinates = (134, 50) (219, 50) (134, 73) (219, 73)
Length, l = 85 mm
Width, w = 23 mm
Area, A = 1955 mm^2

Crack 12 [36]

Original Image

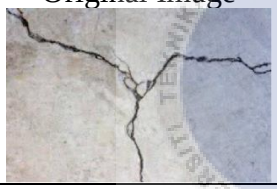

Grayscale Image

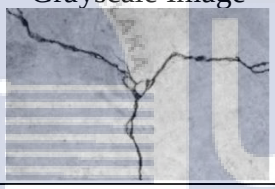

Median Filter

Gaussian Filter

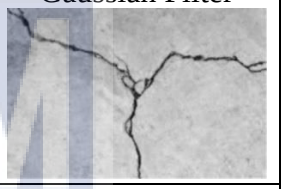

Simple threshold (T = 145)

Otsu Threshold (T = 147)

Edge Detection

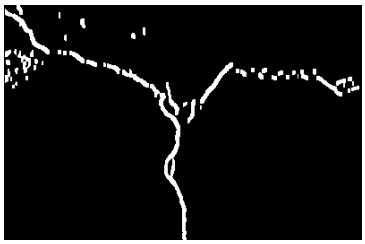

Sobel X

Sobel Y

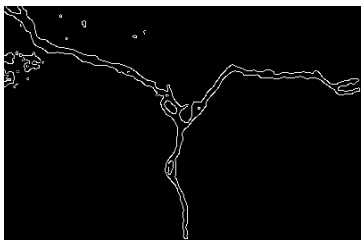

Canny

Area Determination

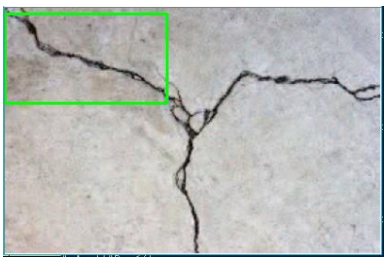

Coordinates = (0, 6) (172, 6) (0, 101) (172, 101)
Length, l = 172 mm
Width, w = 95 mm
Area, A = 16340 mm^2

UNIVERSITI TEKNIKAL MALAYSIA MELAKA

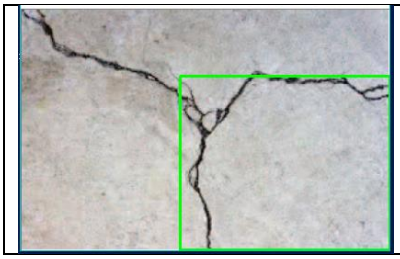

Coordinates = (172, 72) (400, 72) (172, 261) (400, 261)
Length, l = 228 mm
Width, w = 189 mm
Area, A = 43092 mm^2

Crack 13 [36]

Original Image

Grayscale Image

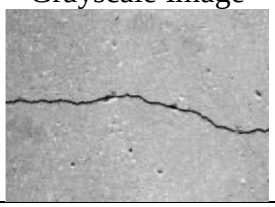

Median Filter

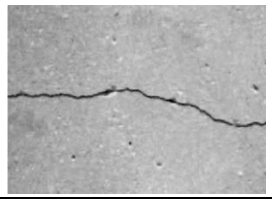

Gaussian Filter

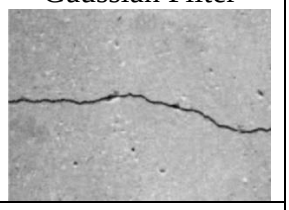

Simple threshold (T = 128)

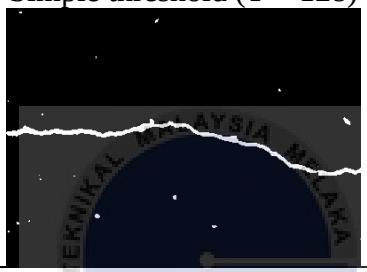

Otsu Threshold (T = 166)

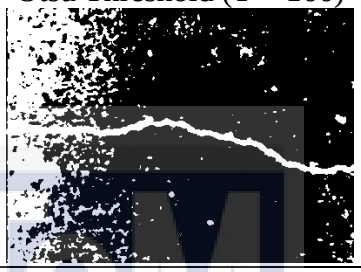

Edge Detection

Sobel X | Sobel Y | Canny

Area Determination

Coordinates = (0, 132) (400, 132) (0, 189) (400, 189)
Length, l = 400 mm
Width, w = 57 mm
Area, A = 22800 mm^2

Crack 14 [36]

Original Image

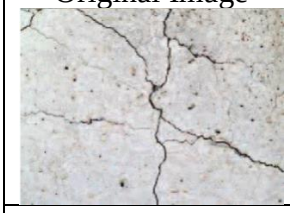

Grayscale Image

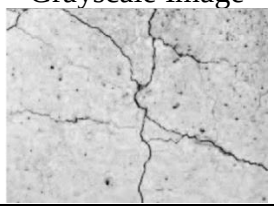

Median Filter

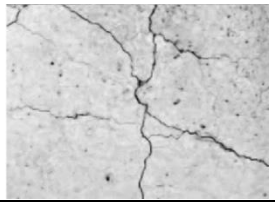

Gaussian Filter

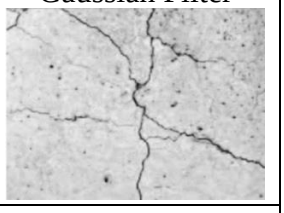

Simple threshold (T = 185)

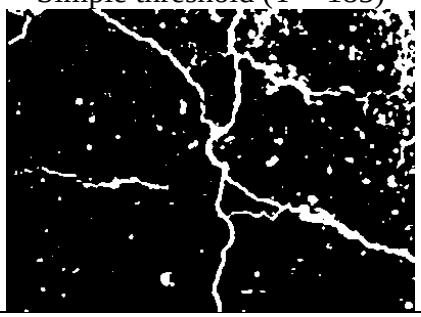

Otsu Threshold (T = 177)

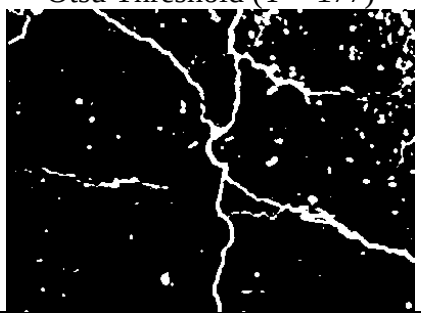

Edge Detection

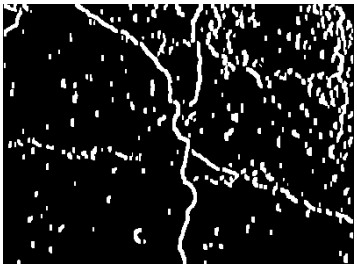

Sobel X

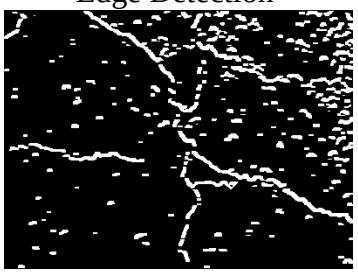

Sobel Y

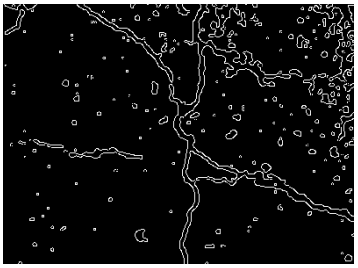

Canny

Area Determination

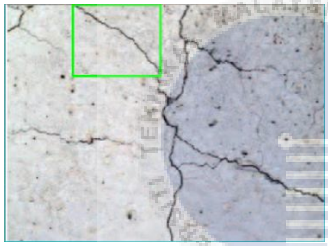

Coordinates = (84, 0) (194, 0) (84, 89) (194, 89)
Length, l = 110 mm
Width, w = 89 mm
Area, A = 9790 mm^2

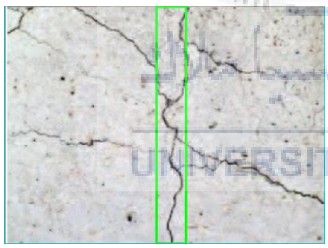

Coordinates = (189, 0) (226, 0) (189, 296) (226, 296)
Length, l = 37 mm
Width, w = 296 mm
Area, A = 10952 mm^2

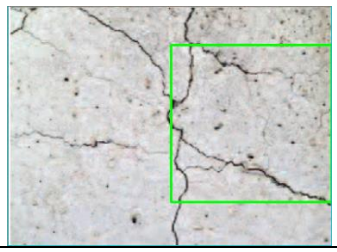

Coordinates = (201, 47) (400, 47) (201, 242) (400, 242)
Length, l = 199 mm
Width, w = 195 mm
Area, A = 38805 mm^2

Crack 15 [45]

Original Image	Grayscale Image	Median Filter	Gaussian Filter
	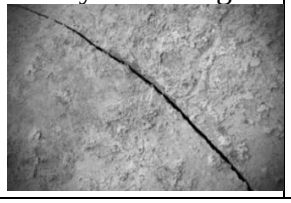	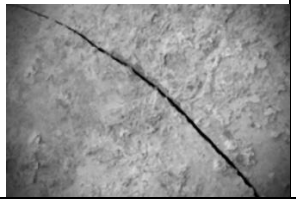	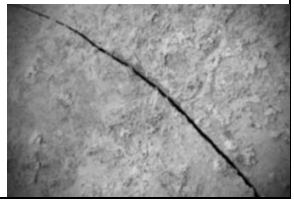

UTeM
UNIVERSITI TEKNIKAL MALAYSIA MELAKA

Simple threshold (T = 92)	Otsu Threshold (T = 129)
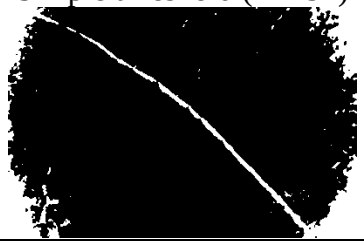	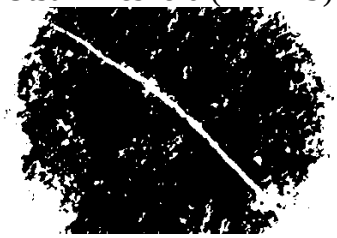

Edge Detection

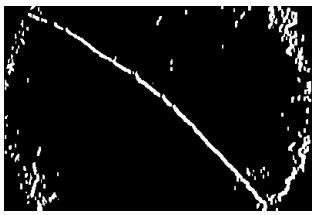
Sobel X

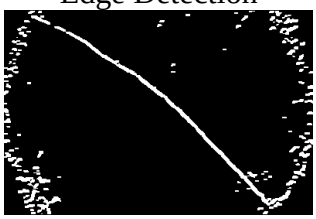
Sobel Y

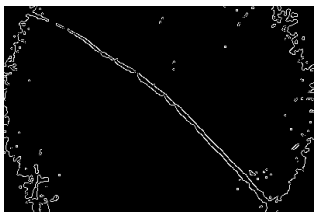
Canny

Area Determination

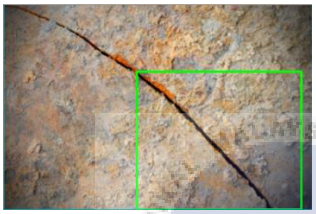

Coordinates = (172, 86) (386, 86) (172, 265) (386, 265)
Length, l = 214 mm
Width, w = 179 mm
Area, A = 38306 mm^2

Coordinates = (93, 35) (169, 35) (93, 84) (169, 84)
Length, l = 76 mm
Width, w = 49 mm
Area, A = 3724 mm^2

Crack 16 [45]

Original Image	Grayscale Image	Median Filter	Gaussian Filter

Simple threshold (T = 88)	Otsu Threshold (T = 179)
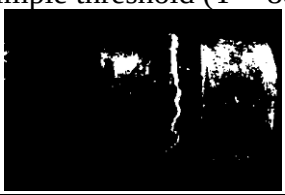	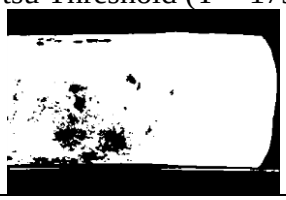

Edge Detection

Sobel X

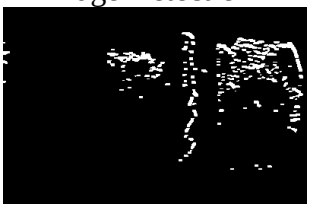
Sobel Y

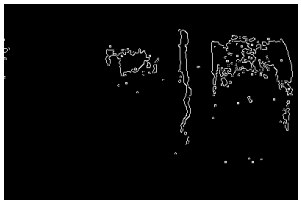
Canny

UNIVERSITI TEKNIKAL MALAYSIA MELAKA

Area Determination

Coordinates = (237, 35) (255, 35) (237, 174) (255, 174)
Length, l = 18 mm
Width, w = 139 mm
Area, A = 2502 mm^2

Crack 17 [46]

Original Image	Grayscale Image	Median Filter	Gaussian Filter
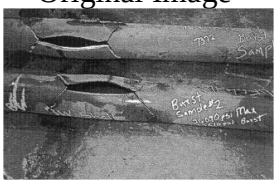	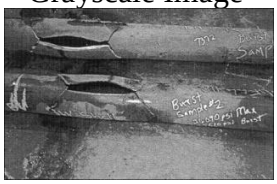	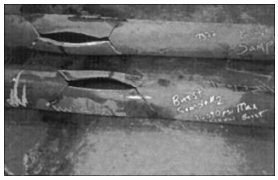	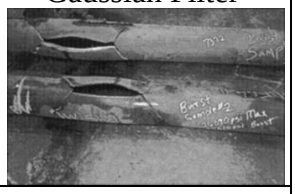

Simple threshold (T = 71)	Otsu Threshold (T = 109)

Edge Detection

Sobel X | Sobel Y | Canny

Area Determination

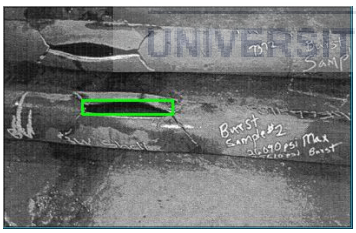

Coordinates = (90, 107) (194, 107) (90, 123) (194, 123)
Length, l = 104 mm
Width, w = 16 mm
Area, A = 1664 mm^2

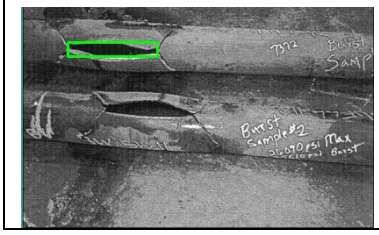

Coordinates = (51, 41) (153, 41) (51, 57) (153, 57)
Length, l = 102 mm
Width, w = 16 mm
Area, A = 1632 mm^2

UNIVERSITI TEKNIKAL MALAYSIA MELAKA

Crack 18 [46]

Original Image	Grayscale Image	Median Filter	Gaussian Filter
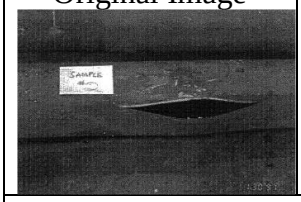		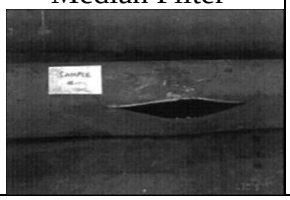	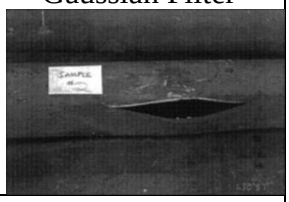

Simple threshold (T = 30)	Otsu Threshold (T = 140)
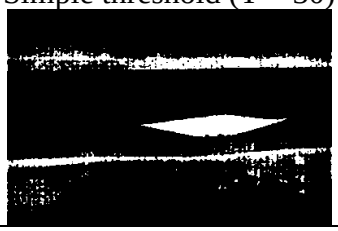	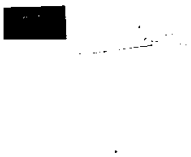

Edge Detection

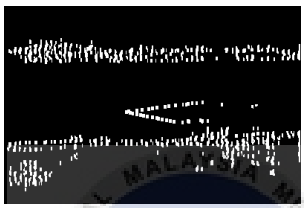
Sobel X

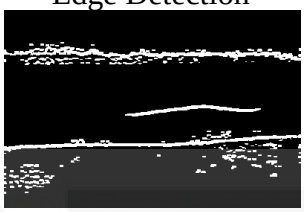
Sobel Y

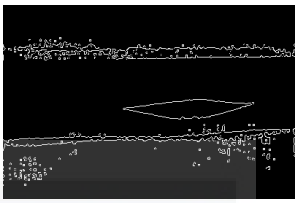
Canny

Area Determination

Coordinates = (166, 129) (341, 129) (166, 157) (341, 157)
Length, l = 175 mm
Width, w = 28 mm
Area, A = 4900 mm^2

Crack 19 [20]

Original Image	Grayscale Image	Median Filter	Gaussian Filter
		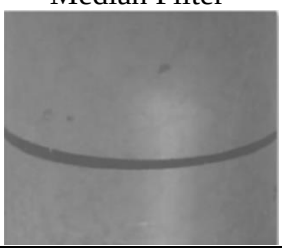	

Simple threshold (T = 111)	Otsu Threshold (T = 129)

UNIVERSITI TEKNIKAL MALAYSIA MELAKA

Edge Detection

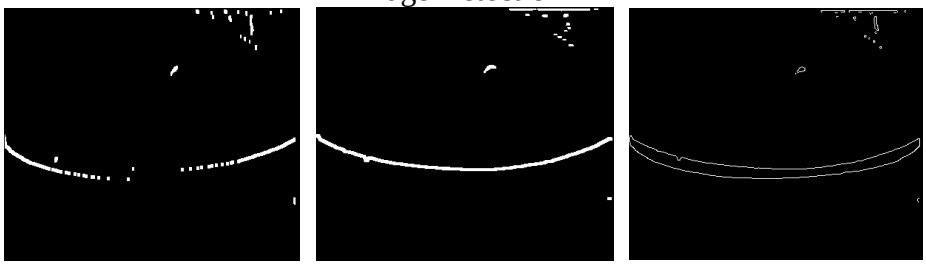

Sobel X | Sobel Y | Canny

Area Determination

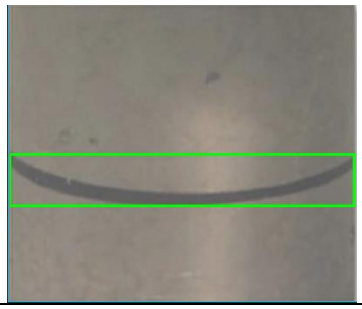

Coordinates = (0, 173) (395, 173) (0, 232) (395, 232)
Length, l = 395 mm
Width, w = 59 mm
Area, A = 23305 mm^2

Crack 21 [20]

Original Image | Grayscale Image | Median Filter | Gaussian Filter

Simple threshold (T = 94) | Otsu Threshold (T = 113)

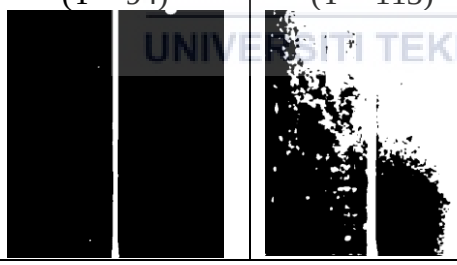

Edge Detection

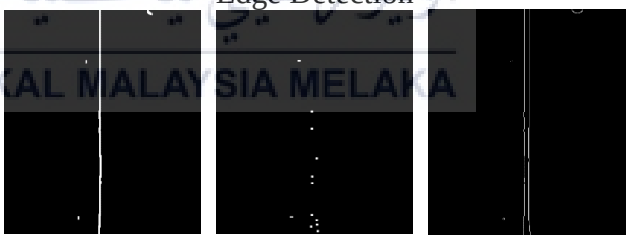

Sobel X | Sobel Y | Canny

Area Determination

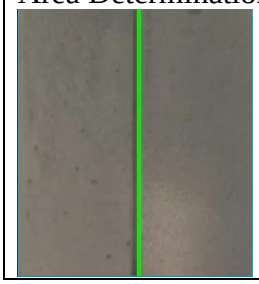

Coordinates = (203, 0) (207, 0) (203, 457) (207, 457)
Length, l = 4 mm
Width, w = 457 mm
Area, A = 1828 mm^2

UNIVERSITI TEKNIKAL MALAYSIA MELAKA

Crack 22 [29]

Original Image	Grayscale Image	Median Filter	Gaussian Filter
		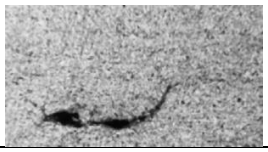	

Simple threshold (T = 117)

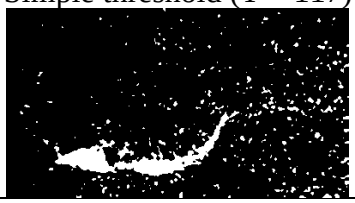

Otsu Threshold (T = 151)

Edge Detection

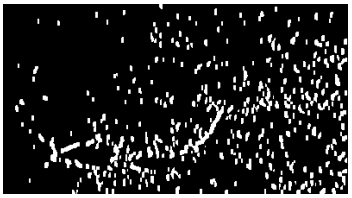
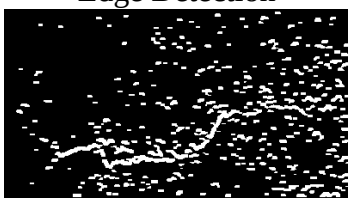
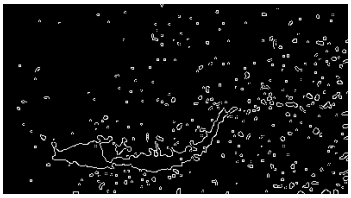

Sobel X | Sobel Y | Canny

Area Determination

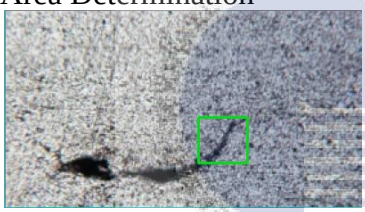

Coordinates = (216, 119) (271, 119) (216, 170) (271, 170)
Length, l = 55 mm
Width, w = 51 mm
Area, A = 2805 mm^2

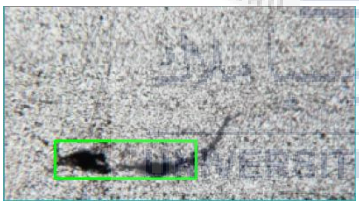

Coordinates = (57, 152) (218, 152) (57, 195) (218, 195)
Length, l = 161 mm
Width, w = 43 mm
Area, A = 6923 mm^2

Crack 23 [29]

Original Image	Grayscale Image	Median Filter	Gaussian Filter
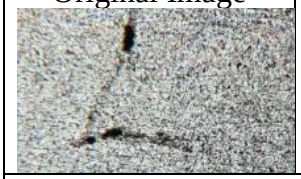	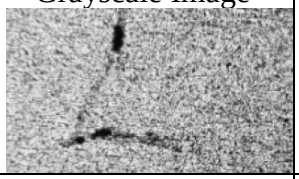	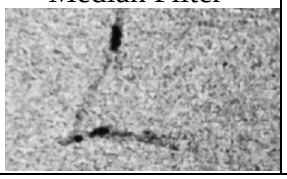	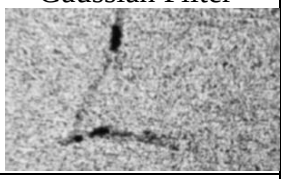

Simple threshold (T = 82)

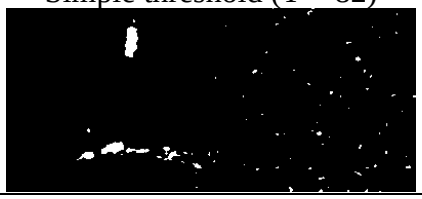

Otsu Threshold (T = 157)

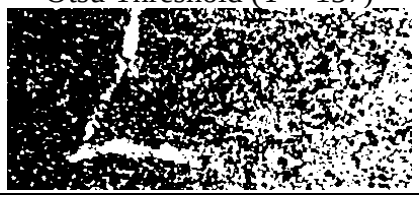

Edge Detection

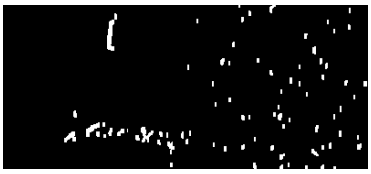
Sobel X

Sobel Y

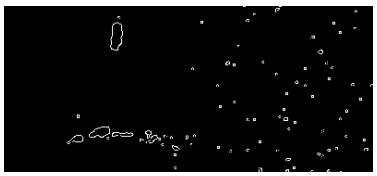
Canny

Area Determination

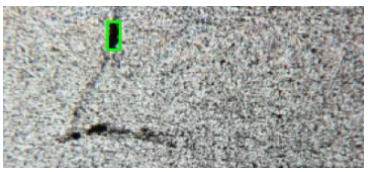

Coordinates = (115, 17) (129, 17) (115, 48) (129, 48)
Length, l = 14 mm
Width, w = 31 mm
Area, A = 434 mm^2

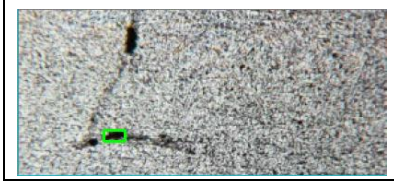

Coordinates = (92, 130) (115, 130) (92, 142) (115, 142)
Length, l = 23 mm
Width, w = 12 mm
Area, A = 276 mm^2

Crack 24 [29]

Original Image

Grayscale Image

Median Filter

Gaussian Filter

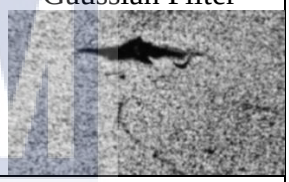

Simple threshold (T = 77)

Otsu Threshold (T = 138)

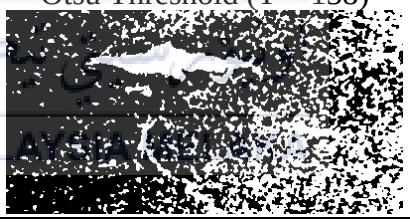

Edge Detection

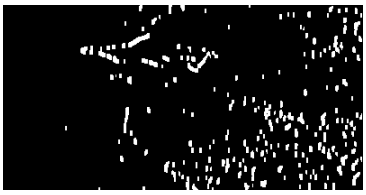
Sobel X

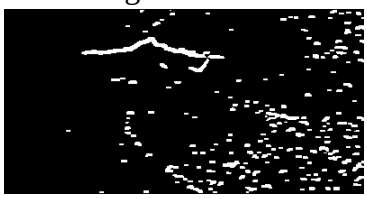
Sobel Y

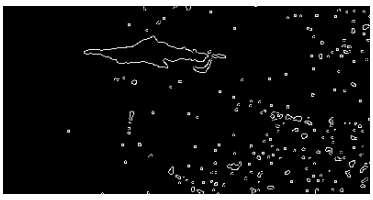
Canny

Area Determination

Coordinates = (115, 17) (129, 17) (115, 48) (129, 48)
Length, l = 14 mm
Width, w = 31 mm
Area, A = 434 mm^2

UNIVERSITI TEKNIKAL MALAYSIA MELAKA

Crack 25 [29]

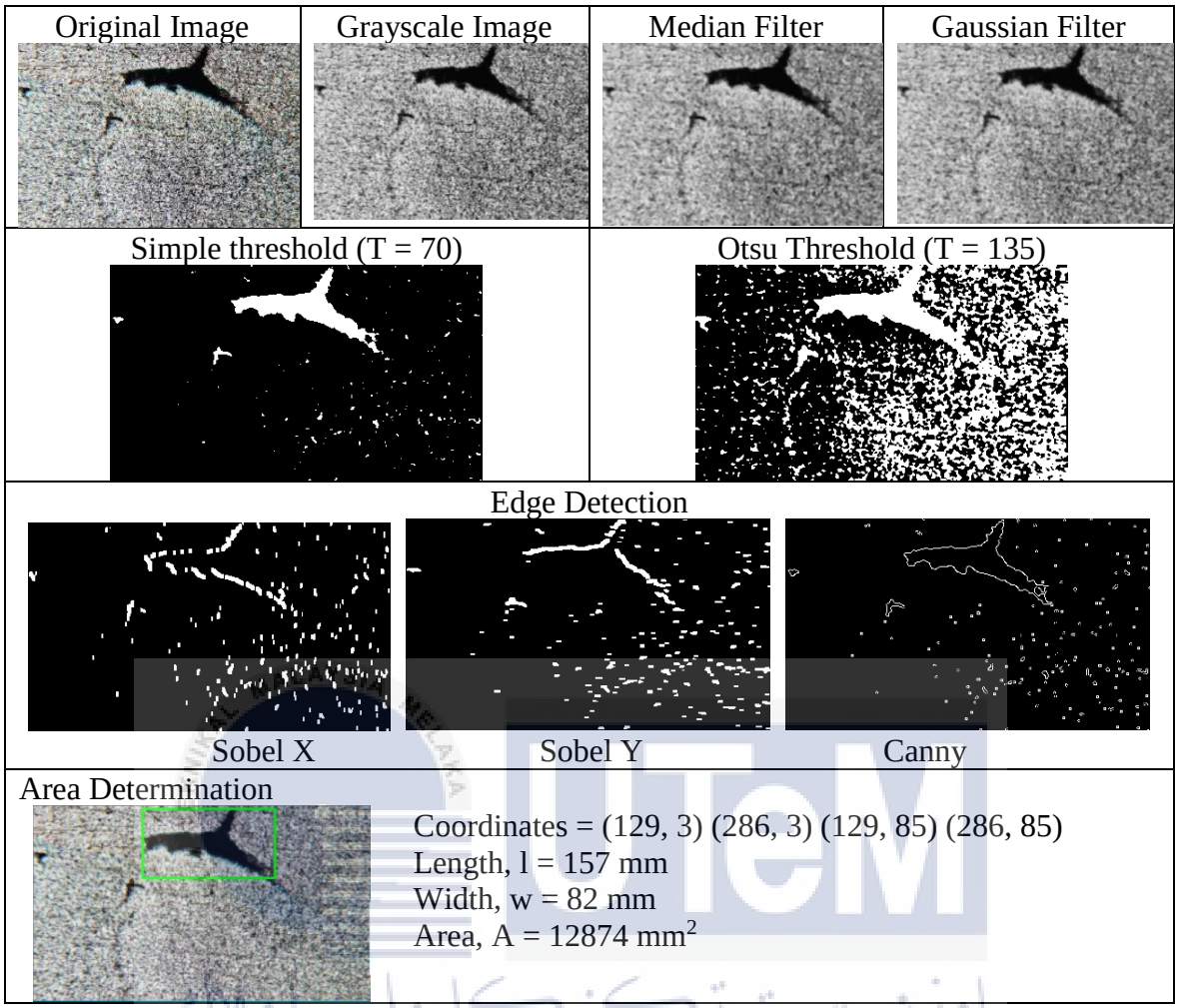

Crack 26 [29]

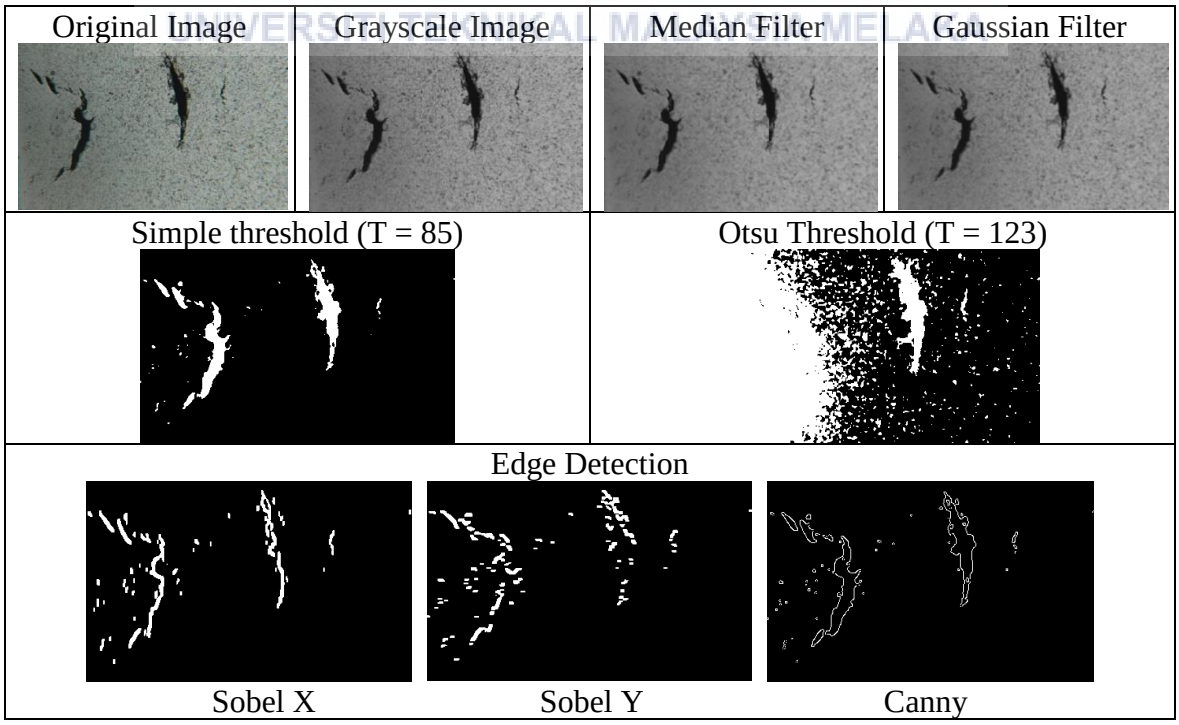

UNIVERSITI TEKNIKAL MALAYSIA MELAKA

Area Determination

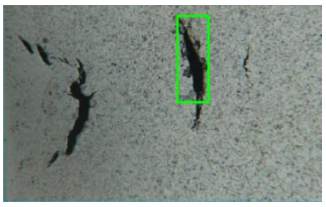

Coordinates = (217, 13) (256, 13) (217, 121) (256, 121)
Length, l = 39 mm
Width, w = 108 mm
Area, A = 4212 mm^2

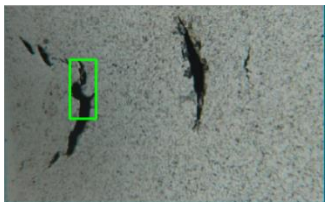

Coordinates = (81, 67) (114, 67) (81, 141) (114, 141)
Length, l = 33 mm
Width, w = 74 mm
Area, A = 2442 mm^2

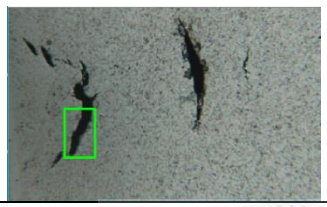

Coordinates = (71, 128) (110, 128) (71, 190) (110, 190)
Length, l = 39 mm
Width, w = 62 mm
Area, A = 2418 mm^2

Crack 27 [29]

Original Image

Grayscale Image

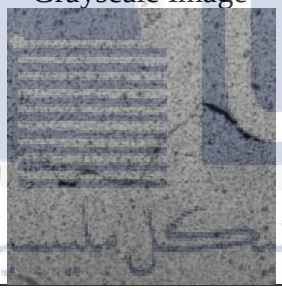

Median Filter

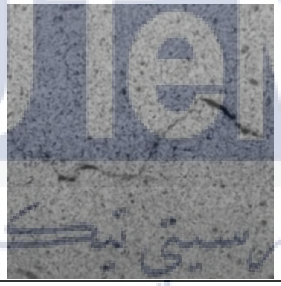

Gaussian Filter

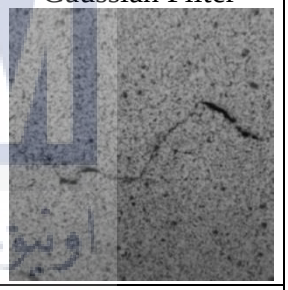

Simple threshold (T = 64)

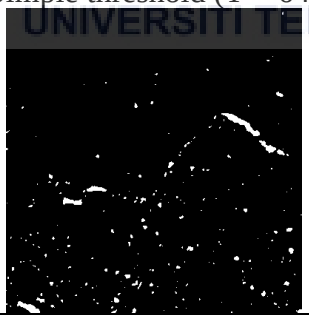

Otsu Threshold (T = 115)

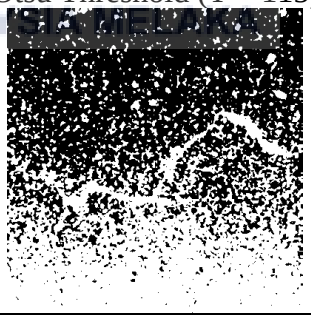

Edge Detection

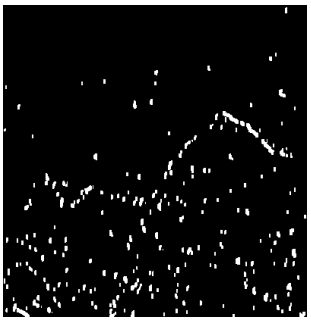

Sobel X

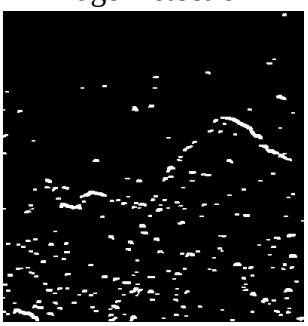

Sobel Y

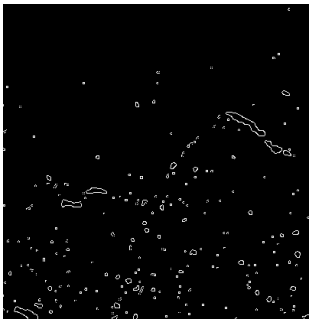

Canny

Area Determination

Coordinates = (291, 141) (343, 141) (291, 173) (343, 173)
Length, l = 52 mm
Width, w = 32 mm
Area, A = 1664 mm^2

Coordinates = (342, 178) (365, 178) (342, 196) (365, 196)
Length, l = 23 mm
Width, w = 22 mm
Area, A = 506 mm^2

Crack 28 [29]

Original Image	Grayscale Image	Median Filter	Gaussian Filter
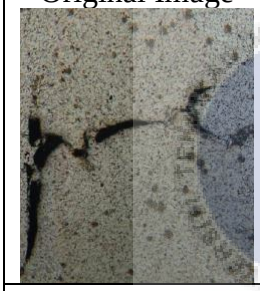	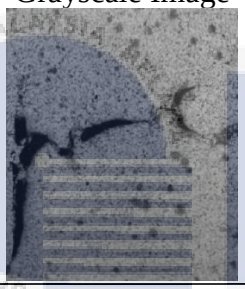		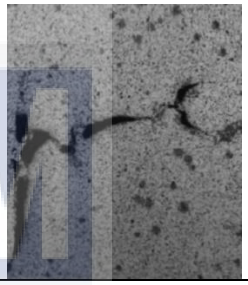

Simple threshold (T = 56)	Otsu Threshold (T = 100)	Edge Detection		
	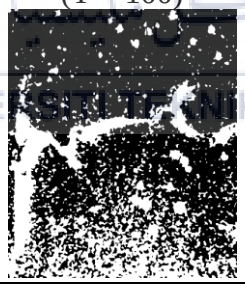			
		Sobel X	Sobel Y	Canny

Area Determination

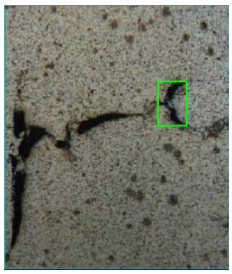

Coordinates = (273, 135) (324, 135) (273, 214) (324, 214)
Length, l = 51 mm
Width, w = 79 mm
Area, A = 4029 mm^2

UNIVERSITI TEKNIKAL MALAYSIA MELAKA

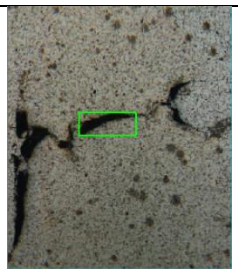

Coordinates = (127, 190) (229, 190) (127, 231) (229, 231)
Length, l = 102 mm
Width, w = 41 mm
Area, A = 4182 mm^2

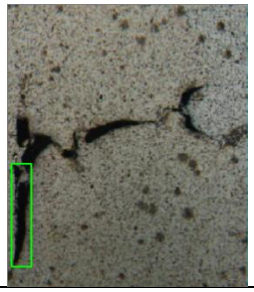

Coordinates = (6, 264) (39, 264) (6, 435) (39, 435)
Length, l = 33 mm
Width, w = 171 mm
Area, A = 5643 mm^2

Crack 29 [31]

Original Image	Grayscale Image	Median Filter	Gaussian Filter
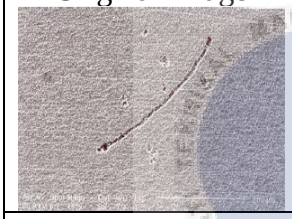	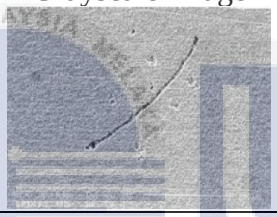		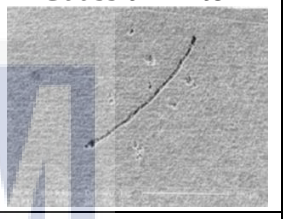

Simple threshold (T = 140)

Otsu Threshold (T = 171)

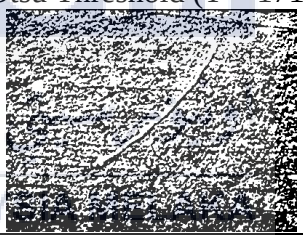

Edge Detection

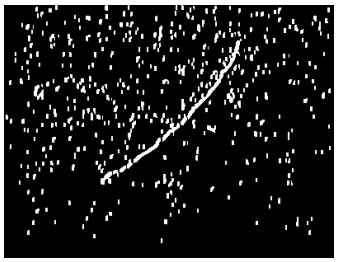

Sobel X

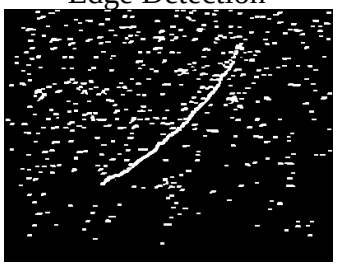

Sobel Y

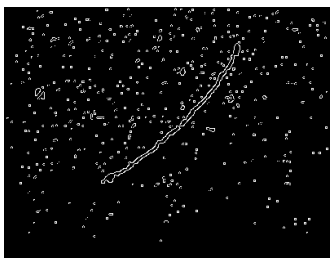

Canny

Area Determination

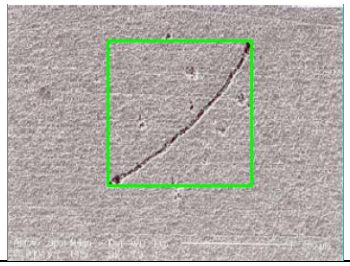

Coordinates = (104, 38) (254, 38) (104, 189) (254, 189)
Length, l = 150 mm
Width, w = 151 mm
Area, A = 22650 mm^2

UNIVERSITI TEKNIKAL MALAYSIA

Crack 30 [47]

Original Image	Grayscale Image	Median Filter	Gaussian Filter
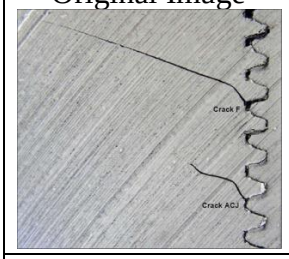	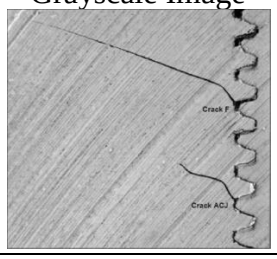	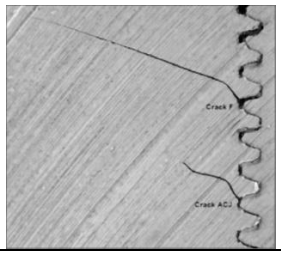	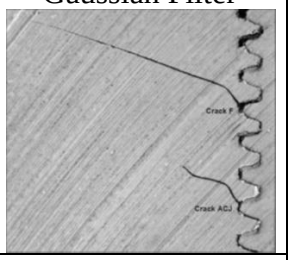

Simple threshold (T = 130)	Otsu Threshold (T = 139)
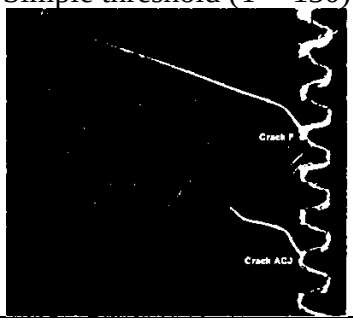	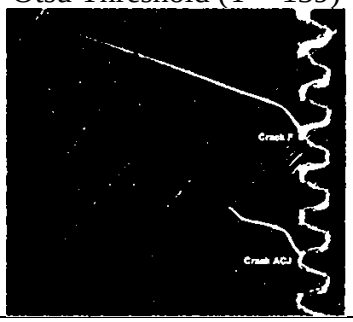

Edge Detection

Sobel X | Sobel Y | Canny

Area Determination

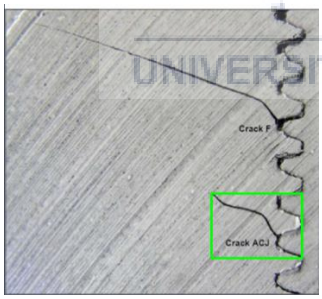

Coordinates = (261, 233) (376, 233) (261, 315) (376, 315)
Length, l = 112 mm
Width, w = 82 mm
Area, A = 9184 mm^2

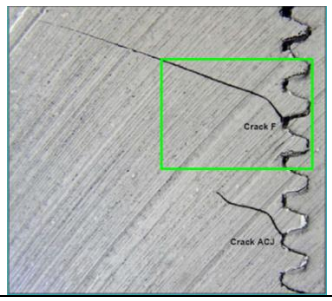

Coordinates = (192, 66) (382, 66) (192, 204) (382, 204)
Length, l = 190 mm
Width, w = 138 mm
Area, A = 26200 mm^2

UNIVERSITI TEKNIKAL MALAYSIA MELAKA

Crack 31 [48]

Original Image	Grayscale Image 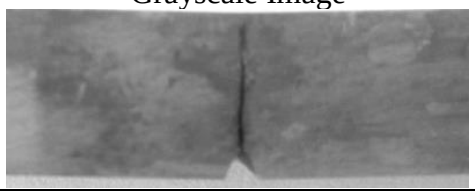
Median Filter 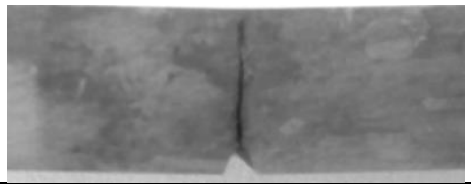	Gaussian Filter 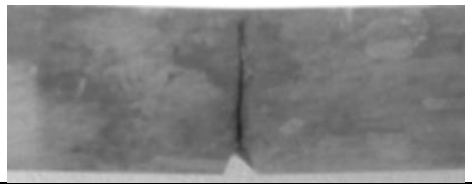
Simple threshold (T = 82) 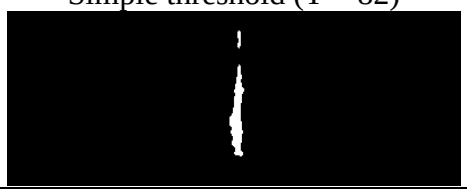	Otsu Threshold (T = 148) 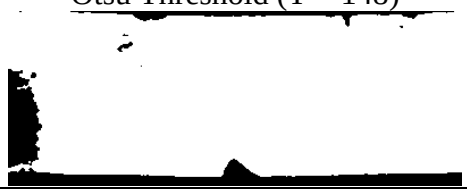
Edge Detection Sobel X Sobel Y Canny	
Area Determination 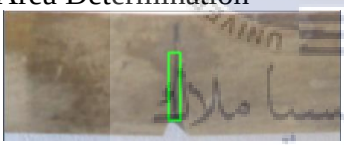	Coordinates = (195, 48) (209, 48) (195, 128) (209, 128) Length, l = 14 mm Width, w = 80 mm Area, A = 1120 mm^2

UNIVERSITI TEKNIKAL MALAYSIA MELAKA

Crack 32 [48]

Original Image	Grayscale Image 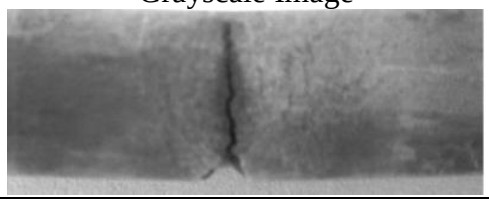
Median Filter 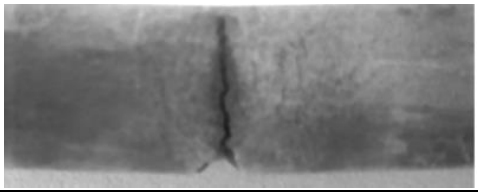	Gaussian Filter 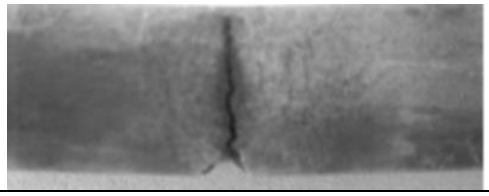
Simple threshold (T = 70) 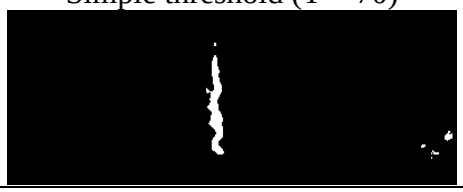	Otsu Threshold (T = 129)

Edge Detection

Sobel X

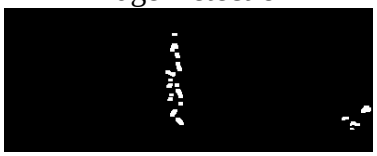
Sobel Y

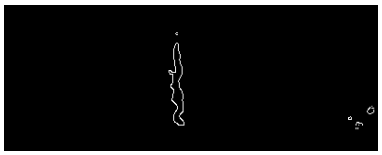
Canny

Area Determination

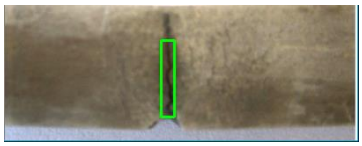

Coordinates = (177, 41) (192, 41) (177, 128) (192, 128)
Length, l = 15 mm
Width, w = 87 mm
Area, A = 1305 mm^2

Crack 33 [48]

Original Image

Grayscale Image

Median Filter

Gaussian Filter

Simple threshold (T = 60)

Otsu Threshold (T = 109)

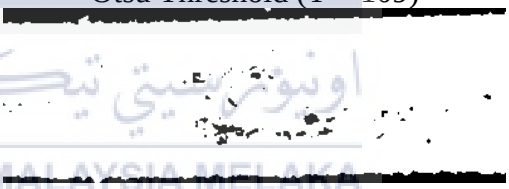

Edge Detection

Sobel X

Sobel Y

Canny

Area Determination

Coordinates = (72, 62) (83, 62) (72, 133) (83, 133)
Length, l = 11 mm
Width, w = 71 mm
Area, A = 781 mm^2

UNIVERSITI TEKNIKAL MALAYSIA MELAKA

Crack 35 [49]

Original Image	Grayscale Image	Median Filter	Gaussian Filter
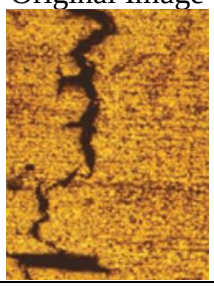		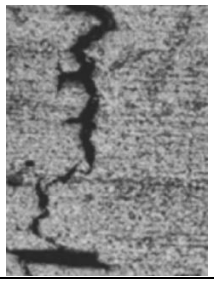	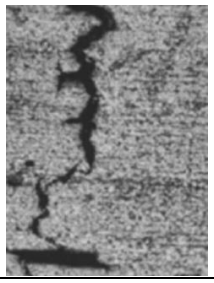

Simple threshold (T = 74)	Otsu Threshold (T = 116)	Edge Detection		
	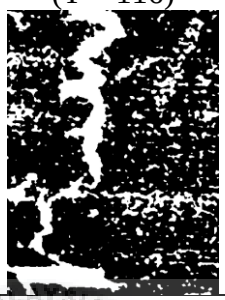	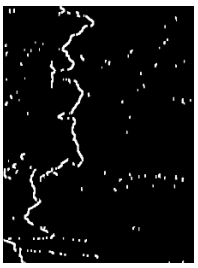		
		Sobel X	Sobel Y	Canny

Area Determination

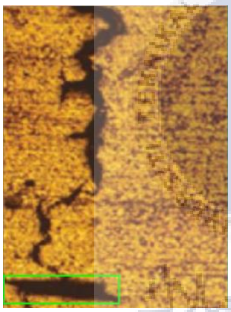

Coordinates = (0, 477) (206, 477) (0, 526) (206, 526)
Length, l = 206 mm
Width, w = 49 mm
Area, A = 10094 mm^2

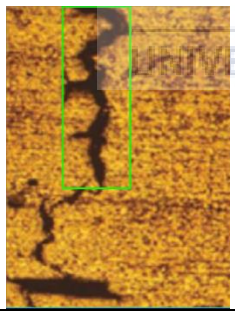

Coordinates = (100, 0) (220, 0) (100, 324) (220, 324)
Length, l = 120 mm
Width, w = 324 mm
Area, A = 38880 mm^2

UNIVERSITI TEKNIKAL MALAYSIA MELAKA

Crack 36 [49]

Original Image	Grayscale Image	Median Filter	Gaussian Filter
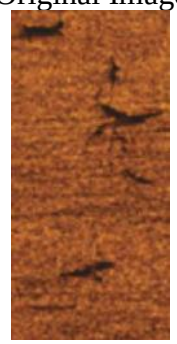	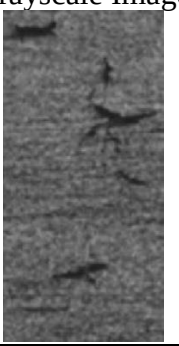	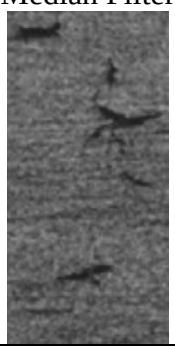	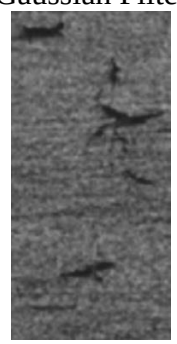

Simple threshold (T = 56)	Otsu Threshold (T = 93)	Edge Detection
		Sobel X Sobel Y Canny

Area Determination

Coordinates = (19, 29) (131, 29) (19, 74) (131, 74)
Length, l = 112 mm
Width, w = 45 mm
Area, A = 5040 mm^2

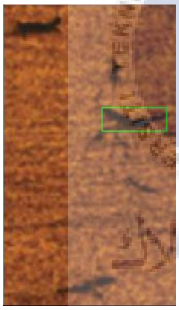

Coordinates = (227, 238) (377, 238) (227, 292) (377, 292)
Length, l = 150 mm
Width, w = 54 mm
Area, A = 8100 mm^2

Coordinates = (124, 630) (257, 630) (124, 674) (257, 674)
Length, l = 133 mm
Width, w = 44 mm
Area, A = 5852 mm^2

UTeM
اونيۏرسيتي تيکنيکل مليسيا ملاک
UNIVERSITI TEKNIKAL MALAYSIA MELAKA

Crack 38 [49]

Original Image	Grayscale Image	Median Filter	Gaussian Filter
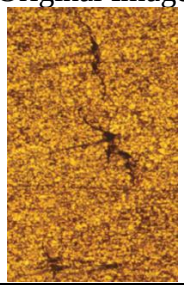	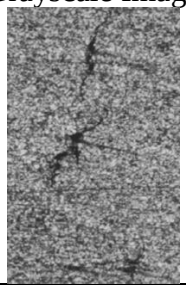	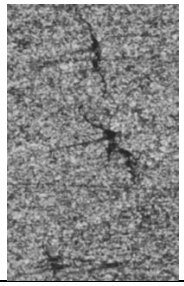	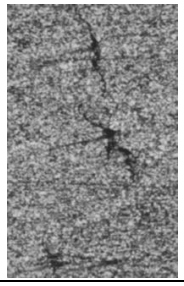

Simple threshold (T = 63)	Otsu Threshold (T = 128)	Edge Detection
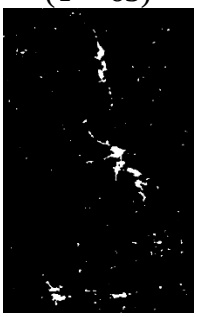		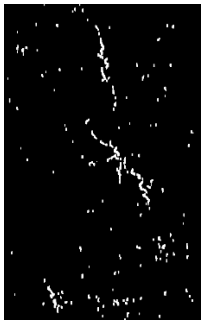 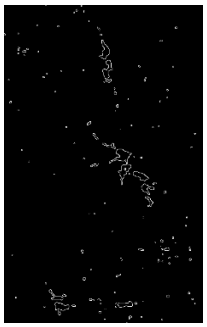 Sobel X Sobel Y Canny

Area Determination

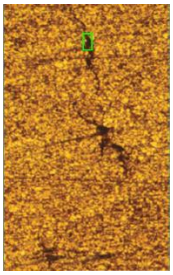

Coordinates = (191, 71) (212, 71) (191, 110) (212, 110)
Length, l = 21 mm
Width, w = 39 mm
Area, A = 819 mm^2

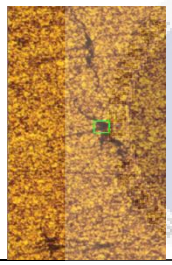

Coordinates = (218, 291) (256, 291) (218, 320) (256, 320)
Length, l = 38 mm
Width, w = 29 mm
Area, A = 1102 mm^2

Crack 39 [49]

Original Image	Grayscale Image	Median Filter	Gaussian Filter
	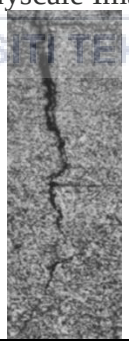	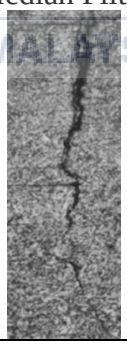	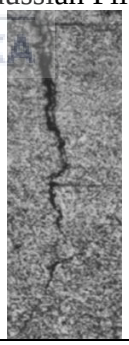

Simple threshold (T = 78)	Otsu Threshold (T = 122)	Edge Detection
	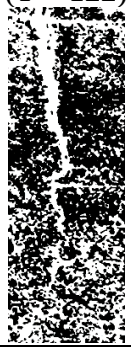	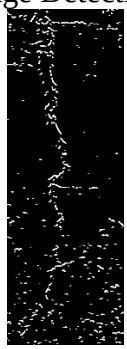 Sobel X Sobel Y Canny

UNIVERSITI TEKNIKAL MALAYSIA MELAKA

Area Determination

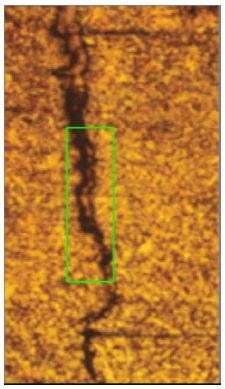

Coordinates = (116, 227) (203, 227) (116, 514) (203, 514)
Length, l = 87 mm
Width, w = 287 mm
Area, A = 24969 mm^2

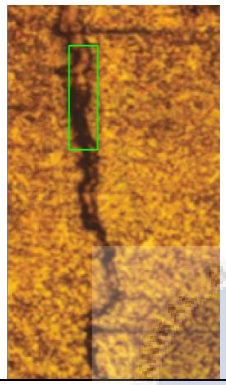

Coordinates = (115, 76) (169, 76) (115, 272) (169, 272)
Length, l = 54 mm
Width, w = 196 mm
Area, A = 10584 mm^2

Crack 39 [49]

Original Image	Grayscale Image	Median Filter	Gaussian Filter
	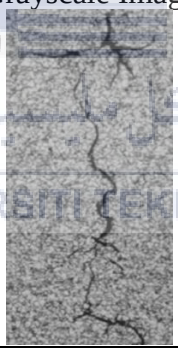	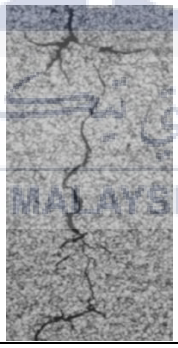	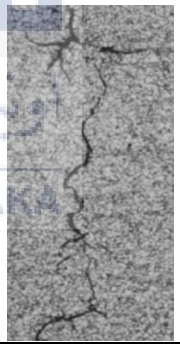

Simple threshold (T = 101)	Otsu Threshold (T = 136)	Edge Detection
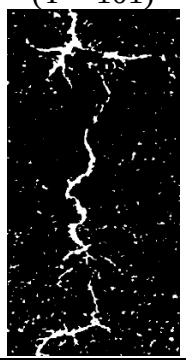	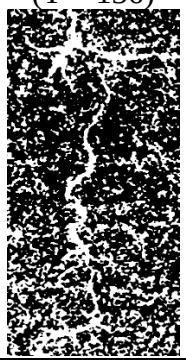	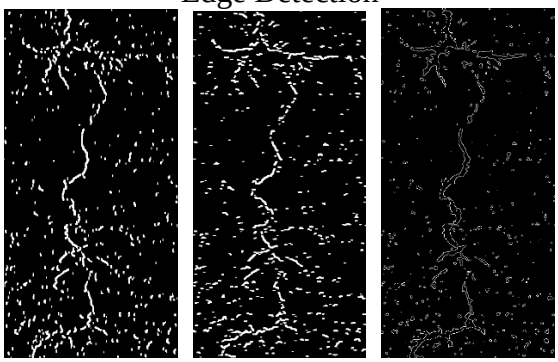

Sobel X Sobel Y Canny

UNIVERSITI TEKNIKAL MALAYSIA MELAKA

Area Determination

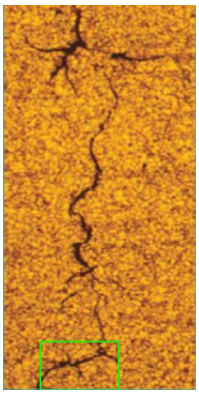

Coordinates = (66, 617) (209, 617) (66, 705) (209, 705)
Length, l = 143 mm
Width, w = 88 mm
Area, A = 12584 mm^2

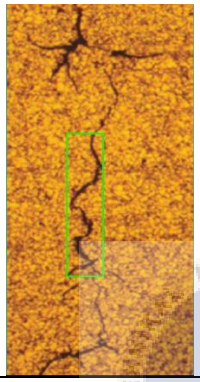

Coordinates = (112, 243) (180, 243) (112, 511) (180, 511)
Length, l = 68 mm
Width, w = 268 mm
Area, A = 18224 mm^2

Crack 41 [49]

Original Image

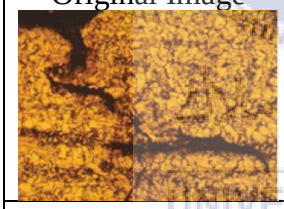

Grayscale Image

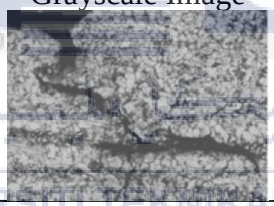

Median Filter

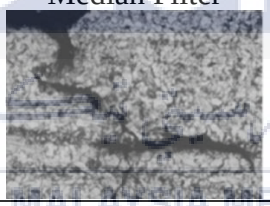

Gaussian Filter

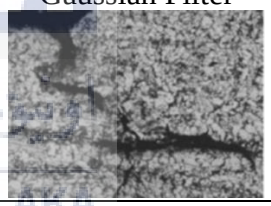

Simple threshold (T = 52)

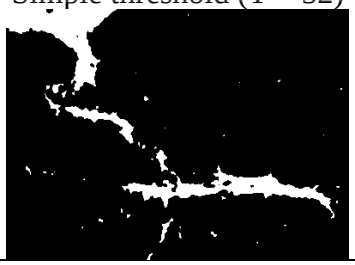

Otsu Threshold (T = 113)

Edge Detection

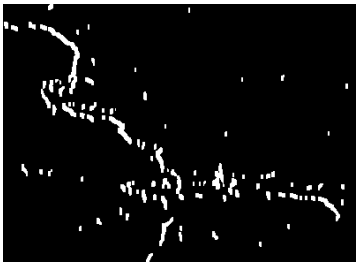

Sobel X

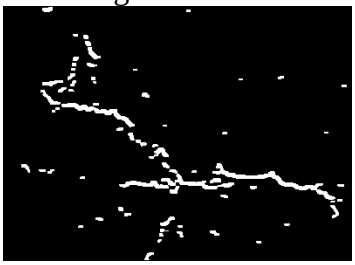

Sobel Y

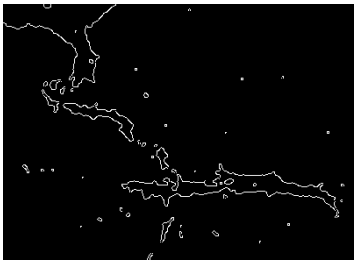

Canny

Area Determination

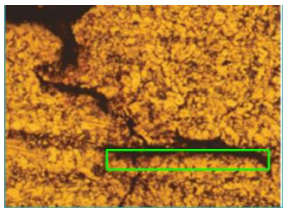

Coordinates = (146, 209) (380, 209) (146, 237) (380, 237)
Length, l = 234 mm
Width, w = 28 mm
Area, A = 6552 mm^2

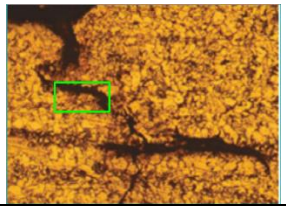

Coordinates = (69, 113) (149, 113) (69, 156) (149, 156)
Length, l = 80 mm
Width, w = 43 mm
Area, A = 3440 mm^2

Crack 42 [49]

Original Image | Grayscale Image | Median Filter | Gaussian Filter

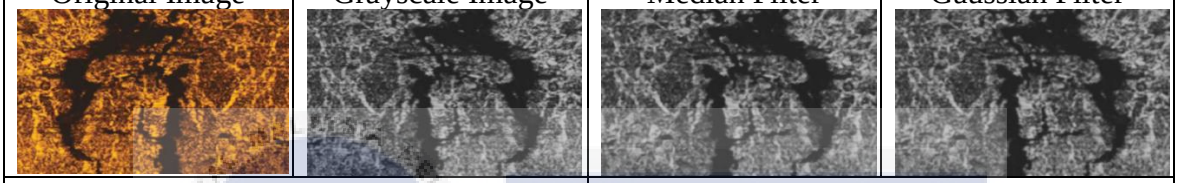

Simple threshold (T = 39) | Otsu Threshold (T = 93)

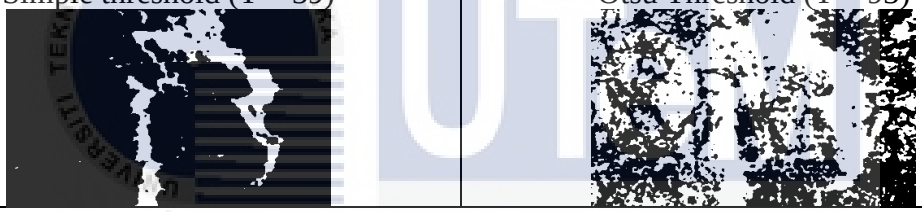

Edge Detection

Sobel X | Sobel Y | Canny

Area Determination

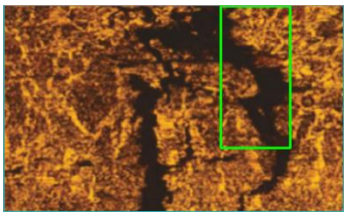

Coordinates = (146, 209) (380, 209) (146, 237) (380, 237)
Length, l = 234 mm
Width, w = 28 mm
Area, A = 6552 mm^2

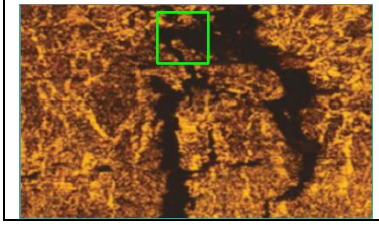

Coordinates = (69, 113) (149, 113) (69, 156) (149, 156)
Length, l = 80 mm
Width, w = 43 mm
Area, A = 3440 mm^2

UNIVERSITI TEKNIKAL MALAYSIA MELAKA

Crack 43 [50]

Original Image	Grayscale Image	Median Filter	Gaussian Filter
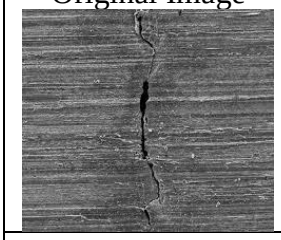		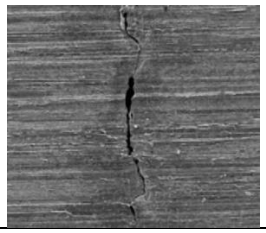	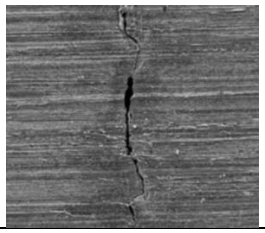

Simple threshold (T = 48)	Otsu Threshold (T = 104)
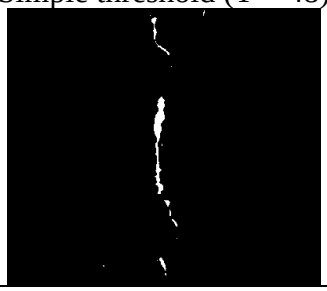	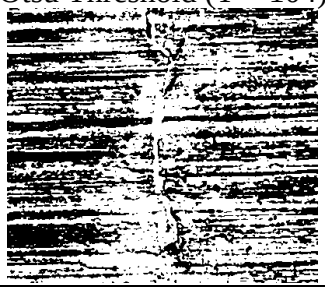

Edge Detection

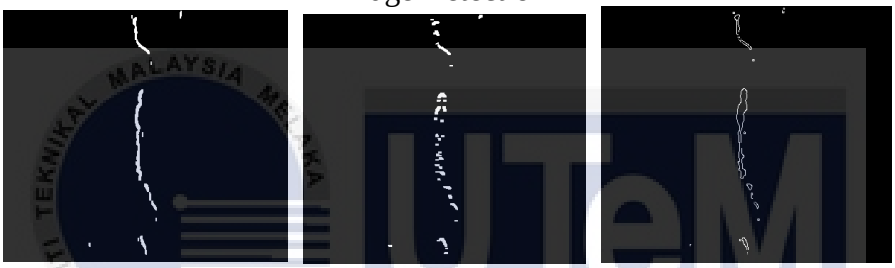

Sobel X | Sobel Y | Canny

Area Determination

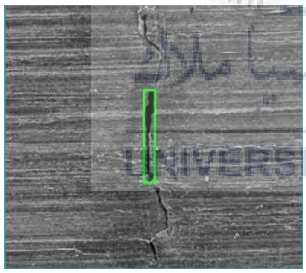

Coordinates = (186, 113) (201, 113) (186, 237) (201, 237)
Length, l = 15 mm
Width, w = 124 mm
Area, A = 1860 mm^2

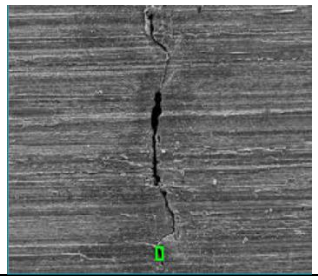

Coordinates = (194, 318) (202, 318) (194, 334) (202, 334)
Length, l = 8 mm
Width, w = 16 mm
Area, A = 128 mm^2

UNIVERSITI TEKNIKAL MALAYSIA MELAKA